Algorithmes itératifs à faible complexité pour le codage de canal et le compressed sensing

Ludovic Danjean

Ph.D. THESIS

presented to

Université de Cergy-Pontoise
École Doctorale Sciences et Ingénierie

to obtain the title of

Doctor of Science of the University of Cergy-Pontoise
Specialty: **Sciences and Technologies of Information and Communication**

Defended by

Ludovic DANJEAN

Low-Complexity Iterative Algorithms for Channel Coding and Compressed Sensing

prepared at
Équipes Traitement de l'Information et Systèmes (ETIS) - UMR 8051
ENSEA - Université de Cergy-Pontoise - CNRS

and

Signal Processing and Coding Lab
Department of Electrical and Computer Engineering - University of Arizona

defense date: November 29, 2012

Jury:

President:	Prof.	Pierre Duhamel	LSS - SUPELEC, France
Reviewer:	Assoc. Prof.	Alexandre Graell	Chalmers University, Sweden
Reviewer:	Prof.	Charly Poulliat	INP - ENSEEIHT, France
Examinator:	Dr.	Vincent Gripon	Télécom Bretagne, France
Advisor:	Prof.	David Declercq	ETIS/ENSEA-UCP-CNRS, France
Advisor:	Prof.	Bane Vasic	University of Arizona, USA

Résumé

L'utilisation d'algorithmes itératifs est aujourd'hui largement répandue dans tous les domaines du traitement du signal et des communications numériques. Dans les systèmes de communications modernes, les algorithmes itératifs sont utilisés dans le décodage des codes "low-density parity-check" (LDPC), qui sont une classe de codes correcteurs d'erreurs utilisés pour leurs performances exceptionnelles en terme de taux d'erreur. Dans un domaine plus récent qu'est le "compressed sensing", les algorithmes itératifs sont utilisés comme méthode de reconstruction afin de recouvrer un signal "sparse" à partir d'un ensemble d'équations linéaires, appelées observations. Cette thèse traite principalement du développement d'algorithmes itératifs à faible complexité pour les deux domaines mentionnés précédemment, à savoir le design d'algorithmes de décodage à faible complexité pour les codes LDPC, et le développement et l'analyse d'un algorithme de reconstruction à faible complexité, appelé "Interval-Passing Algorithm (IPA)", dans le cadre du "compressed sensing".

Dans la première partie de cette thèse, nous traitons le cas des algorithmes de décodage des codes LDPC. Il est maintenu bien connu que les codes LDPC présentent un phénomène dit de "plancher d'erreur" en raison des échecs de décodage des algorithmes de décodage traditionnels du types propagation de croyances, et ce en dépit de leurs excellentes performances de décodage. Récemment, une nouvelle classe de décodeurs à faible complexité, appelés "finite alphabet iterative decoders (FAIDs)" ayant de meilleures performances dans la zone de plancher d'erreur, a été proposée. Dans ce manuscrit nous nous concentrons sur le problème de la sélection de bons décodeurs FAID pour le cas de codes LDPC ayant un poids colonne de 3 et le cas du canal binaire symétrique. Les méthodes traditionnelles pour la sélection des décodeurs s'appuient sur des techniques asymptotiques telles que l'évolution de densité, mais qui ne garantit en rien de bonnes performances sur un code de longueur finie surtout dans la région de plancher d'erreur. C'est pourquoi nous proposons ici une méthode de sélection qui se base sur la connaissance des topologies néfastes au décodage pouvant être présentes dans un code en utilisant le concept de "trapping sets bruités". Des résultats de simulation sur différents codes montrent que les décodeurs FAID sélectionnés grâce à cette méthode présentent de meilleures performances dans la zone de plancher d'erreur comparé au décodeur à propagation de croyances.

Dans un second temps, nous traitons le sujet des algorithmes de reconstruction itératifs pour le compressed sensing. Des algorithmes itératifs ont été proposés pour ce domaine afin de réduire la complexité induite de la reconstruction par "linear program-

ming". Dans cette thèse nous avons modifié et analysé un algorithme de reconstruction à faible complexité dénommé IPA utilisant les matrices creuses comme matrices de mesures. Parallèlement aux travaux réalisés dans la littérature dans la théorie du codage, nous analysons les échecs de reconstruction de l'IPA et établissons le lien entre les "stopping sets" de la représentation binaire des matrices de mesure creuses. Les performances de l'IPA en font un bon compromis entre la complexité de la reconstruction sous contrainte de minimisation de la norme ℓ_1 et le très simple algorithme dit de vérification.

Abstract

Iterative algorithms are now widely used in all areas of signal processing and digital communications. In modern communication systems, iterative algorithms are used for decoding low-density parity-check (LDPC) codes, a popular class of error-correction codes that are now widely used for their exceptional error-rate performance. In a more recent field known as compressed sensing, iterative algorithms are used as a method of reconstruction to recover a sparse signal from a linear set of measurements. This thesis primarily deals with the development of low-complexity iterative algorithms for the two aforementioned fields, namely, the design of low-complexity decoding algorithms for LDPC codes, and the development and analysis of a low complexity reconstruction algorithm called Interval-Passing Algorithm (IPA) for compressed sensing.

In the first part of this thesis, we address the area of decoding algorithms for LDPC codes. It is well-known that LDPC codes suffer from the error floor phenomenon in spite of their exceptional performance, where traditional iterative decoders based on the belief propagation (BP) fail for certain low-noise configurations. Recently, a novel class of decoders called "finite alphabet iterative decoders (FAIDs)" were proposed that are capable of surpassing BP in the error floor at much lower complexity. In this work, we focus on the problem of selection of particularly good FAIDs for column-weight-three codes over the Binary Symmetric channel (BSC). Traditional methods for decoder selection use asymptotic techniques such as the density evolution method, which does not guarantee a good performance on finite-length codes especially in the error floor region. Instead, we propose a methodology for selection that relies on the knowledge of potentially harmful topologies that could be present in a code, using the concept of noisy trapping set. Numerical results are provided to show that FAIDs selected based on our methodology outperform BP in the error floor on several codes.

In the second part of this thesis, we address the area of iterative reconstruction algorithms for compressed sensing. Iterative algorithms have been proposed for compressed sensing in order to tackle the complexity of the LP reconstruction method. In this work, we modify and analyze a low complexity reconstruction algorithm called the IPA which uses sparse matrices as measurement matrices. Similar to what has been done for decoding algorithms in the area of coding theory, we analyze the failures of the IPA and link them to the stopping sets of the binary representation of the sparse measurement matrices used. The performance of the IPA makes it a good trade-off between the complex ℓ_1-minimization reconstruction and the very simple verification decoding.

Contents

List of Figures

List of Tables

Glossary

AMP	Approximate Message-Passing.
AWGNC	Additive White Gaussian Noise Channel.
BasP	Basis Pursuit.
BCH	Bose-Chaudhuri-Hocquenghem.
BCJR	Bahl Cocke Jelinek Raviv.
BP	Belief Propagation.
BPSK	Binary Phase Shift Keying.
BEC	Binary Erasure Channel.
BER	Bit Error Rate.
BSC	Binary Symmetric Channel.
DE	Density Evolution.
FAID	Finite Alphabet Iterative Decoder.
FER	Frame Error-Rate.
GF	Galois Field.
IPA	Interval-Passing Algorithm.
LDPC	Low Density Parity Check.
LLR	Log-Likelihood Ratio.
LT	Linear Threshold.
LP	Linear Programming.
LUT	Look-Up Table.
MAP	Maximum A Posteriori.
ML	Maximum Likelihood.
MP	Message-Passing.
NCNV	Noisy Critical Number Vector.
NLT	Non-Linear Threshold.
PEG	Progressive Edge-Growth.
QAM	Quadrature Amplitude Modulation.
QPSK	Quadrature Phase Shift Keying.
RS	Reed-Solomon.

RIP	Restricted Isometry Property.
SNR	Signal-to-Noise Ratio.
TS	Trapping Set.
TSO	Trapping Set Ontology.

General Introduction

Context and Motivation

Iterative algorithms are nowadays widely used in all areas of signal processing because either they perform at a low complexity, or they provide fast processing on large scale problems, without any significant loss in performance. In most cases iterative methods are even able to provide excellent performance, which explains why iterative algorithms can be found from the first algorithms solving linear system of equations to the most advanced algorithms in signal processing systems that primarily deal with the recovery of a signal that was transmitted, stored, or corrupted somehow.

The aim of this dissertation is to design and analyze low-complexity iterative algorithms for two domains of the signal processing, namely the channel coding, and the more recent field of compressed sensing. In the first half of the dissertation we seek to design low-complexity finite precision iterative decoders. In the second step we address the design and analysis of low-complexity iterative reconstruction algorithms in compressed sensing.

Design of low-complexity finite precision iterative decoders

Since their rediscovery, low-density parity-check (LDPC) codes [1] have been used intensively in channel coding, including in some standards such as the second generation of Digital Video Broadcasting by Satellite, and in the standards of wireless networking like Wifi and Wimax. In spite of their excellent performance under iterative decoding, LDPC codes exhibit an abrupt degradation in the slope of the error rate performance in the high signal-to-noise ratio (SNR) known as the error floor region [44]. The error floor problem have attracted significant interest with emphasis on designing codes and low-complexity decoders to lower error floors in domain where error floor is a major concern for systems like in storage devices where very low error rates are expected.

Recently a new class of low-complexity finite precision iterative decoders, called finite alphabet iterative decoders (FAIDs), was proposed for LDPC codes over the

Binary Symmetric channel (BSC), where the messages can take a finite number of levels [67]. These new decoders exhibit better performance in the error floor region compared to traditional iterative decoders using a very low complexity as only a small number of bits (as small as 3) are required for the message representation. The update functions used at the variable nodes can be easily described by maps which are chosen with the goal of increasing the error correction capability of the code.

Although it has been proven that FAIDs have excellent performance in the error floor, the problem of identifying particularly good FAIDs for a given code is not trivial. This is due to the enormous number of FAIDs that can be designed for a particular number of precision bits. In this dissertation we address the problem of selection of good FAIDs for column-weight-three codes on the BSC using two different approaches. The first approach relies on the structure of a code we want to select a FAID for, and the second approach aims at selecting a set of potential good FAIDs without being code specific.

Finally, we also attempt to extend the design of FAIDs on column-weight-four codes, as these types of codes are present in many practical applications as in storage systems where error floor is a critical issue, and where FAIDs can find their industrial interest.

Design of low-complexity iterative reconstruction algorithms

In compressed sensing, reconstructing a sparse signal from a small set of measurements via compressed sensing [79] has attracted significant attention in the last few years. A k-sparse signal $\mathbf{x} \in \mathbb{R}^n$, i.e. a signal $\mathbf{x}$ with at most k non-zero values, is observed indirectly through a shorter measurement vector $\mathbf{y} \in \mathbb{R}^m$ and obtained from the linear equations $\mathbf{y} = A\mathbf{x}$ where A is an $m \times n$ measurement matrix, with $m \ll n$. The task of compressed sensing is to recover $\mathbf{x}$ from $\mathbf{y}$. The first approach to solve the compressed sensing problem is to find a signal $\mathbf{x}$ with the smallest ℓ_0-norm given $\mathbf{y} = A\mathbf{x}$. The ℓ_0-norm minimization of compressed sensing is known to be NP-hard. Instead, the ℓ_1-norm minimization solution based on linear programming (LP) was introduced to reconstruct $\mathbf{x}$. The LP technique for the compressed sensing problem, called Basis Pursuit [86, 78], has a remarkable performance, but its high complexity and running time makes it impractical in some applications which require fast reconstruction, or when the dimension of a measurement matrix is large.

To tackle the issue of complexity, message-passing algorithms for compressed sensing have been proposed, originating from channel coding mainly based on belief propagation [99], or iterative thresholding [92].

Recently low-complexity message-passing algorithm was proposed [103], which we refer to as Interval-Passing Algorithm (IPA). This algorithm performs at a very low complexity with very promising reconstruction performance compared to the original and complex Basis Pursuit and another very simple algorithm, known as verification

decoding. However, it was introduced primarily for sparse binary measurement matrices.

The goal of this dissertation is to modify the IPA for non-negative real-valued measurement matrices, and analyze its reconstruction possibilities.

Contributions and organization of the dissertation

The main contributions of this dissertation are summarized as follows.

- We introduce FAIDs and propose selection methods for column-weight-three LDPC codes using two approaches, and we design FAIDs for column-weight-four LDPC codes:
  - The first method of selection of FAIDs for column-weight-three codes uses large attractors of iterative decoders, which are the codewords of LDPC codes. We describe this method on the Tanner code where we extracted all the minimum codewords of weight 20, and identified three distinct topologies of codewords. After explaining the limitations of current techniques which analyze harmful structures, we detail the selection method of good FAIDs by simulating error-patterns of weight 5 and 6 on the three types of minimal codewords.
  - In the second approach, the main contribution relies on the methodology to select a group of potential good decoders in the error floor on any column-weight-three code. To process this methodology, new concepts are introduced such as the concepts of noisy trapping sets and noisy critical numbers for the analysis of harmful structures, and the concept of decoder domination to perform the selection of the decoders. Simulation results show indeed that selected FAIDs have excellent performance in the error floor region on a variety of codes.
  - We also provide the first results on the design of FAIDs for column-weight-four LDPC codes using a heuristic-based method on a given high-rate code. We provide a simple procedure to extract some harmful structures responsible for the error floor in this particular code, and then design a FAID which has a better error correction capability on the extracted harmful topologies. Numerical results are provided to validate the efficacy of our method showing that the designed 3-bit and 4-bit precisions FAID can outperform BP (floating-point) as well as offset min-sum in the error floor.

- We present and analyze the IPA for compressed sensing:
  - We modify the original IPA in order to deal with non-negative real-valued sparse measurement matrix, and show that this low-complexity reconstruction algorithm is providing a good complexity/performance trade-off between the complex reconstruction of the linear programming methods, and the very simple verification algorithm.
  - We analyze the reconstruction possibilities of the IPA, by establishing a link between the reconstruction failures of the IPA and the stopping sets of the binary representation of the measurement matrix. Simulation results on codes for which the stopping sets distribution is known, confirm the influence of such structures on the IPA performance.

From the two main topics of the thesis, this manuscript is divided into two parts: chapters 1 and 2 are related to channel coding and low-complexity iterative decoders, and chapters 3 and 4 are related to compressed sensing and low-complexity iterative reconstruction algorithms. The outline of the dissertation is detailed as follows.

In chapter 1, we provide a detailed overview regarding channel coding, introducing the notations and the necessary background on iterative decoders and the error floor phenomenon.

In the chapter 2 we introduce the FAIDs, both approaches to select good FAID for column-weight-three codes in the error floor region, as well as the first study on FAID for column-weight-four codes.

Chapter 3 reviews recent work on compressed sensing with a description of the problem setting, the traditional approach using linear programming techniques, and the suggested iterative reconstruction methods.

In the chapter 4 we present the modified version of the IPA, and provide a complete analysis of the reconstruction possibilities of the IPA.

At the present date, this thesis has led to the following publications:

Journal paper:

1. S. K. Planjery, D. Declercq, L. Danjean and B. Vasic, "Finite alphabet iterative decoders for LDPC codes surpassing floating-point iterative decoders," in *IET Electron. Lett.*, vol. 47, no. 16, pp. 919–921, Aug. 2011.

2. V. Ravanmehr, L. Danjean, B. Vasic, D. Declercq, "Interval-Passing Algorithm for Non-Negative Measurement Matrices: Performance and Reconstruction Analysis," *IEEE J. on Emerging and Selected Topics in Circuits and Systems* (accepted for publication), vol. 2, no. 3, Oct. 2012.

3. S. K. Planjery, D. Declercq, L. Danjean and B. Vasic, "Finite Alphabet Iterative Decoders, Part I: Decoding Beyond Belief Propagation on BSC," submitted to *IEEE Trans. Comm.*, 2012.

International Conferences:

1. S. K. Planjery, S. K. Chilappagari, B. Vasic, D. Declercq, L. Danjean, "Iterative Decoding Beyond Belief Propagation," in *Proc. Inform. Theory and Applicat. Workshop* (invited paper), San Diego, CA, USA, Feb. 2010.

2. D. Declercq, L. Danjean, E. Li, S. Planjery, B.Vasic, "Finite Alphabet Iterative Decoding (FAID) of the (155,64,20) Tanner Code," in *Proc. IEEE Int. Symp. on Turbo-Codes and Iterative Inform. Process.* (invited paper), Brest, France, Sep. 2010.

3. L. Danjean, D. Declercq, S. K. Planjery and B. Vasic, "On the Selection of Finite Alphabet Iterative Decoders for LDPC codes on the BSC," in *Proc. IEEE Inform. Theory Workshop*, Paraty, Brazil, Oct. 2011.

4. V. Ravanmehr, L. Danjean, D. Declercq and B. Vasic, "On Iterative Compressed Sensing Reconstruction of Sparse Non-negative Vectors," in *Proc. Int. Symp. on Applied Sci. in Biomedical and Commun. Technologies* (invited paper), Barcelona, Spain, Oct. 2011.

5. L. Danjean, V. Ravanmehr, D. Declercq and B. Vasic, "Iterative Reconstruction Algorithms in Compressed Sensing," in *Proc. Telecommun. Forum* (invited paper), Belgrade, Serbia, Nov. 2011.

6. V. Ravanmehr, L. Danjean, D. Declercq and B. Vasic, "Signal Recovery Performance of the Interval-Passing Algorithm," in *Proc. Int. Symp. on Turbo-Code and Iterative Process.*, Gothenburg, Sweden, Aug. 2012.

National Conferences:

1. L. Danjean, D. Declercq, S. K. Planjery and B. Vasic, "Décodeurs multi-niveaux pour le décodage quasi-optimal des codes LDPC," in *Proc. MajecSTIC*, Bordeaux, France, Oct. 2010.

2. L. Danjean, D. Declercq, S. K. Planjery and B. Vasic, "Trapping sets bruités pour la sélection des décodeurs multi-niveaux des codes LDPC," in *Proc. XXIIIe colloque GRETSI*, Bordeaux, France, Sep. 2011.

Chapter 1

Introduction on Channel Coding

EVER since its inception in the 1950's, error-correcting codes have played an indispensable role in ensuring high reliability and low power consumption in wireless/wired data transmissions as well as in data storage, and have now become ubiquitous in all modern communication and data storage systems. An error-correction code essentially consists of an encoder and a decoder; information that is to be transmitted is encoded by adding redundancy in a specific manner at the transmitter and decoding is performed at the receiver to correct some or all of the errors contained in the received noisy data. In particular, a specific class of error-correcting codes called *low-density parity-check codes* (LDPC) [1] has not only revolutionized the communications and storage industry, but also sparked a widespread research interest over the past two decades, leading to the so-called field of *modern coding theory*.

Since the first goal of this dissertation is centrally themed around LDPC codes, we begin this chapter by providing a brief overview of the historical background of error-correcting codes especially related to LDPC codes, and provide the necessary preliminaries required for understanding this contribution of this dissertation in this field.

1.1 Historical background

The origin of error-correcting codes dates back to the work of Hamming during his time at Bell Labs in the late 1940's. At that time, Hamming got motivated to develop error-correcting codes when he became increasingly frustrated with relay computers he was working with, which would halt any submitted jobs containing errors. He eventually designed the first type of error-correcting linear block codes, now known as Hamming codes, which could correct a single error, and later published his work in 1950 [2]. This led to the development of other important early codes such as the triple error-correcting Golay code [3] and the Reed-Muller (RM) codes [4, 5].

Meanwhile, Shannon, who happened to be a colleague of Hamming at Bell Labs, published his landmark paper [6] in 1948 that led to the birth of the field of information theory. The paper essentially laid down the fundamental limits of error-free transmission by introducing the notion of *channel capacity*. Shannon pointed out that every channel has an associated capacity, and he proved using random coding arguments that for transmission rates less than the channel capacity, there exists a code that can achieve arbitrarily low error-rates asymptotically with the length of the code. However, Shannon did not provide any insights into the explicit design of capacity-achieving codes, and thus, the quest for the search of such codes began.

In the ensuing years, much of the research was dedicated towards the design of linear block codes that had good error-correcting capabilities and good minimum distance. Initial code designs were for hard-decision channels and relied heavily on algebraic structure based on finite-field algebra. Codes such as the Bose-Chaudhuri-Hocquenghem (BCH) codes [7, 8] and the Reed-Solomon (RS) codes [9] became widely used especially in magnetic recoding applications such as magnetic tape systems. The codes were decoded by an efficient algorithm developed by Berlekamp and Massey [10]. However, algebraic-based codes were still far from achieving the limits of Shannon's capacity in their asymptotic performance, and they lacked the random-like properties originally envisioned by Shannon.

Concurrently, another class of codes called *convolutional* codes were developed by Elias [11], which had a more probabilistic approach to channel coding. Interpreted as discrete-time finite-state systems, these codes had an underlying special structure known as the *trellis* which enabled linear-time encoding and inherently allowed for the capability to use practical soft-decision decoding algorithms. One of the most important decoding algorithms for these codes was developed by Viterbi, famously known as the *Viterbi algorithm* [12], which optimally estimated the most likely sequence of transmitted bits. This proved to be a major attraction for these codes, and they were capable of providing substantial coding gains even though their asymptotic performance was still far from Shannon's capacity. Another algorithm that was developed in the same probabilistic spirit was the BCJR algorithm by Bahl, Cocke, Jelinek, and Raviv [13] which estimated the *a posteriori* probability of each transmitted bit. At the time, the BCJR algorithm was considered to be purely of theoretical interest as it was regarded too complex for practical implementations. However, the BCJR algorithm along with the class of convolutional codes turned out to be the most crucial steps for paving the way towards the development of capacity-achieving codes.

The breakthrough in the search for capacity-achieving codes was finally reached in 1993 by Berrou, Glavieux, and Thitimajshima with their discovery of *turbo codes* [14]. A key feature of these codes was the use of *iterative decoding*, which involved using the BCJR algorithm to iteratively exchange soft information between two convolutional codes concatenated in parallel. This proved to be pivotal for achieving near-Shannon-limit performance with reasonable decoding complexity. Subsequently,

the class of *low-density parity-check* (LDPC) codes, originally invented by Gallager in early 1960's but remained forgotten for nearly thirty years, was rediscovered by MacKay [15] who showed that these codes were also capable of capacity-achieving performance. This led to a renaissance in the field of modern coding theory with LDPC codes becoming one of the most active topics of research.

LDPC codes are essentially linear-block codes whose parity-check matrices have a sparse number of non-zero entries. These codes are conveniently represented as bipartite graphs known as the *Tanner graphs* [16], and the decoding algorithm operates on the Tanner graph of the code. The decoding algorithms used for LDPC codes are based on a central iterative algorithm known as the *belief propagation* (BP). The BP is a message-passing algorithm that involves propagating probabilistic messages along the edges of the graph in order to estimate the *a posteriori* probabilities of the codeword bits thereby lending itself to low complexity implementations. The notion of using graph-based decoding was eventually extended to other codes such as Turbo codes through the significant contributions of Tanner [16] and much later Wiberg [17]. Under BP decoding, LDPC codes are able to achieve an unprecedentedly good error-rate performance which has made them the overwhelming choice among existing codes for both present and emerging technologies in digital communications and data storage.

Within the past decade, with LDPC codes steadily gaining popularity, there has been an outburst of research related to the design of capacity-achieving LDPC codes as well as in the development and analysis of decoding algorithms. Richardson and Urbanke proposed the key technique of *density evolution* [19] for determining the decoding threshold of a given LDPC code under BP decoding, which is a threshold of noise below which the bit error probability tends to zero asymptotically with the length of the code. Using density evolution, Richardson, Shokrollahi and Urbanke optimized capacity-achieving irregular code ensembles for the best (highest) decoding thresholds that were very close to the Shannon limit. The technique was also subsequently used in the design of reduced-complexity BP decoders by Chen *et al.* [20] and Fossorier [21]*et al.*, and quantized BP decoders by Lee and Thorpe [22]. Another important asymptotic technique that was proposed for analyzing decoding algorithms simpler than BP (such as bit flipping) was the use of expander arguments and expander codes proposed by Sipser and Speilman [23]. Burshtein and Miller [24] applied expander arguments to message-passing to show that they could correct a linear fraction of errors. For finite-length analysis of codes, a novel approach to decoding called linear programming (LP) decoding was proposed by Feldman *et al.* [25], where the decoding problem is transformed to an LP formulation.

The problem of constructing codes with desirable structural properties and good minimum distance while maintaining their capacity-achieving ability also gained significant attention, with many applications facing stringent constraints in terms of storage requirements and implementation complexity. A particularly broad class of codes called *quasi-cyclic* codes generated great appeal to the industry, where the parity-check

matrices of these codes consist of blocks of circulants enabling much more efficient encoding and decoding implementations. Some of the notable works on quasi-cyclic codes include the codes proposed by Fossorier [26], the Protograph codes developed by Thorpe [27] and Divsalar *et al.* [28], the algebraic-based quasi-cyclic codes proposed by Lan *et al.* [29], finite geometry codes by Kou *et al.* [30], and combinatorially constructed codes by Vasic *et al.* [31]. Another class of codes that recently gained limelight are LDPC convolutional codes [32, 33], which are the convolutional counterparts to the conventional linear block code version of LDPC codes, and were recently shown by Lentmaier *et al.* to be capable of having BP thresholds nearly matching the MAP thresholds [34].

LDPC codes have already found their way into various standards such as the DVB-S2 (Digital Video Broadcasting), IEEE 802.3an (Ethernet), and are also being considered for the IEEE 802.16e (Wimax) and IEEE 802.11n (Wifi) standards. However, in spite of their excellent error-rate performance under BP decoding and their obvious advantages, they still have a major weakness that manifests itself in the form of an *error floor*. The error floor is an abrupt degradation in the performance of the code in the high signal-to-noise (SNR) region. This problem mainly arises due to the sub-optimality of BP decoding on finite-length codes with loopy graphs, especially when codes are designed to be asymptotically close to Shannon's limit. It could prove to be a major disadvantage particularly for applications requiring very low target error-rates such as storage devices. Therefore, the error floor problem has been widely regarded as one of the most important problems in coding theory and has attracted significant research interest over the past few years. Addressing the error floor problem is one of the main goals of this dissertation along with taking into account the effects of finite-precision for decoder realizations.

1.2 LDPC codes: fundamentals and notations

In this section, we will provide the necessary preliminaries related to LDPC codes starting from the basics of linear block codes to the general concept of message-passing and graph-based decoding. Along the way, we will introduce the required notations that will be used throughout this dissertation.

1.2.1 Linear block codes

An (N, K) binary linear block code $\mathcal{C}$ [35] is a K-dimensional subspace of $\mathrm{GF}(2)^N$, which is the vector space over the field GF(2) consisting of all possible binary N-tuples. Thus, the code $\mathcal{C}$ contains 2^k N-tuples or *codewords*. Given a message vector of k information bits, this vector is mapped to one of the codewords of length N in the code $\mathcal{C}$. The code $\mathcal{C}$ is said to have a *code rate* of $R = K/N$, which represents the

amount of redundancy added by the code.

The support of a codeword $\mathbf{x} = (x_1, x_2, \ldots, x_N)$, denoted by supp($\mathbf{x}$), is the set of all positions i such that $x_i \neq 0$. The *hamming weight* (or simply weight) of $\mathbf{x}$ denoted $w(\mathbf{x})$, is the cardinality of supp($\mathbf{x}$). The *hamming distance* (or simply distance) between any two codewords is the number of positions for which they differ in value. The minimum distance of a code $\mathcal{C}$, denoted by d_{min} is the smallest possible distance between any pair of codewords in $\mathcal{C}$. A codeword vector that has zero in all its positions is referred to as the *all-zero codeword*. Since a linear block must include the all-zero codeword, the minimum distance is simply the weight of the nonzero codeword that has the smallest weight.

The process of mapping a message vector of k information bits to a codeword of length N in the code $\mathcal{C}$ is known as *encoding*. Encoding is carried out through a $K \times N$ generator matrix $\mathbf{G}$ of the code $\mathcal{C}$, whose rows correspond to the basis vectors of $\mathcal{C}$, i.e., the linearly independent codewords. Given a message vector of k bits, say, $\mathbf{u} = (u_1, u_2, \ldots, u_k)$, a codeword $\mathbf{x} \in \mathcal{C}$ can obtained by performing $\mathbf{x} = \mathbf{uG}$.

A linear block code is also characterized by its parity-check matrix $\mathbf{H}$, which is an $M \times N$ matrix whose rows span the null space of $\mathbf{G}$, i.e., $\mathbf{GH}^T = 0$. Consequently, every codeword $\mathbf{x}$ is orthogonal to the rows of $\mathbf{H}$ so that $\mathbf{xH}^T = 0$. Given a vector $\mathbf{x}' \in \mathrm{GF}(2)^N$, the parity-check matrix can be used to verify whether $\mathbf{x}'$ is a codeword belonging to $\mathcal{C}$ or not. Therefore, each row of $\mathbf{H}$ is referred to as a *parity-check constraint* and there are M such parity-check constraints. The value of M is related to the code parameters by $M \geq (N - K)$, where the equality holds if $\mathbf{H}$ is a full-rank matrix.

Once a given message $\mathbf{u}$ is encoded to a codeword $\mathbf{x}$, it is then transmitted over a noisy channel and is received as $\mathbf{r} = (r_1, r_2, \ldots, r_N)$. *Decoding* is then performed to estimate the transmitted codeword $\mathbf{x}$ based on the received vector $\mathbf{r}$. The optimal decision rule used for determining the estimate $\hat{\mathbf{x}}$ is the *maximum a posteriori* (MAP) decoding rule, which essentially chooses a codeword $x \in \mathcal{C}$ that maximizes the a posteriori probability $\Pr(\mathbf{x}|\mathbf{r})$ (the probability that the transmitted codeword is $\mathbf{x}$ given that $\mathbf{r}$ was received). More precisely,

$$\hat{\mathbf{x}} = \arg\max_{\mathbf{x} \in \mathcal{C}} \Pr(\mathbf{x}|\mathbf{r}).$$

We shall assume that all codewords are equally likely to be transmitted. Under this assumption, the MAP decoding problem reduces to the *maximum likelihood* (ML) decoding problem which determines the codeword that maximizes the $\Pr(\mathbf{r}|\mathbf{x})$. If $\mathbf{r} \in \mathrm{GF}(2)^N$, then the ML decoding problem is equivalent to finding the nearest neighbor of $\mathbf{r}$ in the vector space $\mathrm{GF}(2)^N$ that is a codeword in $\mathcal{C}$. Therefore the code's error-correcting capability is linked to its minimum distance d_{min} as the code is guaranteed to correct $\lfloor (d_{min} - 1)/2 \rfloor$ errors. In general, ML decoding on a linear-block code is NP-hard as it requires a brute-force search of all codewords in the vector space $\mathrm{GF}(2)^N$. Hence, sub-optimal decoding algorithms that enable efficient implementations are used

in practice.

1.2.2 Channel assumptions

Let us assume that a codeword $\mathbf{x} = (x_1, x_2, \ldots, x_N) \in \mathcal{C}$ is transmitted over a noisy channel and is received as a vector $\mathbf{r}$. If the channel is memoryless, then the probability $\Pr(\mathbf{r}|\mathbf{x})$ can be expressed as

$$\Pr(\mathbf{r}|\mathbf{x}) = \prod_{i=1}^{N} \Pr(r_i|x_i).$$

This implies that the effect of the channel on every bit in the transmitted codeword is independent from one another. Hence, during decoding, it suffices to decide the value for each x_i independently based on maximizing $\Pr(r_i|x_i)$. This probability is also referred to as a *likelihood*.

For soft-decoding algorithms, the received vector $\mathbf{r}$ is mapped to a vector of probabilities or log-likelihood ratios before serving as input to the decoder. Let $\mathbf{y} = (y_1, y_2, \ldots, y_N)$ denote the vector that is input to a given decoder. We shall refer to the values y_i in vector $\mathbf{y}$ as *channel values*, to signify the fact they are determined based on the values received from the channel. If $\mathbf{y}$ is a vector of log-likelihoods, then the log-likehood ratio (LLR) corresponding to a bit position i is given by

$$y_i = \log\left(\frac{\Pr(r_i|x_i = 0)}{\Pr(r_i|x_i = 1)}\right).$$

Examples of memoryless channels include the Binary Symmetric channel (BSC), the Binary erasure channel (BEC), and the Additive White Gaussian channel (AWGNC). Examples of channels with memory include partial-response channels and other channels in magnetic recording that cause inter-symbol interference (ISI).

For this dissertation, we shall only focus on the BSC. The BSC is a binary-input binary-output memoryless channel and therefore the received vector $\mathbf{r}$ is also binary N-tuple. The channel flips a bit in the transmitted codeword with a *cross-over probability* of α. Fig. 1.1 shows an illustration of the BSC. A transmitted bit 0 is received as 0 with probability $1 - \alpha$ and as a 1 with probability α.

For the BSC, given a cross-over probability α,the LLR is determined from $\mathbf{r}$ as follows

$$y_i = \begin{cases} \log\left(\frac{1-\alpha}{\alpha}\right) & \text{if } r_i = 0 \\ \log\left(\frac{\alpha}{1-\alpha}\right) & \text{if } r_i = 1 \end{cases}$$

Note that by the definition above, y_i being positive implies that the corresponding codeword bit is more likely to be a zero, and y_i being negative implies the negative

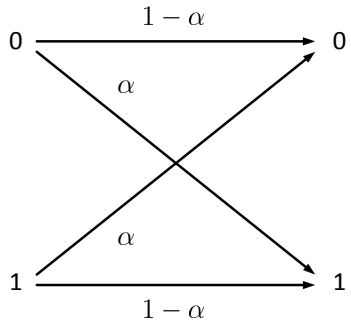

Figure 1.1: Illustration of the Binary Symmetric channel

corresponding codeword bit is more likely to be a one.

1.2.3 Tanner graph representation

LDPC codes are linear block codes that have sparse parity-check matrices. Any (N, K) linear block code $\mathcal{C}$ can be represented by a bipartite graph G, also known as the Tanner graph, which consists of two sets of nodes: the set of variable nodes $V = \{v_1, \cdots, v_N\}$ and the set of check nodes $C = \{c_1, \cdots, c_M\}$. Given the parity-check matrix $\mathbf{H}$ of a code $\mathcal{C}$, the Tanner graph is obtained by assigning a variable node corresponding to each codeword bit and a check node corresponding to each parity-check constraint, and then connecting variable nodes to certain check nodes based on the parity-check matrix. An edge connection between a particular variable node and a particular check node is made if the codeword bit associated with the variable node participates in the parity-check constraint associated with the check node. This is illustrated with the help of an example.

Example 1.1. *Consider the parity-check matrix of an* $(8, 4)$ *extended Hamming code with* $d_{min} = 4$*, which is given by*

$$\mathbf{H} = \begin{bmatrix} 1 & 0 & 1 & 0 & 1 & 0 & 1 & 0 \\ 0 & 1 & 1 & 0 & 0 & 1 & 1 & 0 \\ 0 & 0 & 0 & 1 & 1 & 1 & 1 & 0 \\ 1 & 1 & 1 & 1 & 1 & 1 & 1 & 1 \end{bmatrix}$$

In order to generate the Tanner graph, first observe that the graph must contain 8 variable nodes corresponding to the 8 columns, and 4 check nodes corresponding to the 4 parity-check constraints. Therefore $V = \{v_1, v_2, v_3, v_4, v_5, v_6, v_7, v_8\}$ *and* $C = \{c_1, c_2, c_3, c_4\}$*. By convention,* $\bigcirc$ *is used to depict a variable node, and* $\square$ *is used to depict a check node in the Tanner graph. Now looking at the first column in* $\mathbf{H}$*, there is a 1 in the first row and in the fourth row. Therefore,* v_1 *is connected to check nodes*

c_1 and c_4. Similarly, all other variable nodes are connected to the appropriate check nodes. Fig. 1.2 shows the resulting Tanner graph of the code.

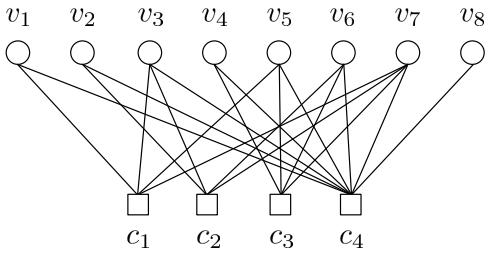

Figure 1.2: Tanner graph of the $(8, 4)$ extended Hamming code

The check nodes (variable nodes respectively) connected to a variable node (check node respectively) are referred to as its *neighbors*. The set of neighbors of a node v_i is denoted as $\mathcal{N}(v_i)$, and the set of neighbors of node c_j is denoted by $\mathcal{N}(c_j)$. The degree of a node is the number of its neighbors. Let $\mathbf{x} = (x_1, x_2, \ldots, x_N)$ be a vector such that x_i denotes the value of the codeword bit associated with the variable node v_i. We shall refer to this value as the *bit value* of node v_i. $\mathbf{x}$ is a codeword if and only if for each check node, the modulo two sum of the bit values of its neighbors is zero.

An LDPC code is to be *regular*, if in its corresponding Tanner graph G, all variable nodes have the same degree d_v, and all check nodes have the same degree d_c. A code is said to be a column-weight-d_v (or d_v-left-regular) code if all variable nodes have the same degree d_v, which is also referred to as *left degree*. A code is said to be *irregular* if there are variable nodes as well as check nodes that have different degrees. The (8,4) extended Hamming code provided above is an example of an irregular code.

The girth of the Tanner graph g is length of the shortest cycle present in the Tanner graph of the code. A cycle of length g is referred to as a g-cycle. For this dissertation, we will be mostly concerned with column-weight-three LDPC codes. Henceforth, for convenience, Tanner graphs shall be simply referred to as graphs.

1.2.4 Message-passing decoders

Message-passing (MP) decoders are a class of iterative decoders that operate on the graph of the code. The a posteriori probability of a codeword bit associated to each variable node in the graph is calculated by exchanging messages iteratively between the set of variable nodes and the set of check nodes along the edges of the graph. A major attraction with MP decoders is that all the computations are carried out locally at each node, and therefore an efficient decoder implementation can be realized.

Recall that $\mathbf{y} = (y_1, y_2, \ldots, y_N)$ is the input to the MP decoder. Let $\mathcal{Y}$ denote the alphabet of all possible channel values. Let $\mathcal{M}$ denote the alphabet of all possible

values that the messages can assume. Let $m^{(k)}(v_i, c_j)$ denote the message passed by a variable node $v_i \in V$ to its neighboring check node $c_j \in C$ in the k^{th} iteration and $m^{(k)}(c_j, v_i)$ denote the vice versa. Let $m^{(k)}(\mathcal{N}(v_i), v_i)$ denote the set of all incoming messages to variable node v_i and $m^{(k)}(\mathcal{N}(v_i)\backslash c_j, v_i)$ denote the set of all incoming messages to variable node v_i except from check node c_j. Let $m^{(k)}(\mathcal{N}(c_j)\backslash v_i, c_j)$ and $m^{(k)}(\mathcal{N}(c_j)\backslash v_i, c_j)$ be defined similarly.

Any MP decoder requires two update functions: Φ_v used for update at the variable nodes, and Φ_c used for check nodes. Both update functions are symmetric functions on the incoming messages, i.e., they remain unchanged by any permutation of its messages. Thus without abuse of notation, if the arguments of a function are written as a set, we imply that the order of these arguments is insignificant.

We now describe the MP decoding process. Initially, all the messages are set to zero, i.e., $m^{(0)}(\mathcal{N}(v_i), v_i) = 0 \ \ \forall v_i \in V$ and $m^{(0)}(\mathcal{N}(c_j), c_j) = 0 \ \ \forall c_j \in C$. Then for every iteration $k > 0$, messages are propagated in the following manner:

$$\begin{aligned} m^{(k)}(v_i, c_j) &= \Phi_v\left(y_i, m^{(k-1)}(\mathcal{N}(c_j)\backslash v_i, c_j)\right) \\ m^{(k)}(c_j, v_i) &= \Phi_c\left(m^{(k)}(\mathcal{N}(c_j)\backslash v_i, c_j)\right) \end{aligned}$$

An important feature of MP decoding that can be noted from the above is that during the update of messages at a particular node, the outgoing message from the node on an edge is determined as a function of all local messages incoming from its neighbors excluding the message incoming on that particular edge. We refer to such messages as *extrinsic incoming messages*. By doing so, the node is to an extent treating all its incoming messages as independent messages. This is the subtle difference between MP decoding and iterative bit-flipping decoding algorithms. Fig. 1.3 and 1.4 describes the update of the messages at a degree-three variable node and check node, respectively.

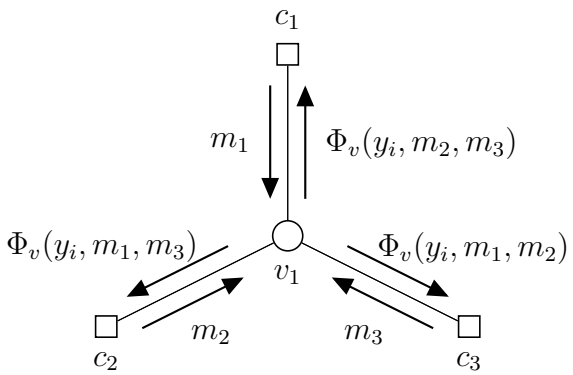

Figure 1.3: Update of the messages at a variable node.

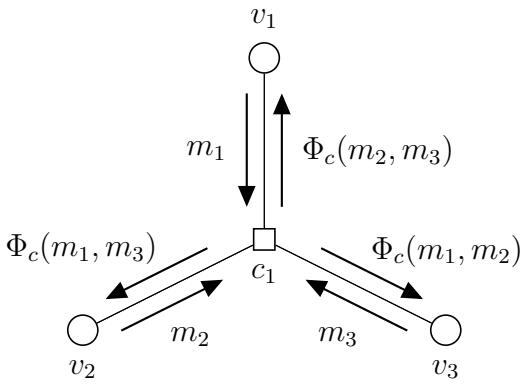

Figure 1.4: Update of the messages at a check node.

At the end of each iteration, a symmetric *decision function* Ψ, is used to decide the bit value of each node $v_i \in V$ based on its incoming messages. Let $\hat{\mathbf{x}}^{(k)} = (\hat{x}_1^{(k)}, \hat{x}_2^{(k)}, \ldots, \hat{x}_N^{(k)})$ denote the vector of bit values decided at the end of the k^{th} iteration. The bit value $\hat{x}_i^{(k)}$ of each node v_i is determined by

$$\hat{x}_i^{(k)} = \Psi\left(y_i, m^k(\mathcal{N}(v_i), v_i)\right).$$

The estimate $\hat{\mathbf{x}}^{(k)}$ is then verified to check whether it is a codeword or not. This is easily done by passing the decided bit values along the edges and verifying whether every check node is *satisfied* or not. A check node is satisfied if the modulo 2 sum of all the bit values of its neighbors is zero. If all check nodes are satisfied, then $\hat{\mathbf{x}}^{(k)}$ is a codeword and the decoding is terminated.

In conventional MP decoders, the decision function is either a simple majority rule (if messages are binary), or simply the sign of the sum of its arguments (if messages are log-likelihoods). More precisely, for a node v_i with degree d_v

$$\Psi(y_i, m^k(\mathcal{N}(v_i), v_i)) = \begin{cases} 1 & \text{if } \left(y_i + \sum m^{(k)}(\mathcal{N}(v_i), v_i)\right) > 0 \\ 0 & \text{if } \left(y_i + \sum m^{(k)}(\mathcal{N}(v_i), v_i)\right) < 0 \\ \text{sgn}(y_i) & \text{otherwise} \end{cases}$$

where the sgn function outputs a 0 if the sign of the argument is positive, and a 1 if it is negative.

The algorithm runs until either $\hat{\mathbf{x}}^{(k)}$ is a codeword, or until the maximum number of iterations is reached, whichever occurs first. We say that the decoder has *converged* if $\hat{\mathbf{x}}^{(k)}$ is a codeword for some k, else we say that the decoder has *failed*. A *success* is declared if the decoder converges to the right codeword, and a *miss-correction* is

declared if the decoder converges to a wrong codeword.

Note that during our general description of MP decoding, we inherently assumed that the scheduling used is a *flooding* scheduling, which involves updating all variable nodes simultaneously update followed by a simultaneous update of all check nodes. In contrast, a *serial* or layered scheduling could also be carried out for [36]. Discussions regarding scheduling are beyond the scope of this dissertation, and throughout we shall implicitly assume that the flooding scheduling is used for any MP decoder being described.

MP decoders can be broadly classified into two classes: hard decoding algorithms (where the messages assume binary values) such as the Gallager A and the Gallager B algorithms [1], and soft decoding algorithms (where the messages assume real values) which are conventionally based on the BP algorithm such as the sum-product algorithm and the min-sum algorithm [20]. We now discuss the BP algorithm in greater detail.

1.2.5 Belief propagation: Sum-Product and other low-complexity variants

All conventional MP algorithms used for decoding LDPC codes are based on the BP algorithm [37]. The BP has its roots in the broad class of Bayesian inference problems [38], and it is used to compute marginals of functions on a graphical model. Although exact inference in Bayesian belief networks is hard in general and inference using BP is exact only on loop-free graphs (trees), it provides surprisingly close approximations to exact marginals on loopy graphs.

The problem of decoding on the graph of the code is also a Bayesian inference problem, and therefore the BP algorithm is well-suited for this purpose. As a decoding algorithm for LDPC codes, the BP propagates probabilistic messages along the edges of the Tanner graph in an iterative fashion. BP can be implemented in two domains, namely the probabilistic domain where the messages are probabilities, and the LLR domain where messages are LLRs. We shall describe the BP algorithm in the LLR, domain which is more commonly used due to it being less sensitive to numerical precision issues. The BP algorithm is also known as the *Sum-Product* algorithm.

In the LLR domain, the messages and channel values are real-valued LLRs, i.e., $\mathcal{M} = \mathbb{R}$ and $\mathcal{Y} = \mathbb{R}$. The function $\Phi_v : \mathbb{R} \times \mathbb{R}^{d_v - 1} \to \mathbb{R}$ is the update function used at a variable node of degree d_v, and $\Phi_c : \mathbb{R}^{d_c - 1} \to \mathbb{R}$ is the update rule used at a check node with degree d_c.

Let $m_1, m_2, \ldots, m_{l-1}$ denote the $l-1$ extrinsic incoming messages of a node with degree l, which are used in the calculation of the outgoing message. The update rules

for the BP algorithm are given as follows:

$$\Phi_v(y_i, m_1, \ldots, m_{d_v-1}) = y_i + \sum_{j=1}^{d_v-1} m_j \tag{1.1}$$

$$\Phi_c(m_1, \ldots, m_{d_c-1}) = 2\tanh^{-1}\left(\prod_{j=1}^{d_c-1}\tanh\left(\frac{m_j}{2}\right)\right). \tag{1.2}$$

When the magnitudes of the messages reach a large value, the check node update function of the BP algorithm can be approximated to:

$$\Phi_c(m_1, \ldots, m_{d_c-1}) = \left(\prod_{j=1}^{d_c-1}\operatorname{sgn}(m_j)\right)\min_{j\in\{1,\ldots,d_c-1\}}(|m_j|) \tag{1.3}$$

where sgn denotes the standard sign function. The check node update function defined in Eq. (2.1) along with variable node update function defined in Eq. (1.1) together constitute the min-sum decoder. Thus, the min-sum is an approximation of BP decoding.

Clearly the min-sum decoder is much lower in complexity than the BP algorithm due to its simplified check node operation. However, the performance loss arising from using min-sum instead of BP is quite large. Hence, many low-complexity variants have been proposed which attempt to reduce this gap in performance. All of the variants proposed typically deal with simplifying the check node update function while keeping the variable node update function intact, as defined in Eq. (1.1).

One important low-complexity variant of BP that requires mentioning is the *offset min-sum* decoder proposed by Chen *et al.* [20]. For this algorithm, an offset factor γ is introduced into the check node update function. This offset factor serves to reduce the overstimate of the outgoing message produced by a check node using the rule in Eq. (2.1), especially when the magnitudes of the incoming messages are small. Therefore, the offset factor is also often referred to as a *correction factor*. The modified check node update function is as follows:

$$\Phi_c(m_1, \ldots, m_{d_c-1}) = \left(\prod_{j=1}^{d_c-1}\operatorname{sgn}(m_j)\right)\max\left(\min_{j\in\{1,\ldots,d_c-1\}}(|m_j|) - \gamma, 0\right). \tag{1.4}$$

The offset factor γ could be fixed or could be varied as a function of the SNR. Also the value for γ can be chosen using the density evolution technique for maximizing the decoding threshold as done in [20], or by a brute-force simulation on a given code that checks different values of γ and selects the one giving the best performance.

1.3 Error floor problem

For any typical finite-length LDPC code, the error-rate performance curve plotted as a function of SNR under iterative decoding, consists of two distinct regions: the waterfall region, and the error floor region. In the waterfall region (which is the low SNR region), the error-rate drops significantly with increase in SNR making the curve look like a waterfall. On the other hand, in the error floor region (which is the high SNR region), the decrease in the error-rate dramatically slows down and the curve tends to flatten out turning into an error floor. Fig. 1.5 illustrates the two regions on a typical FER performance curve of an LDPC code plotted as a function of the cross-over probability α of the BSC.

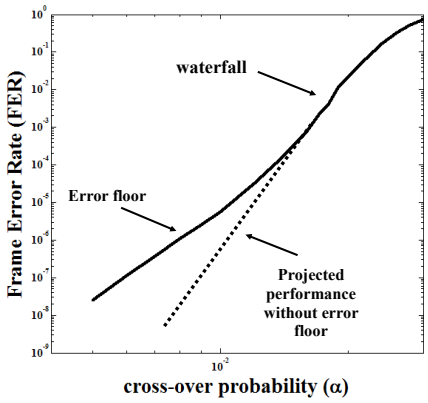

Figure 1.5: Typical performance of BP decoding on an LDPC code over the BSC

The error floor problem arises due to the suboptimality of BP decoding on loopy graphs. It can be troublesome for applications requiring very low target error-rates, and especially when high-rate codes are employed, which have relatively dense graphs. Although asymptotic techniques such as density evolution provide an accurate prediction of the FER performance in the early waterfall region, the point at which the error floor starts as well as its slope are greatly dependent on the particular structure of a code, and hence cannot be predicted by density evolution. Therefore, finite-length analysis techniques are required for the study of error floors. Besides, for codes with moderate to large lengths, the ability to predict error floors becomes even more critical as the error floor may be unreachable by Monte-Carlo simulations.

1.3.1 Prior work on error floor estimation

The first crucial observation on error floors was made by MacKay and Postol [39], who found that the minimum distance of an LDPC code did not necessarily play a dominant role in the error floor of a code. In their investigations with a Margulis

construction of an LDPC code for the AWGNC, they observed that it showed a high error floor in spite of its good minimum distance, and they attributed it to the presence of *near-codewords* in the graph. Another notion proposed in the spirit of finite-length analysis was the notion of *pseudocodewords* originally introduced by Wiberg [17], and later further developed by Frey *et al.* [40] and Forney *et al.* [41]. Pseudocodewords are essentially outputs of the decoder that are not necessarily codewords and stem from the different possible binary configurations of the computation tree. These works further motivated investigations into finite-length analysis of codes under iterative decoding with attempts to characterize the error floors for different channels.

For the BEC, the error floor could be well-characterized through the work of Di *et al.* [42], who introduced the notion of *stopping sets* which are purely combinatorial objects. Later Orlitsky *et al.* [43] provided asymptotic results on the stopping set distribution for different code ensembles.

However, a huge stride towards the understanding of the error floor problem in a general setting, was made through the pioneering work of Richardson [44], who showed that the problem is at least partially combinatorial in nature. Richardson introduced the notion of *trapping sets*, which are certain problematic loopy structures present in the graph of the code that cause the decoder to fail for certain low-noise configurations, and are a function of both the code and the decoding algorithm in operation. Using this notion, he proposed a semi-analytical method for estimating the error-rates of BP decoding on the AWGNC in the error floor by identifying the dominant trapping sets. Another approach based on statistical physics was also proposed for the AWGNC by Stepanov *et al.* [45] through the notion of *instantons*, which are certain low-noise configurations that swayed the decoding trajectory away from the correct codeword. Later, Chilappagari *et al.* [46] in line with Richardson's work, presented results on the error floor estimation for the BSC under Gallager B decoding. Another notion called *absorbing sets*, was proposed by Dolecek *et al.* [47], which are a special type of trapping sets that are purely combinatorial and stable under the bit-flipping algorithm, and this notion enabled them to perform a detailed analysis on array-based LDPC codes.

Many other works also subsequently emerged that further developed on the notion of pseudocodewords. Vontobel and Koetter introduced the concept of *graph covers* to explain failures of iterative decoding [49], and showed that pseudocodewords arising from graph covers are identical to pseudocodewords of the linear programming (LP) decoding [25] which constituted the vertices of the *fundamental polytope*. Later, Kelly and Sridhara [50] used graph covers to derive bounds on the minimum pseudocodeword weight in terms of girth and the minimum left-degree of the graph. The pseudocodeword analysis was also extended to the class LDPC-convolutional codes by Smarandache *et al.* [51]. However, pseudocodewords are purely topological in nature and do not take a particular decoding algorithm into account. Therefore, the notion of trapping sets is required for studying failures of a particular iterative decoder.

It is evident from previous discussions that the main utility behind the notion of trapping sets is in enabling the error floor estimation of a given code under a particular decoding algorithm. If the relevant topological structures corresponding to different trapping sets could be identified a priori and enumerated on the graph of a given code without the need for simulation, a reasonable estimate of the error floor could be obtained provided that each trapping set's contribution towards the error floor is known or determined.

Although it was shown by McGregor and Milenkovic [53] that performing an exhaustive search of all trapping sets in the graph of a given code is NP-hard, several good practical approaches have been proposed. Milenkovic *et al.* [54] examined the asymptotic trapping set distributions for both regular and irregular LDPC code ensembles. Cole *et al.* [55] proposed a method to estimate the error floor based on importance sampling, which is similar to Richardson's approach in [44]. Wang *et al.* proposed an efficient algorithm to exhaustively enumerate both trapping sets and stopping sets for codes with relatively short to moderate block lengths ($N \approx 500$). Abu-Surra *et al.* [56] proposed an efficient improved impulse method that could enumerate trapping sets by augmenting the Tanner graph with auxiliary variable nodes, and treating the problem as if it were searching for low-weight codewords. Although the method does not guarantee enumeration of all trapping sets, it is reasonably reliable and is applicable to any arbitrary graph. A method that uses the *branch-and-bound* approach to enumerate stopping sets in a given code was proposed by Rosnes and Ytrehus [57]. Karimi and Bannihasemi [58] recently proposed an algorithm which could efficiently enumerate the dominant trapping sets present in any arbitrary graph by recursively expanding the cycles present in the graph. More recently, Zhang and Siegel [59] proposed an efficient technique that expanded on the branch-and-bound approach by transforming the bounding step to an LP formulation, and which allowed a complete enumeration of trapping sets up to a certain size with reasonable computation time.

In spite of the fact that all the above works are useful for enumerating trapping sets in a given graph which aid in estimating the error floor, none of them directly address the issue of how to utilize the knowledge of trapping sets for constructing better codes or improving the decoding algorithms. For instance, it is highly non-trivial to determine which particular subgraphs (that correspond to certain trapping sets) should be avoided during the construction of codes in order to improve the error floor performance. Vasić *et al.* [60] proposed the *trapping set onotology*, which is a hierarchy of trapping sets that exploits the topological relations, and can be utilized for code construction or decoder design. We shall use this in our dissertation in the decoder design.

For the remainder of this section, we shall elaborate on some of the relevant notions used to characterize decoder failures, and describe the trapping set ontology.

1.3.2 Characterization of failures of iterative decoders

We begin by defining the notion of *trapping sets* and their related terminologies as originally provided by Richardson in [44]. Note that for purpose of exposition, we shall assume that the all-zero codeword was transmitted. This is a valid assumption as the MP decoders considered and the channel (BSC) are symmetric [19]. Recall that $\mathbf{y}$ is the decoder input, and $\hat{\mathbf{x}}^{(k)}$ is the estimate on the codeword bits after k iterations. Let I denote the maximum number of iterations allowed for decoding.

Definition 1.1. *A variable node v_i is said to be eventually correct if there exists a positive integer l such that for all $l \leq k \leq I$, $\hat{x}_i^{(k)} = 0$*

Definition 1.2. *For a decoder input $\mathbf{y}$, a trapping set $\mathbf{T}(\mathbf{y})$ is a non-empty set of variable nodes that are not eventually corrected by the decoder.*

The above definition is quite general as it includes all possible decoder failures such as stable fixed points as well as failures resulting from the oscillatory behavior of the decoder output among different states constituting a basin of attraction. Note that if $\mathbf{T}(\mathbf{y}) = \emptyset$, then the decoding is successful on input $\mathbf{y}$.

A trapping set (TS) $\mathbf{T}(\mathbf{y})$ is said to be an (a, b) TS, if it has a variable nodes, and b odd-degree check nodes in the subgraph induced by $\mathbf{T}(\mathbf{y})$. For convenience, we shall use the notation $\mathcal{T}(a, b)$ to denote the topological structure associated with an (a, b) TS, which is simply a graph consisting of a variable nodes and b odd-degree check nodes. Note that two trapping sets can share the same parameters (a, b) but have different underlying topologies.

If the degree of a check node is at most two in the graph, then the TS is said to be an *elementary* TS. It has been observed by many researchers that the dominant trapping sets in the error floor are typically elementary trapping sets [44, 52]. Therefore, we shall place more focus on elementary trapping sets during our discussions. Fig. 1.6 shows an example of a subgraph corresponding to an elementary $(5, 3)$ TS. Note that ■ is used to denote an odd-degree check node, and will be used throughout this dissertation for any future graphical illustrations.

Note that non-zero codewords (under the all-zero codeword assumption) are $(a, 0)$ trapping sets whose corresponding graphs have only even-degree check nodes. These are precisely the only trapping sets under ML decoding. However, for any sub-optimal iterative decoder, there will be other (a, b) TSs.

Stopping sets [42] are a sub-class of trapping sets that were introduced to characterize failures on the BEC. Note that for the BEC, a transmitted bit is either received correctly or is erased. Let S denote a subset of variable nodes and let $\mathcal{N}(S)$ denote the set of neighbors $\{\mathcal{N}(v_i) : \forall v_i \in S\}$. The definition is given below.

Definition 1.3. *A stopping set is a subset of variable nodes S in the graph G, such that every neighbor in $\mathcal{N}(S)$ is connected to subset S at least twice.*

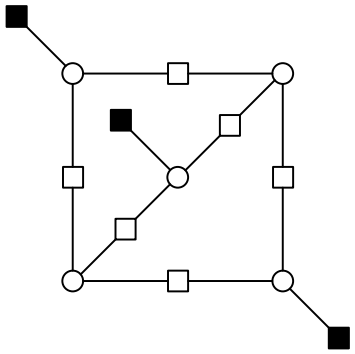

Figure 1.6: Subgraph corresponding to a $(5, 3)$ TS

The above definition implies that stopping sets are (a, b) TSs whose corresponding graphs do not contain any degree-one check node. For the BEC, iterative decoding fails if all a variable nodes of an (a, b) stopping set are erased, regardless of its neighborhood in the original graph G and the number of iterations allowed. Therefore, stopping sets can be treated as purely combinatorial objects, and the error floor can be completely characterized for the BEC under iterative decoding. Fig. 1.7 shows an example of an $(8, 2)$ stopping set whose corresponding graph contains two degree-3 check nodes.

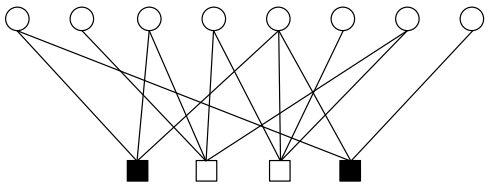

Figure 1.7: Subgraph corresponding to a $(8, 2)$ stopping set

An *absorbing set* [47] is a special type of (a, b) TS that is stable under the bit-flipping decoding. For a given subset S of variable nodes, let $\mathcal{E}(S)$ (resp. $\mathcal{O}(S)$) denote the set of neighboring checks of S that are even-degree (resp. odd-degree).

Definition 1.4. *An absorbing set is a subset of variable nodes S in the graph G, such that each variable node in S has strictly greater neighbors in $\mathcal{E}(S)$ than in $\mathcal{O}(S)$. In addition, if all remaining variable nodes in $V \setminus S$ also have strictly greater neighbors in $\mathcal{E}(S)$ than in $\mathcal{O}(S)$, then it is said to be a fully absorbing set.*

Another closely related type of trapping set is a *fixed set* that was introduced by Chilappagari and Vasić [48] to characterize failures of Gallager A/B decoding on the BSC. It is defined as follows.

Definition 1.5. *For a received vector $\mathbf{r}$ from the BSC and decoder input $\mathbf{y}$, a trapping set $\mathbf{T}(\mathbf{y})$ is said to be a fixed set, if $\mathbf{T}(\mathbf{y}) = \mathrm{supp}(\mathbf{y})$.*

The necessary and sufficient conditions for a set of variable nodes to form a fixed set for the Gallager A/B algorithm is provided through the following theorem [48].

Theorem 1.1. *Let $\mathcal{C}$ be an LDPC code with d_v-left-regular graph G. Let $\mathbf{T}$ be a subset of a variable nodes with induced subgraph $\mathcal{T}$. Let the checks in $\mathcal{T}$ be partitioned into two disjoint subsets; $\mathcal{O}$ consisting of checks with odd degree and $\mathcal{E}$ consisting of checks with even degree. Then $\mathcal{T}$ is a fixed set for the Gallager A/B algorithm iff : (a) Every variable node in $\mathcal{I}$ has at least $\lceil \frac{d_v}{2} \rceil$ neighbors in $\mathcal{E}$ and (b) No $\lfloor \frac{d_v}{2} \rfloor$ of $\mathcal{O}$ share a neighbor outside $\mathcal{I}$.*

Note that the definition of absorbing set satisfies the above theorem and therefore is always a fixed set; however the opposite is not necessarily true. For column-weight-three codes though, they are the same. For this dissertation, we shall mainly utilize the notion of trapping sets to characterize decoder failures.The notion of fixed set will be used only mainly for discussing the trapping set ontology which will be introduced shortly.

Given an (a, b) TS, it is also important to determine a measure of relative *harmfulness* of the TS which is based on its underlying topological structure. Again for the BSC under the Gallager B decoding, Chilappagari and Vasic [46] introduced the notion of *critical number* as a measure of harmfulness. Given the subgraph corresponding to a TS is $\mathcal{T}(a, b)$, let $\mathbf{y}_\mathcal{T}$ denote the vector of channel values received by the variable nodes in $\mathcal{T}(a, b)$. Let $\mathbf{T}(\mathbf{y}_\mathcal{T})$ denote the set of nodes that failed to converge to the right values.

Definition 1.6. *The critical number n_c of a trapping set whose subgraph is $\mathcal{T}(a, b)$, is the minimum number of errors introduced in the subgraph $\mathcal{T}(a, b)$ that causes the Gallager-B decoder. More precisely,*

$$n_c = \min_{\mathbf{T}(\mathbf{y}_\mathcal{T}) \neq \emptyset} |\mathrm{supp}(\mathbf{y}_\mathcal{T})|.$$

Note that the dominant trapping sets are the subgraphs with the least critical number. Although this notion is limited to Gallager-B decoding, later on, we will generalize this notion to include other decoding algorithms as well.

Henceforth, for convenience, whenever we refer to a TS, we shall implicitly refer to its underlying topological structure, which is a subgraph induced by the variable nodes belonging to the TS.

1.3.3 Trapping set ontology

The trapping set ontology (TSO) [60] is a database of trapping sets that is organized as a hierarchy based on their topological relations. This topological relationship between trapping sets is specified in the form of a *parent-child* relationship. A trapping set $\mathcal{T}_1$

is said to be a *parent* of a trapping set $\mathcal{T}_2$ if $\mathcal{T}_2$ contains $\mathcal{T}_1$, and $\mathcal{T}_2$ is then considered to be a *child* of $\mathcal{T}_1$. The main objective for using the TSO is to make the identification of relevant trapping sets independent of a given code, as well as to serve as a guide for code construction or decoder design in addition to enabling efficient enumeration techniques.

The development of TSO was primarily motivated by the work of Chilappagari *et al.* in [61], who observed that the trapping sets found for various iterative decoders over different channels are closely related. For instance on a given code, many trapping sets found for the BP decoding over the AWGN were either the same as the trapping sets of Gallager B over BSC, or bigger subgraphs containing them. This implies that there exists a topological interrelation among trapping sets and in a broader sense, a topological interrelation among error patterns that cause decoding failures for various algorithms on different channels. Relying on this fact, the TSO is generated based on the notion of fixed sets for Gallager B, with the purpose of capturing these topological relations in order to provide a hierarchy.

Since the necessary and sufficient conditions for a fixed set of Gallager B are clearly defined through Theorem 1.1, this notion is used to generate the TSO. Also it is well-known that, in general, trapping sets are subgraphs formed by cycles or union of cycles [44]. Therefore, assuming that any code considered has at least girth g and left degree d_v, the TSO is generated as follows. Starting with a g-cycle, variable nodes of d_v degree are added to the g-cycle in all possible ways thereby expanding the g-cycle to a chosen maximum size, while enforcing the constraint that the resulting subgraph after each addition of a variable node, is elementary and satisfies Theorem 1.1. Once all different expanded subgraphs are generated, a hierarchy is then established based on their parent-child relationship. The procedure is then repeated starting with a $(g+2)$-cycle, and so on.

Note that although the methodology is restricted by using Theorem 1.1 for fixed sets, it can be easily generalized for generating other types of subgraphs, provided that the constraints or desired properties of the subgraph are clearly specified. Moreover, as previously pointed out, since failures of other iterative decoders over channels other than BSC are also topologically linked to failures of Gallager B decoding on the BSC, we regard the subgraphs in the TSO as a good starting point for consideration in decoder design or code construction.

Chapter 2

Finite Alphabet Iterative Decoders: Selection and Design

THE goal of this chapter is to introduce the new class of finite precision iterative decoders on the BSC, which we refer to as *Finite Alphabet Iterative Decoders* (FAIDs), and which are able to surpass the BP in the error floor region at a very low-complexity. We then propose two selection methods based on two approaches for column-weight-three codes. The first approach is code dependent, and deals with the FAID selection on minimal codewords of a given code which are seen as larger attractors than the sole trapping sets. The second approach provides a methodology to select candidate FAIDs that are potentially good in the error floor without considering any specific code. This approach relies on the introduction of three essential concepts, namely the noisy critical numbers, the noisy trapping sets, and the decoder domination. Finally, this chapter addresses also the design of FAID for column-weight-four codes, providing good performing 3-bit FAID derived from the extraction of harmful structures on the given code.

2.1 Preliminaries

Let G denote the Tanner graph of an (N, K) binary LDPC code $\mathcal{C}$ of rate $R = K/N$, which consists of the set of variable nodes $V = \{v_1, \cdots, v_N\}$ and the set of check nodes $C = \{c_1, \cdots, c_M\}$. The degree of a node in G is the number of its neighbors in G. A code $\mathcal{C}$ is said to have a regular column-weight d_v if all variable nodes in V have the same degree d_v. The set of neighbors of a node v_i is denoted as $\mathcal{N}(v_i)$, and the set of neighbors of node c_j is denoted by $\mathcal{N}(c_j)$. The girth of G is the length of shortest cycle present in G.

Let $\mathbf{x} = (x_1, x_2, \ldots, x_N)$ denote a codeword of $\mathcal{C}$ that is transmitted over the BSC, where x_i denotes the value of the bit associated with variable node v_i, and let the vector

received from the BSC be $\mathbf{r} = \{r_1, r_2, \ldots, r_N\}$. Let $\mathbf{e} = (e_1, e_2, \ldots, e_N)$ denote the *error pattern* introduced by the BSC such that $\mathbf{r} = \mathbf{x} \oplus \mathbf{e}$, and $\oplus$ is the modulo-two sum. The support of an error vector $\mathbf{e} = (e_1, e_2, \ldots, e_N)$, denoted by $\text{supp}(\mathbf{e})$, is defined as the set of all positions i such that $e_i \neq 0$. Let $\mathbf{y} = (y_1, y_2, \ldots, y_N)$ be the input to the decoder, where each y_i is calculated based on the received value r_i. We shall also refer to the values y_i as *channel values*. During the analysis of decoders, we shall assume that the all-zero codeword was transmitted. This is a valid assumption since the decoders we consider are symmetric [19].

We remind that a trapping set (TS) denoted by $\mathbf{T}(\mathbf{y})$ (as originally defined in [44]) is a non-empty set of variable nodes that are not eventually corrected for a given decoder input $\mathbf{y}$. If $\mathbf{T}(\mathbf{y})$ is empty, then the decoding is successful. Note that $\mathbf{T}(\mathbf{y})$ will depend on the number of decoding iterations. A common notation used to denote a TS is (a, b), where $a = |\mathbf{T}(\mathbf{y})|$, and b is the number of odd-degree check nodes in the subgraph induced by $\mathbf{T}(\mathbf{y})$.

Let $\mathcal{T}(a, b)$ denote the topology associated with a (a, b) TS, which is a graph consisting of a variable nodes and b odd-degree check nodes. This standard notation is however not sufficient to describe in details the topologies which are the supports of the TS's. In particular, there could be several different topologies which have the same values a and b. To circumvent this problem, we extend the notation of TS by adding to the first two parameters, an additional topological information which allows to distinguish between different structures with the same a and b. We propose the following notation:

$$\mathcal{T}(a, b)\ n_{c_3} - n_{c_4} - n_{c_5} - n_{c_6} - n_{c_7} - n_{c_8}$$

where n_{c_k} represents the number of cycles containing k variable nodes. For example the Fig. 2.1 shows the two different topologies for a $(6, 4)$ TS (considering girth-eight, and TS for column-weight-three codes) which differs only in the cycles contained in these two structures. In this figure, ● denotes a variable node, □ denotes a degree-two check node and ■ denotes a degree-one check node.

A TS is said to be elementary if $\mathcal{T}$ contains only degree-one or/and degree-two check nodes. Throughout this chapter, we restrict our focus to elementary TS's, since they are known to be dominant in the error floor [44, 46]. Also, whenever we refer to a TS, we will implicitly refer to its topological structure $\mathcal{T}$.

2.2 Finite alphabet iterative decoders

We now introduce a new type of finite precision decoders which we refer to as FAIDs [63, 64]. An N_s-level FAID denoted by D is defined as a 4-tuple given by $\mathrm{D} = (\mathcal{M}, \mathcal{Y}, \Phi_v, \Phi_c)$. The finite alphabet $\mathcal{M}$ defined as
$\mathcal{M} = \{-L_s, \ldots, -L_2, -L_1, 0, L_1, L_2, \ldots, L_s\}$, where $L_i \in \mathbb{R}^+$ and $L_i > L_j$ for any $i > j$, consists of $N_s = 2s + 1$ levels for which the message values are confined to.

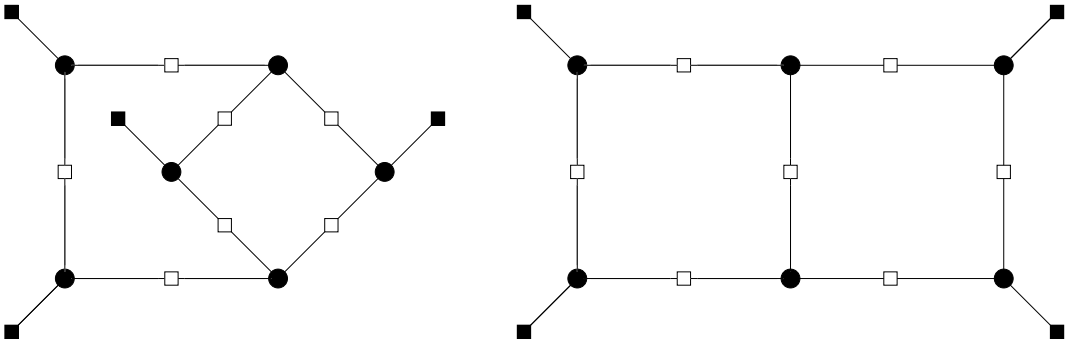

(a) $\mathcal{T}(6,4)$ $0-2-0-1-0-0-0-0$. (b) $\mathcal{T}(6,4)$ $0-1-2-0-0-0-0-0$.

Figure 2.1: The two different structures for a $(6,4)$ TS.

The sign of a message $x \in \mathcal{M}$ can be interpreted as the estimate of the bit associated with the variable node for which x is being passed to or from (positive for zero and negative for one), and the magnitude $|x|$ as a measure of how reliable this value is.

The set $\mathcal{Y}$ denotes the set of all possible channel values. For FAIDs over the BSC, $\mathcal{Y}$ is defined as $\mathcal{Y} = \{\pm \mathrm{C}\}$, where $\mathrm{C} \in \mathbb{R}^+$, and the value $y_i \in \mathcal{Y}$ for node v_i is determined by $y_i = (-1)^{r_i}\mathrm{C}$, i.e., we use the mapping $0 \rightarrow \mathrm{C}$ and $1 \rightarrow -\mathrm{C}$. Note that for the BP and min-sum algorithms (where the messages are log-likelihoods), the decoder input $\mathbf{y}$ is a real-valued vector ($\mathcal{Y} = \mathbb{R}$). Let $m_1, \cdots, m_{l-1}$ denote the extrinsic incoming messages to a node with degree l.

2.2.1 Definitions of the update functions Φ_v and Φ_c

The function $\Phi_c : \mathcal{M}^{d_c-1} \rightarrow \mathcal{M}$ used for update at a check node with degree d_c is defined as

$$\Phi_c(m_1, \ldots, m_{d_c-1}) = \left(\prod_{j=1}^{d_c-1} \mathrm{sgn}(m_j) \right) \min_{j \in \{1,\ldots,d_c-1\}} (|m_j|). \tag{2.1}$$

Note that this is the same function used in the min-sum decoder, and hence the novelty in the proposed decoders lies in the definition of the variable node update function Φ_v.

The function $\Phi_v : \mathcal{Y} \times \mathcal{M}^{d_v-1} \rightarrow \mathcal{M}$ is the update function used at a variable node with degree d_v, and is defined in closed form as

$$\Phi_v(y_i, m_1, m_2, \cdots, m_{d_v-1}) = Q\left(\sum_{j=1}^{d_v-1} m_j + \omega_i \cdot y_i \right) \tag{2.2}$$

where the function $Q(.)$ is defined below based on a threshold set $\mathscr{T} = \{T_i : 1 \leq i \leq$

$s+1\}$ with $T_i \in \mathbb{R}^+$ and $T_i > T_j$ if $i > j$, and $T_{s+1} = \infty$.

$$Q(x) = \begin{cases} \text{sgn}(x)L_i, & \text{if } T_i \leq |x| < T_{i+1} \\ 0, & \text{otherwise} \end{cases}$$

The weight ω_i is computed using a symmetric function $\Omega : \mathcal{M}^{d_v-1} \rightarrow \{0,1\}$. Based on this definition, the function Φ_v can be classified as a linear-threshold (LT) function or a non-linear-threshold (NLT) function. If $\Omega = 1$ (or constant), i.e., if the value of ω_i is always 1 (or constant) for all possible inputs of Ω, then Φ_v is an LT function and a FAID with such a Φ_v is classified as an LT FAID. Else, Φ_v is an NLT function and a FAID with such a Φ_v is an NLT FAID.

Note that for an LT FAID, Φ_v takes a linear combination of its arguments and then applies the function Q to determine its output. Therefore, Φ_v will always output the same value for any possible set of incoming messages for a given y_i, if their sum remains the same. For example, for a node with $d_v = 3$, $\Phi_v(-\text{C}, m_1, m_2) = \Phi_v(-\text{C}, m_3, m_4)$ when $m_1 + m_2 = m_3 + m_4$. This is also a typical property present in existing quantized decoders such as quantized BP and min-sum.

On the other hand, for an NLT FAID, Φ_v takes a non-linear combination of its arguments (due to Ω) before applying the function Q on the result. Therefore, Φ_v can output different values even for distinct sets of incoming messages that have the same sum. For instance, consider a map Φ_v for a node with $d_v = 3$ such that $\Phi_v(-\text{C}, -L_3, L_3) = 0$ and $\Phi_v(-\text{C}, -L_2, L_2) = -L_1$. In this case, the two distinct sets of incoming messages are $\{-L_3, L_3\}$ and $\{-L_2, L_2\}$, and the sums are zero for both the sets. However, Φ_v still gives different outputs for each of the sets namely, 0 and $-L_1$ respectively. Hence these decoders are different from existing quantized message-passing decoders. Note that the function Φ_v satisfies the following two properties.

Definition 2.1 (Symmetry property)**.** *A FAID is a symmetric decoder if its update function Φ_v satisfies $\Phi_v(y_i, m_1, ..., m_{d_v-1}) = -\Phi_v(-y_i, -m_1, ..., -m_{d_v-1})$.*

Definition 2.2 (Lexicographic ordering)**.** *A FAID is said to be lexicographically ordered if Φ_v satisfies $\Phi_v(-\text{C}, m_1, \ldots, m_{d_v-1}) \geq \Phi_v(-\text{C}, m'_1, \ldots, m'_{d_v-1})$ $\forall m_i \geq m'_i$, $i \in \{1, \ldots, d_v - 1\}$.*

The property of *lexicographic ordering* ensures that for a given channel value, the output is always non-decreasing with increase in the values of incoming messages. For instance, a map Φ_v where $\Phi_v(-\text{C}, L_1, L_2) = L_2$ and $\Phi_v(-\text{C}, L_2, L_2) = L_1$ is forbidden, since $\Phi_v(-\text{C}, L_2, L_2) \geq \Phi_v(-\text{C}, L_1, L_2)$. This is a typical property also present in existing message-passing decoders.

The decision rule used in FAIDs at the end of each iteration, to determine the bit value corresponding to each node v_i, is simply the sign of the sum of all incoming messages plus the channel value y_i (positive implies zero and negative implies one).

It is evident from the definition that Φ_v can be uniquely described either by assigning real values to the elements of $\mathcal{M}$, $\mathscr{T}$ and $\mathcal{Y}$, and defining Ω, or by providing a set of constraints which the assigned values can take. As examples, we provide the closed-form description of Φ_v for a 5-level NLT FAID and a 7-level LT FAID defined for column-weight-three codes.

Example 2.1 (5-level NLT FAID)**.** *The constraints on the values assigned to elements of $\mathcal{M}$ and $\mathscr{T}$ that describe this map are: $\mathrm{C} = L_1$, $L_2 = 3L_1$, $T_1 = L_1$, $T_2 = L_2$, and the function Ω is given by $\omega_i = \Omega(m_1, m_2) = 1 - \big(\mathrm{sgn}(m_1) \oplus \mathrm{sgn}(m_2)\big) \cdot \delta(|m_1| + |m_2| - 2L_2)$.*

Example 2.2 (7-level LT FAID)**.** *The constraints on the values assigned to elements of $\mathcal{M}$ and $\mathscr{T}$ that describe this map are: $L_1 < \mathrm{C} < 2L_1$, $L_2 = 2L_1$, $L_3 = 2L_2 + \mathrm{C}$, and $T_1 = L_1$, $T_2 = L_2$, and $T_3 = L_3 - C$, where $\Omega = 1$ since it is an LT function.*

Note in Ex. 2.1, $\mathrm{sgn}(x) = 1$ if $x < 0$, and $\mathrm{sgn}(x) = 0$ otherwise. Also note that although the rule defined in Ex. 2.2 appears to be similar to a quantized min-sum decoder, the messages in this decoder are not quantized probabilities or log-likelihoods.

2.2.2 Describing the maps of Φ_v as arrays

Let us alternatively define $\mathcal{M}$ to be $\mathcal{M} = \{M_1, M_2, \cdots, M_{N_s}\}$ where $M_1 = -L_s$, $M_2 = -L_{s-1}$,$\cdots$, $M_s = -L_1$, $M_{s+1} = 0$, $M_{s+2} = L_2$,$\cdots$, $M_{N_s} = L_s$. Then, Φ_v can be defined using d_{v-1}-dimensional arrays or look-up tables (LUTs) rather than as closed-form functions, which enables simple implementations and also may be more convenient for decoder selection.

For column-weight-three codes, the map specifying Φ_v is a simple two-dimensional array defined by $[l_{i,j}]_{1 \le i \le N_s, 1 \le j \le N_s}$, where $l_{i,j} \in \mathcal{M}$, such that $\Phi_v(-\mathrm{C}, M_i, M_j) = l_{i,j}$ for any $M_i, M_j \in \mathcal{M}$. The values for $\Phi_v(\mathrm{C}, M_i, M_j)$ can be deduced from the symmetry of Φ_v. Table 2.1 shows an example of a Φ_v defined as an array for a 7-level FAID when $y_i = -\mathrm{C}$, that have been identified as a NLT FAID.

Fig. 2.2 shows the error-rate performances of the 5-level NLT and 7-level LT FAIDs defined in the two examples, and the 7-level NLT FAID defined by the Table 2.1, along with the floating-point BP and min-sum decoders on the well-known $(155, 64)$ Tanner code. All decoders were run for a maximum of 100 iterations. From the plot, we see that all the FAIDs significantly outperform the floating-point BP and min-sum on the code. We will provide in the sequel of this chapter the methodology used to identify good FAIDs. We also provide in the Table 2.2 and 2.3 the arrays corresponding to the Example 2.1 and 2.2, respectively.

Table 2.1: LUT for Φ_v of a 7-level FAID with $y_i = -\mathrm{C}$ (NLT FAID).

$\boldsymbol{m_1/m_2}$	$\boldsymbol{-L_3}$	$\boldsymbol{-L_2}$	$\boldsymbol{-L_1}$	$\boldsymbol{0}$	$\boldsymbol{+L_1}$	$\boldsymbol{+L_2}$	$\boldsymbol{+L_3}$
$\boldsymbol{-L_3}$	$-L_3$	$-L_3$	$-L_3$	$-L_3$	$-L_3$	$-L_3$	$-L_1$
$\boldsymbol{-L_2}$	$-L_3$	$-L_3$	$-L_3$	$-L_3$	$-L_2$	$-L_1$	$+L_1$
$\boldsymbol{-L_1}$	$-L_3$	$-L_3$	$-L_2$	$-L_2$	$-L_1$	$-L_1$	$+L_1$
$\boldsymbol{0}$	$-L_3$	$-L_3$	$-L_2$	$-L_1$	0	0	$+L_1$
$\boldsymbol{+L_1}$	$-L_3$	$-L_2$	$-L_1$	0	0	$+L_1$	$+L_2$
$\boldsymbol{+L_2}$	$-L_3$	$-L_1$	$-L_1$	0	$+L_1$	$+L_1$	$+L_3$
$\boldsymbol{+L_3}$	$-L_1$	$+L_1$	$+L_1$	$+L_1$	$+L_2$	$+L_3$	$+L_3$

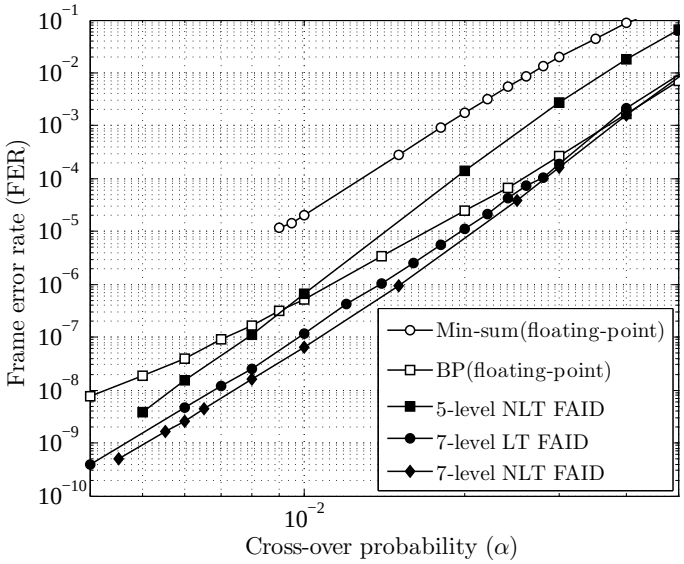

Figure 2.2: Performance comparisons between the floating-point decoders: BP and min-sum , and the 3-bit precision decoders: 5-level NLT, 7-level LT, and 7-level NLT FAIDs on the $(155, 64)$ Tanner code.

Table 2.2: LUT for Φ_v of a 5-level FAID with $y_i = -\mathrm{C}$ (NLT FAID).

$\boldsymbol{m_1/m_2}$	$\boldsymbol{-L_2}$	$\boldsymbol{-L_1}$	$\boldsymbol{0}$	$\boldsymbol{+L_1}$	$\boldsymbol{+L_2}$
$\boldsymbol{-L_2}$	$-L_2$	$-L_2$	$-L_2$	$-L_2$	0
$\boldsymbol{-L_1}$	$-L_2$	$-L_2$	$-L_1$	$-L_1$	$+L_1$
$\boldsymbol{0}$	$-L_2$	$-L_1$	$-L_1$	0	$+L_1$
$\boldsymbol{+L_1}$	$-L_2$	$-L_1$	0	$+L_1$	$+L_2$
$\boldsymbol{+L_2}$	0	$+L_1$	$+L_1$	$+L_2$	$+L_2$

Table 2.3: LUT for Φ_v of a 7-level FAID with $y_i = -\mathrm{C}$ (LT FAID).

$\boldsymbol{m_1/m_2}$	$\boldsymbol{-L_3}$	$\boldsymbol{-L_2}$	$\boldsymbol{-L_1}$	$\boldsymbol{0}$	$\boldsymbol{+L_1}$	$\boldsymbol{+L_2}$	$\boldsymbol{+L_3}$
$\boldsymbol{-L_3}$	$-L_3$	$-L_3$	$-L_3$	$-L_3$	$-L_3$	$-L_3$	0
$\boldsymbol{-L_2}$	$-L_3$	$-L_3$	$-L_3$	$-L_2$	$-L_2$	$-L_1$	L_1
$\boldsymbol{-L_1}$	$-L_3$	$-L_3$	$-L_2$	$-L_2$	$-L_1$	0	L_2
0	$-L_3$	$-L_2$	$-L_2$	$-L_1$	0	L_1	L_2
$\boldsymbol{L_1}$	$-L_3$	$-L_2$	$-L_1$	0	0	L_1	L_2
$\boldsymbol{L_2}$	$-L_3$	$-L_1$	0	L_1	L_1	L_2	L_3
$\boldsymbol{L_3}$	0	L_1	L_2	L_2	L_2	L_3	L_3

Note that a particular choice of $[l_{i,j}]_{1\leq i\leq N_s, 1\leq j\leq N_s}$ gives rise to a particular Φ_v, and the choice must ensure that both properties of Φ_v are satisfied. A natural question that arises at this point is how many FAIDs exist for a given N_s. This can be easily enumerated by establishing a connection between FAIDs and symmetric plane partitions.

2.2.3 Symmetric plane partition representation of Φ_v

A symmetric plane partition π is an array of nonnegative integers $(\pi_{i,j})_{i\geq 1, j\geq 1}$ such that $\pi_{i,j} \geq \pi_{i+1,j}$, $\pi_{i,j} \geq \pi_{i,j+1}$ $\forall i, j \geq 1$, and $\pi_{i,j} = \pi_{j,i}$. If $\pi_{i,j} = 0$ $\forall i > r$, $\forall j > s$, and $\pi_{i,j} \leq t$ $\forall i, j$, then the plane partition is said to be *contained* in a box with side lengths (r, s, t). The value $\pi_{i,j}$ is represented as a box of height $\pi_{i,j}$ positioned at (i, j) coordinate on a horizontal plane.

Due to the imposition of the lexicographic ordering and symmetry of Φ_v, there exists a bijection between the array $[l_{i,j}]_{1\leq i\leq N_s, 1\leq j\leq N_s}$ and a symmetric plane partition contained in a $(N_s \times N_s \times N_s - 1)$ box, where each $\pi_{i,j}$ is determined based on $l_{i,j}$. Fig. 2.3 shows the visualization of a plane partition corresponding to Φ_v of the 7-level FAID defined in Table 2.1. Kuperberg in [65] gave an elegant formula for the enumeration of symmetric plane partitions contained in a box, and we can directly utilize this for the enumeration of N_s-level FAIDs as well.

Theorem 2.1 (Number of N_s-level FAID)**.** *The total number $K_A(N_s)$ of symmetric lexicographically ordered N_s-level FAIDs is given by*

$$K_A(N_s) = \frac{H_2(3N_s)H_1(N_s)H_2(N_s-1)}{H_2(2N_s+1)H_1(2N_s-1)}$$

where $H_k(n) = (n-k)!\,(n-2k)!\,(n-3k)!\ldots$ is the staggered hyperfactorial function.

Proof. The proof of the theorem follows from the bijection between the map Φ_v of a FAID and a symmetric boxed plane partition. □

The total number of FAIDs for $N_s = 5$ and $N_s = 7$ levels are 28,314 and 530,803,988 respectively. However for $N_s = 7$, we have identified *only* 6,392,620 FAIDs with a practical interest, the discarded ones having a very poor density evolution threshold.

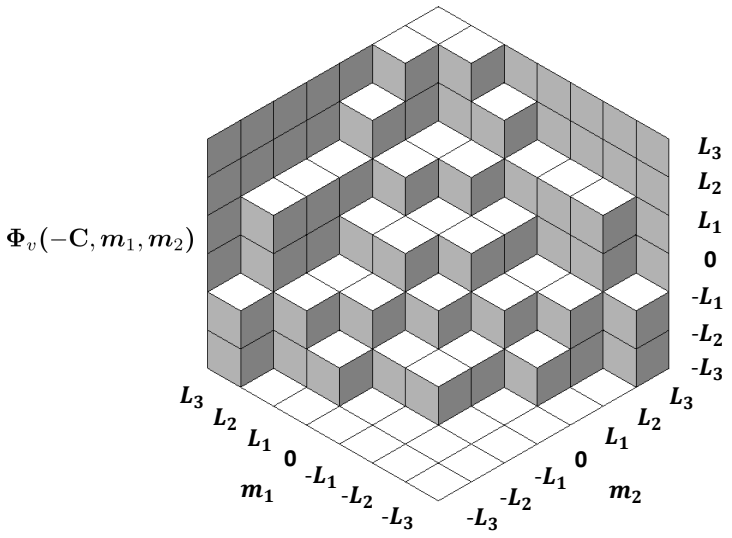

Figure 2.3: A visualization of the plane partition as stacked boxes for the 7-level FAID whose Φ_v is described in Table 2.1.

2.3 Selection of finite alphabet iterative decoders

It is evident from the previous section that identifying particularly good FAIDs from the set of all possible FAIDs is highly non-trivial since the number of such FAIDs is very large. As a first attempt of selection, one can think to rely on the computation of the density evolution (DE) to determine the decoding threshold (α^*) of each FAIDs. In Fig. 2.4 we present the performance comparison on the Tanner code between the floating-point BP, the 5-level FAID (Table 2.1), the 7-level FAID (Table 2.3), and the 5-level and 7-level FAIDs which have the best DE thresholds among all their peers. It is clearly evident that these last ones are not the best decoders, in fact they are presenting a pretty high error-floor. The DE threshold have been computed on the class of ($d_v = 3$,$d_c = 5$) LDPC codes, class which includes the Tanner code. The thresholds of the different FAIDs are given as follows: 5-level FAID of the Table 2.1: $\alpha^* = 0.09781$, 7-level FAID of Table 2.3: $\alpha^* = 0.010155$, best threshold 5-level FAID: $\alpha^* = 0.10319$ and best threshold 7-level FAID: $\alpha^* = 0.010349$. We can then conclude, that the selection of FAIDs only based on the DE threshold is not efficient, hence the need of other techniques, presented in the sequel of this section.

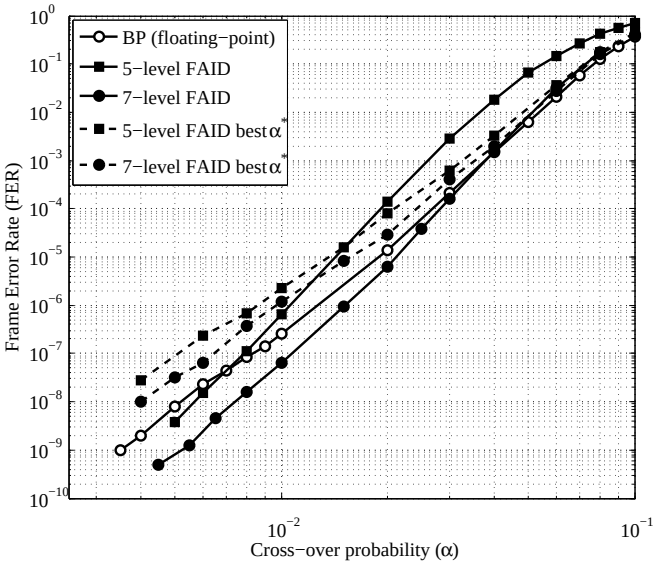

Figure 2.4: Performance comparisons between the floating-point BP, the 5-level FAID from the Table 2.1, the 7-level FAID from the Table 2.3, and 5-level and 7-level FAID exhibiting the best DE thresholds α^*.

We now describe a general approach that can be used to identify a subset of candidate N_s-level FAIDs, one or several of which are potentially good for any column-weight-three code. Our main aim behind this approach is to restrict the choice of FAIDs to a possibly small subset containing good candidates. Given a particular code, it would then be feasible to identify the best performing FAID from this subset by using brute-force simulation or emulation or some other technique on the code. Moreover, since the performance of a FAID on a given code depends on its structure, the goal of identifying several candidate FAIDs is more realistic than identifying a single good FAID, and allows for devising a selection method that is not code-specific. Another important objective of our approach is to ensure that any FAID belonging to this subset is capable of surpassing BP in the error floor not just on a single code but on several codes.

The approach we use relies on the knowledge of potentially harmful subgraphs that could be TS's for traditional iterative decoders when present in a given code. The candidate FAIDs are chosen by analyzing their behavior on each of these subgraphs with errors introduced in them. We will first introduce some important notions that form the basis of our approach, then we present a first approach of selection based on Monte-Carlo simulations on TS's of large sizes, and then present the proposed methodology for FAID selection for column-weight-three codes.

2.3.1 Critical number and isolation assumption

The notion of *critical number* associated with a TS of type $\mathcal{T}(a, b)$ was originally introduced for Gallager-A/B algorithms on the BSC [66]. It is computed by analyzing the Gallager-A/B decoding on errors contained in the topology $\mathcal{T}$ that is present in a code, assuming that all nodes outside the topology are initially correct. It provides a measure of how harmful a TS is, and hence, this notion is not only useful for predicting the error floor performance [46] but also for determining the harmful subgraphs that should be avoided in the code designs.

In order to be able to extend the notion of critical number for FAIDs, we introduce the notion of *isolation assumption* [67] which is used to analyze the decoder on a potential $\mathcal{T}(a, b)$ TS. Under this assumption, the neighborhood of the TS is such that the messages flowing into the TS from its neighborhood are not in any way influenced by the messages flowing out of the TS. Therefore, the messages flowing into the TS can be computed while completely disregarding the neighborhood [67, Theorem 1]. We now precisely define this notion.

Let $\mathscr{T}_i^k(G)$ denote the computation tree corresponding to an iterative decoder on G enumerated for k iterations with node $v_i \in V$ as its root. A node $w \in \mathscr{T}_i^k(G)$ is a *descendant* of a node $u \in \mathscr{T}_i^k(G)$ if there exists a path starting from node w to root v_i that traverses through node u.

Definition 2.3 (Isolation assumption)**.** *Let H be a subgraph of G induced by $P \subseteq V$ with check node set $W \subseteq C$. The computation tree $\mathscr{T}_i^k(G)$ with the root $v_i \in P$ is said to be isolated if for any node $u \notin P \cup W$ in $\mathscr{T}_i^k(G)$, u does not have any descendant belonging to $P \cup W$. If $\mathscr{T}_i^k(G)$ is isolated $\forall v_i \in P$, then H is said to satisfy the isolation assumption in G for k iterations.*

The *critical number* can now be defined in the framework of FAIDs.

Definition 2.4. *The critical number of a FAID denoted by D on a subgraph H is the smallest number of errors introduced in H for which D fails on H under the isolation assumption.*

Remark: We set the critical number to ∞ if D corrects all possible error patterns on H.

The critical number can now be used as possible parameter for decoder selection where a decoder is chosen to maximize the critical number on a given TS or set of TS's. In principle, one could consider a database of potential TS's that are generated either through analytical or empirical evaluations of traditional decoders such as BP and min-sum on several different codes, and then select a FAID based on its critical numbers on all these TS's. The critical number is then supposed to be more representative than the TS itself to measure its impact in the error floor region. For example, a $(7, 3)$ TS with critical number 4 will have a larger contribution to the error floor than a $(5, 3)$ TS with critical number 5.

However, the isolation assumption of a TS typically does not hold in an actual code for more than few iterations and hence the critical number may not reflect the true error-correction capability of the FAID on a code containing the TS. This is especially true for TS's of small sizes. Therefore, unless a very large database of TS's is considered or unless TS's with large sizes are considered such that isolation assumption holds for many more iterations , the strategy will remain ineffective. This motivates the need for a new notion that considers to an extent the influence of the neighborhood.

Before presenting the main tool that will be useful in general in the selection of good FAIDs, the next section provides a first approach based on TS's with large sizes in order to detect good FAID based on Monte Carlo simulations on a given code. These large attractors are taken to be the codewords of the given codes. We present the developed methodology throughout the example of the Tanner code, but it can be applied to any code, provided the distribution of the codewords is known.

2.3.2 Investigation of the (155,64,20) Tanner code

As preliminaries, we briefly review the construction and the details regarding the Tanner code, before presenting in the next few sections a first methodology to identify good FAIDs on this particular code. The choice of this code is not random as its short length allows a deep analysis of the failures of iterative decoding.

The Tanner code has been constructed in [68] and recall in [69, 70]. We expose here the principle of the construction of the (155,64,20) Tanner code, with the code length $N = 155$, and the number of information bits $K = 64$.

The parity-check matrix of the Tanner code is made of $d_v \times d_c$ block of permutation matrices. Each permutation matrix is an $m \times m$ matrix obtained by circularly shifting the identity matrix of size m. For the code we are using the parameters are $m = 31$, $d_v = 3$ and $d_c = 5$. We denote here I_p the matrix obtained by circularly shifting the identity matrix p times. The LDPC matrix obtained is given by :

$$H_{[155,64,20]} = \begin{bmatrix} I_1 & I_2 & I_4 & I_8 & I_{16} \\ I_5 & I_{10} & I_{20} & I_9 & I_{16} \\ I_{25} & I_{19} & I_7 & I_{14} & I_{28} \end{bmatrix}_{(93\times155)}$$

We refer to [68] for a complete explanation on the permutation indices of the parity-check matrix. The girth of the Tanner graph associated with the matrix is 8, and the resulting code has a minimal distance $d_{min} = 20$.

2.3.2.1 Trapping sets distributions

We now detail the topologies of the Tanner code which are supposed to be dominant in the error floor region of the frame error rate curves, namely the smallest structures in

terms of number of bits involved in it. Using expansion of the neighboring tree from each variable node, it is quite easy to derive an algorithm which detects and counts the small closed topologies, and therefore TS's, in a graph. Different algorithms have been suggested to detect TS's [56, 71]. We have reported on Table 2.4 the distribution of TS's up to $a = 7$ bits which are present in the Tanner Code. Two examples of these TS's are drawn on Fig. 2.5(a) and Fig. 2.5(b).

The $(5, 3)$ TS is the corner point of the weakness of iterative decoders on the Tanner code. This *very small* TS makes several iterative decoders fail when the bits in error are located on the 5 bits which compose the TS.

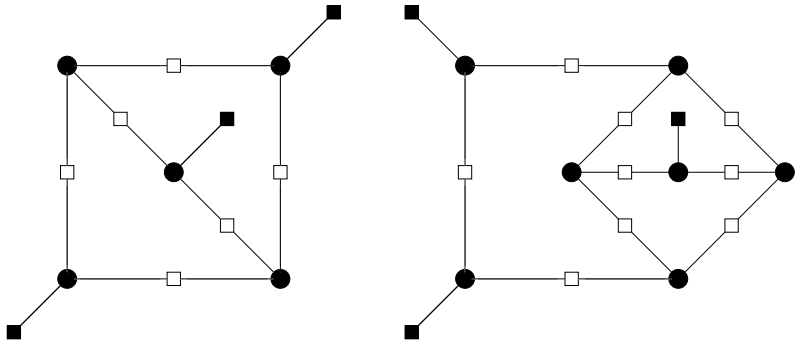

(a) The $(5, 3)$ TS. (b) A $(7, 3)$ TS.

Figure 2.5: Two different structures of TS present in the Tanner code

Table 2.4: Trapping Set spectrum of the Tanner Code.

(155,64,20) Tanner code		
$\mathcal{T}(5,3)\ 0-3-0-0-0-0$	$\rightarrow$	**155**
$\mathcal{T}(6,4)\ 0-1-2-0-0-0$	$\rightarrow$	**930**
$\mathcal{T}(7,3)\ 0-3-2-0-2-0$	$\rightarrow$	**930**
$\mathcal{T}(7,5)\ 0-1-1-0-1-0$	$\rightarrow$	**11160**
$\mathcal{T}(7,5)\ 0-1-0-2-0-0$	$\rightarrow$	**2790**

2.3.2.2 Minimal codeword structures

The knowledge of the dominant TS's could be sufficient to predict the behavior of usual decoders in the error floor region [46, 44]. However, as demonstrated in the next section, when the iterative decoder is more general, which is the case of the FAID decoders, looking at the TS alone is not sufficient. The natural and obvious thing to do is then to look at bigger structures which are also attractor points of the decoders. Instead of considering larger and larger TS, we propose to study the behavior of the

decoders on the closed structures which form the codewords of the Tanner code. The main reason is that the multiplicity of TS with constant $b > 1$ becomes rapidly cumbersome with increasing a. Looking at error events located inside a codeword should give a lot of information about iterative decoding convergence points, although a TS is not necessarily nested in a codeword.

The Hamming distance spectrum of the Tanner code is given on Table 2.5. This spectrum has been obtained with the impulse algorithm presented in [72]. We will focus on the minimum codewords of weight $d_{min} = 20$ for the sake of simplicity of the analysis. Note that these minimal codewords are actually $(20, 0)$ TS's.

By analysis of the topologies of these codewords, we have identified that there are only 3 types of structures for the minimal codewords, which we will denote Type-I, Type-II and Type-III. This means that each and every codeword of weight 20 belongs to one of the automorphism group of the subgraph induced by one of the 3 types of codewords. This is especially interesting since we can restrict the study of the decoders on 3 subgraphs instead of 1023 subgraphs. Another observation is that only 2 out of the 3 types contain the minimal TS, *i.e.* the $(5, 3)$ TS. We have drawn on the Fig. 2.6(a), 2.6(b) and 2.6(c) the structure of Type-I, Type-II and Type-III codewords, respectively. We emphasized the $(5, 3)$ TS on the Fig. 2.6(a) and 2.6(b).

Table 2.5: Codeword distribution of the Tanner Code.

(155,64,20) Tanner code		
weight 20	$\rightarrow$	**1023**
weight 22	$\rightarrow$	**6200**
weight 24	$\rightarrow$	**43865**
weight 26	$\rightarrow$	**259918**

2.3.2.3 Limitations of predicting decoder behavior based on minimal trapping sets

We have computed and indicated on the Table 2.8 the critical numbers of 4 different FAIDs, and for all TS's present in the Tanner code up to 8 bits. The 4 FAIDs considered are the NLT 5-level FAID of the Table 2.2 denoted $\Phi_v^{(1)}$, the 5-level FAIDs of the Table 2.6 and 2.7 denoted $\Phi_v^{(2)}$ and $\Phi_v^{(3)}$, respectively, and the LT 7-level FAID of the Table 2.3, denoted $\Phi_v^{(4)}$.

Without big surprise, the $(8, 2)$ TS (displayed later in this chapter in the Fig. 2.9(b)) is the most difficult TS to cope with for all decoders. Note that all 4 FAIDs have infinite critical number on the 2 smallest TS's, namely the $(5, 3)$ TS and the $(6, 4)$ TS, which seems to indicate that it is possible to derive quantized decoders, even with very few quantization bits, which are not trapped by the TS's of usual decoders (Gallager-B, Min-sum).

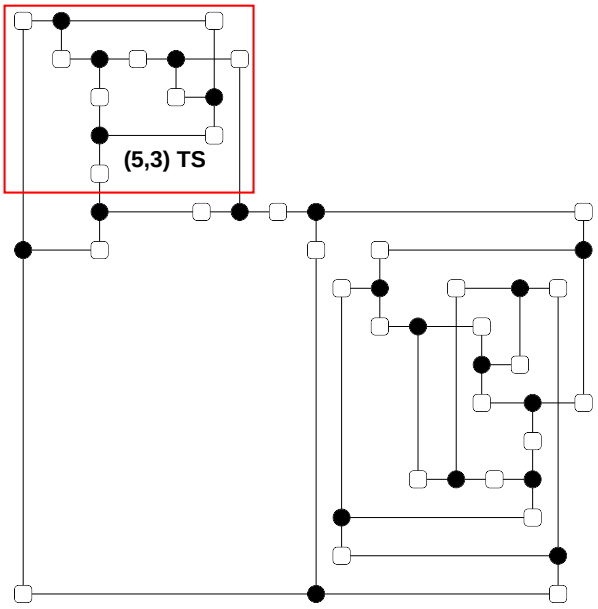

(a) Type-I

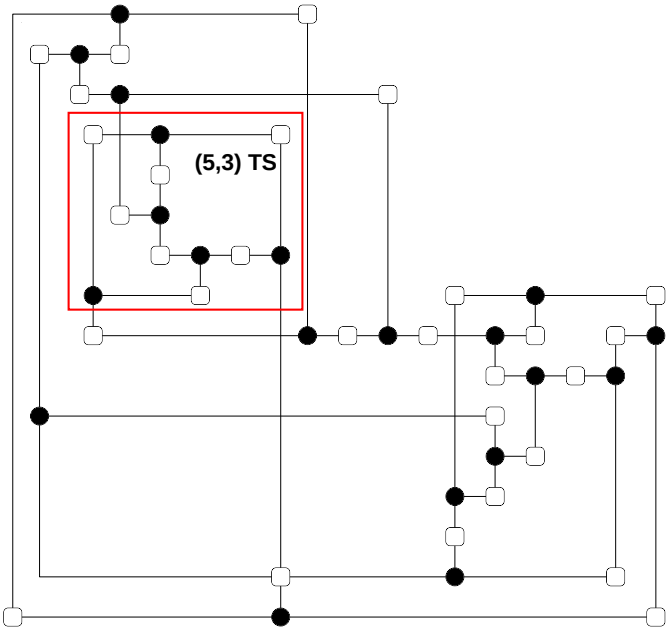

(b) Type-II

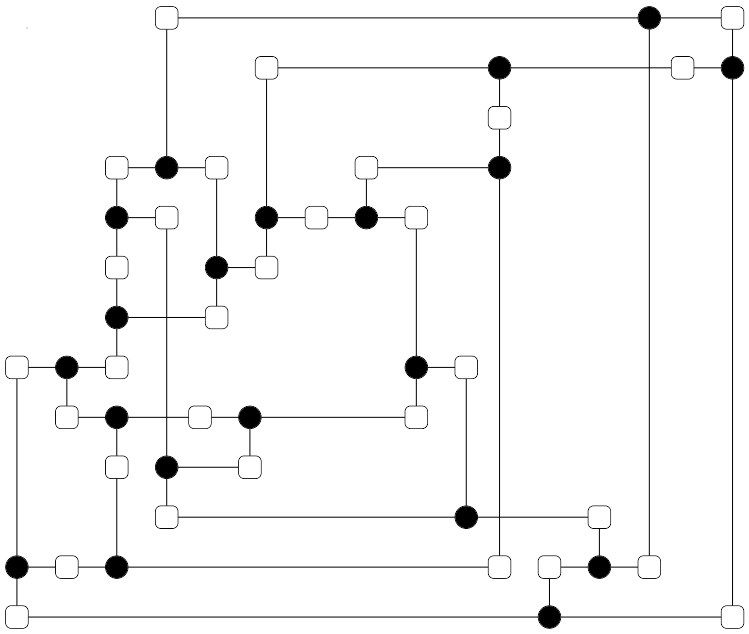

(c) Type-III

Figure 2.6: Topological structures of the minimal codewords of the Tanner code

Table 2.6: LUT for Φ_v of a 5-level FAID with $y_i = -\mathrm{C} - \Phi_v^{(2)}$.

$\boldsymbol{m_1 \backslash m_2}$	$\boldsymbol{-L_2}$	$\boldsymbol{-L_1}$	$\boldsymbol{0}$	$\boldsymbol{+L_1}$	$\boldsymbol{+L_2}$
$\boldsymbol{-L_2}$	$-L_2$	$-L_2$	$-L_2$	$-L_2$	0
$\boldsymbol{-L_1}$	$-L_2$	$-L_2$	$-L_1$	$-L_1$	$+L_1$
$\boldsymbol{0}$	$-L_2$	$-L_1$	$-L_1$	0	$+L_2$
$\boldsymbol{+L_1}$	$-L_2$	$-L_1$	0	$+L_1$	$+L_2$
$\boldsymbol{+L_2}$	0	$+L_1$	$+L_2$	$+L_2$	$+L_2$

Table 2.7: LUT for Φ_v of a 5-level FAID with $y_i = -\mathrm{C} - \Phi_v^{(3)}$.

$\boldsymbol{m_1 \backslash m_2}$	$\boldsymbol{-L_2}$	$\boldsymbol{-L_1}$	$\boldsymbol{0}$	$\boldsymbol{+L_1}$	$\boldsymbol{+L_2}$
$\boldsymbol{-L_2}$	$-L_2$	$-L_2$	$-L_2$	$-L_2$	0
$\boldsymbol{-L_1}$	$-L_2$	$-L_1$	$-L_1$	$-L_1$	$+L_2$
$\boldsymbol{0}$	$-L_2$	$-L_1$	$-L_1$	0	$+L_2$
$\boldsymbol{+L_1}$	$-L_2$	$-L_1$	0	$+L_2$	$+L_2$
$\boldsymbol{+L_2}$	0	$+L_2$	$+L_2$	$+L_2$	$+L_2$

Table 2.8: Critical numbers on the TS's of the Tanner code for the selected decoding rules. The DE threshold of each rule is also shown.

Trapping Set Label	rule $\Phi_v^{(1)}$	rule $\Phi_v^{(2)}$	rule $\Phi_v^{(3)}$	rule $\Phi_v^{(4)}$
$(5,3)\ 0-3-0-0-0-0$	∞	∞	∞	∞
$(6,4)\ 0-1-2-0-0-0$	∞	∞	∞	∞
$(7,3)\ 0-3-2-0-2-0$	7	∞	∞	6
$(7,5)\ 0-1-1-0-1-0$	∞	∞	∞	∞
$(7,5)\ 0-1-0-2-0-0$	∞	∞	∞	∞
$(8,2)\ 0-3-4-2-4-2$	6	5	5	6
$(8,4)\ 0-3-0-2-0-2$	∞	∞	∞	6
$(8,4)\ 0-1-3-1-1-1$	∞	∞	∞	7
$(8,4)\ 0-1-2-2-2-0$	∞	∞	∞	7
$(8,6)\ 0-1-0-1-0-1$	∞	∞	∞	∞
$(8,6)\ 0-1-0-0-2-0$	∞	∞	∞	∞
Decoding threshold α^*	0.09781	0.09778	0.09777	0.10155

These critical numbers are however not predictive at all when the isolation assumption is not fulfilled. We have verified some error correction properties with extensive Monte Carlo simulations on the whole Tanner code. It turns out that although the rule $\Phi_v^{(3)}$ has the exact same statistics as rule $\Phi_v^{(2)}$ and even better statistics than rule $\Phi_v^{(1)}$ in terms of critical numbers, rule $\Phi_v^{(3)}$ fails on 110 five-error patterns when we simulate the rule on the whole Tanner code, while rule $\Phi_v^{(1)}$ and rule $\Phi_v^{(2)}$ correct all five-errors patterns in less than 100 iterations. Another contradiction is that the critical number for rule $\Phi_v^{(2)}$ on $(8,2)$ TS is 5, which means that there are five-error patterns such that decoder $\Phi_v^{(2)}$ fails in an isolated way, but the rule $\Phi_v^{(2)}$ successfully corrects the five errors when the $(8,2)$ TS is simulated in the whole Tanner code. As we can see, contradictions in the analysis of the isolated critical numbers are in both positive and negative directions, which makes it difficult to make use in the goal of choosing a good decoder for a particular code.

In Fig. 2.7, we compared the frame error rate (FER) performance of the FAID rules $\Phi_v^{(1)}$ and $\Phi_v^{(3)}$ on the Tanner code. All curves have been plotted with a maximum of 100 iterations, and at least 300 frame errors have been recorded for each simulation points. The difference between the two rules is not large, although the curves start to split apart in the error floor region due to the fact that $\Phi_v^{(1)}$ corrects all five-error patterns while $\Phi_v^{(1)}$ does not. As a catastrophic counter-example of using only isolated critical numbers for designing FAID rules, we have also plotted the performance of a FAID rule which have *all its critical numbers* equal to $+\infty$ (labeled as 'Bad Rule' in the figure). The DE for this rule is only $\alpha^* = 0.07778$, and then is a lot worse than the

thresholds of the FAIDs considered.

Of course, brute force simulations on the whole code would give the desired ordering between rules, but at the price of a too large computational burden. The problem of finding the best decoding rules for a specific code cannot be solved with the knowledge of critical numbers alone, and remains an open issue. In the following, we propose a first approach to partially solve this issue which is still based on Monte Carlo simulations, but on larger structures than the smallest TS.

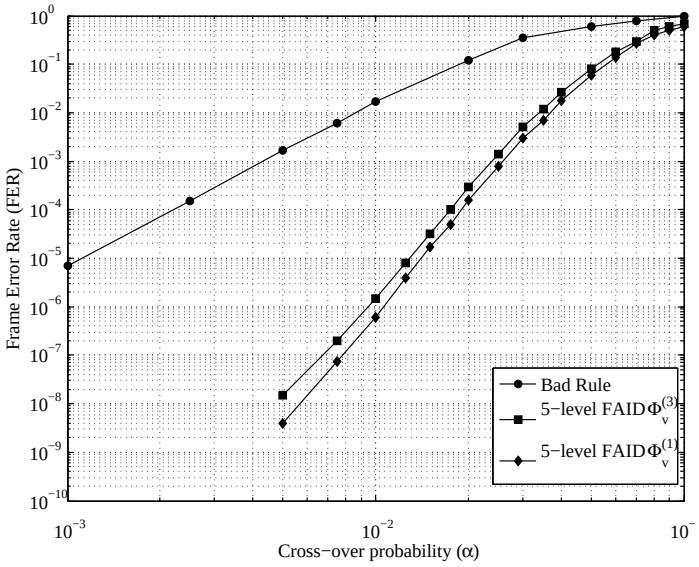

Figure 2.7: Performance comparisons of different FAIDs on the Tanner Code

2.3.2.4 Selection of FAIDs by Monte-Carlo simulations on larger structures

We propose to make the selection of FAIDs with respect to the ordering between FAID rules, by simulations of n_e-errors patterns on the subgraphs induced by the minimal codewords of weight 20. Although we do not claim that simulation results on these subgraphs are strictly predictive, looking at the codeword structures makes sense with respect to the isolation assumption described in the preceding section. As a matter of fact, a codeword is a particular $(a, 0)$ TS, and then is connected to the rest of the graph only by edges which have already even degree inside the TS. More importantly, there is no edge which connects the codeword to the rest of the graph, and which outputs from a variable node. From our observations on TS's, the isolation assumption is more often *'broken'* when the external paths go through a variable node than when they go only through check nodes of the TS. It seems that codewords are *almost isolated*, at least during a number of iterations more important than other types of TS.

We have simulated all 5-errors patterns and all 6-errors patterns on the 3 types of codewords, for a large number of FAIDs. We report on Table 2.9 the results for the 5-level decoders of Tables 2.2, 2.6 and 2.7. The numbers in the table indicate the number of error patterns which are *not* corrected by the decoders, and in the case all error events are corrected, we indicate in brackets the maximum number of iterations needed to correct all events.

Table 2.9: Low-weight error event correction on the codewords.

	5-errors patterns			6-errors patterns		
	$\Phi_v^{(1)}$	$\Phi_v^{(2)}$	$\Phi_v^{(3)}$	$\Phi_v^{(1)}$	$\Phi_v^{(2)}$	$\Phi_v^{(3)}$
type-I	3	2	> 10	172	138	> 500
type-II	$0^{(7)}$	$0^{(8)}$	$0^{(9)}$	$0^{(16)}$	$0^{(21)}$	> 21
type-III	$0^{(4)}$	$0^{(4)}$	$0^{(4)}$	$0^{(4)}$	$0^{(4)}$	$0^{(5)}$

As a first observation, we can see that the 3 types of codewords have completely different behaviors. Type-I codewords seem to be the most problematic ones, and Type-III codewords the easiest to decode. Remember that Type-III codewords do not contain $(5, 3)$ TS, which could explain why they have the best behaviors with iterative decoding. This is a very interesting differentiation of codewords which have although the same Hamming weight, and therefore cannot be differentiated with Maximum Likelihood Decoding.

In terms of ordering of the different rules, those statistics are in better accordance with the simulations on the whole Tanner code than the critical numbers of Table 2.8. It is readily seen on these statistics that rule $\Phi_v^{(3)}$ is worse than rules $\Phi_v^{(1)}$ and $\Phi_v^{(2)}$. Since we verified that rule $\Phi_v^{(3)}$ does not correct all five-error patterns on the Tanner code while $\Phi_v^{(1)}$ and $\Phi_v^{(2)}$ do, we can see that the ordering of rules made with simulations on the codewords is somewhat more predictive than the isolated critical numbers. A more important result is that we performed those statistics for all possible 5-level decoders (we remind that there are 28,314 possible FAIDs with $N_s = 5$), and rules $\Phi_v^{(1)}$ and $\Phi_v^{(2)}$ have the best overall statistics of all decoders. Since this approach of simulating error patterns on codewords appears to be predictive, we conjecture that we have found the best 5-level decoders for the (155,64,20) Tanner code, that is decoders $\Phi_v^{(1)}$ and $\Phi_v^{(2)}$ for which the FER curves are very close. As we already reported in Fig. 2.2 where we remind that the $\Phi_v^{(1)}$ is the 5-level NLT FAID, and $\Phi_v^{(4)}$ being the 7-level LT FAID, both FAIDs $\Phi_v^{(1)}$ and $\Phi_v^{(4)}$ beat the BP decoder in the error floor region, as expected with our conjectures from the minimal codewords in the Tanner code.

To conclude this preliminary part on the selection we should note that the selection of good FAIDs on the Tanner code was a possible task to do due to its short length, and then its easiness to compute the contained TS, the minimal codewords,... For longer codes, this methodology might appear as not tractable as the exhaustive search

of minimal codewords might not be doable. Indeed, for the Tanner code we are able to list all codewords of minimal weight, but it seems way more difficult for other codes, hence we need another tool to select FAIDs that rely only on the knowledge of dominant TS's. This other tool needs the definition of other concepts presented in the next section.

2.3.3 Noisy trapping sets and noisy critical numbers

Let us consider a harmful topology $\mathcal{T}(a, b)$ that has been identified as a potential TS on a given code. We introduce the notion of *initialization vector* which allows us to partially capture the influence of its arbitrary (unknown) neighborhood during the analysis of a FAID on the $\mathcal{T}$.

Definition 2.5. *An initialization vector on a TS $\mathcal{T}(a, b)$ is defined as a vector $\mathbf{\Theta} = (\theta_1, ..., \theta_b)$ where $\theta_i \in \mathcal{M}$, such that during the message-passing of a FAID on $\mathcal{T}$, the message passed by the i^{th} degree-one check node in any iteration is θ_i. The TS $\mathcal{T}(a, b)$ is said to be initialized by such a vector and is referred to as a noisy trapping set.*

A FAID can now be analyzed by introducing errors into the variable nodes of the TS $\mathcal{T}(a, b)$ and passing messages iteratively on the edges of $\mathcal{T}$ under a given initialization vector. Note that the initialization vector on a TS is carried out only through the degree-one check nodes, and also that the initialization vector $\mathbf{\Theta}$ is not iteration-dependent.

As a first example, Fig. 2.8 depicts how a FAID is analyzed for a three-error pattern on a $\mathcal{T}(6, 2)$ initialized by a vector $\mathbf{\Theta} = (\theta_1, \theta_2)$. A ● denotes a variable node initially wrong (v_1, v_2, and v_4) and a ○ denotes a node initially correct (v_3, v_5, and v_6). A □ denotes a degree-two check node and a ■ denotes a degree-one check node. Initially all the messages passed by all nodes except the degree-one check nodes are set to zero. Then the messages are iteratively updated using the maps Φ_v and Φ_c by treating the topology $\mathcal{T}$ as if it were the Tanner graph of a code but with the exception that a degree-one check node sends θ_1 (or θ_2) to its neighbors in all iterations of the message-passing. The message update on a single edge from a variable node is shown in the figure for each of the nodes v_1, v_2, v_3 , and v_5 (v_4 and v_6 are similar to v_2 and v_3 respectively). Note that the messages $m_1, m_2, \ldots, m_6$ denote the extrinsic incoming messages to these nodes.

Let N_I denote the maximum number of iterations allowed for message-passing under a particular FAID on TS $\mathcal{T}(a, b)$. We examine whether an error pattern is corrected by the FAID within N_I iterations under a given initialization vector on the TS $\mathcal{T}(a, b)$.

As a second example Fig. 2.9(a) illustrates the initialization of a $\mathcal{T}(5, 3)$ with a static initialization vector $\mathbf{\Theta}$ on the odd-degree check nodes. In order to demonstrate how the initialization can mimic the influence of the neighborhood, consider the Fig. 2.9(b) where a $\mathcal{T}(8, 2)$ is formed by adding three extra variable nodes to $\mathcal{T}(5, 3)$. The initialization vector of the $\mathcal{T}(5, 3)$ indicates the 3 possible messages that could enter

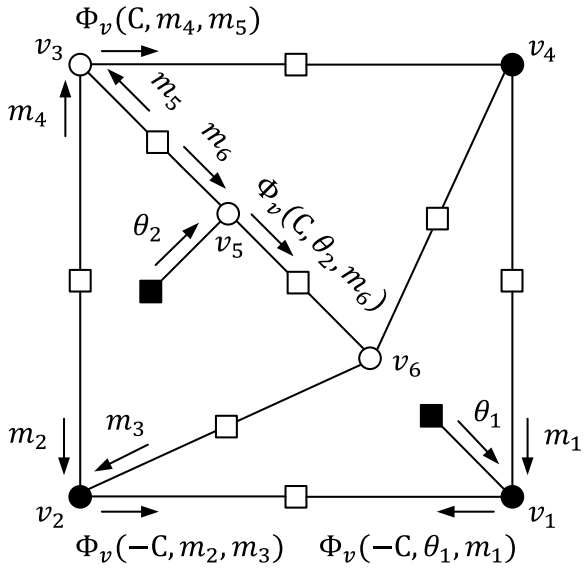

Figure 2.8: An example of a noisy $\mathcal{T}(6,2)$ initialized by a vector $\boldsymbol{\Theta}$.

$\mathcal{T}(5,3)$ due to the influence of its neighborhood defined by $\mathcal{T}(8,2)$. Tables 2.10(a) and 2.10(b) show the observations of the evolution of messages θ_1, θ_2, and θ_3 for the first 10 decoding iterations when the 5-level FAID of Table 2.2 was employed on the Tanner code. Table 2.10(a) corresponds to the case where all 5 errors are introduced on a $\mathcal{T}(5,3)$ contained in $\mathcal{T}(8,2)$. Table 2.10(b) corresponds to the case of adding an extra 6th error in the neighborhood of $\mathcal{T}(5,3)$. From the Tables, we can see that not only does the isolation assumption not hold as messages do not remain $+L_2$ after iteration 3, but at certain iterations even messages such as 0 and $-L_1$ begin to enter the $\mathcal{T}(5,3)$ due to the neighborhood.

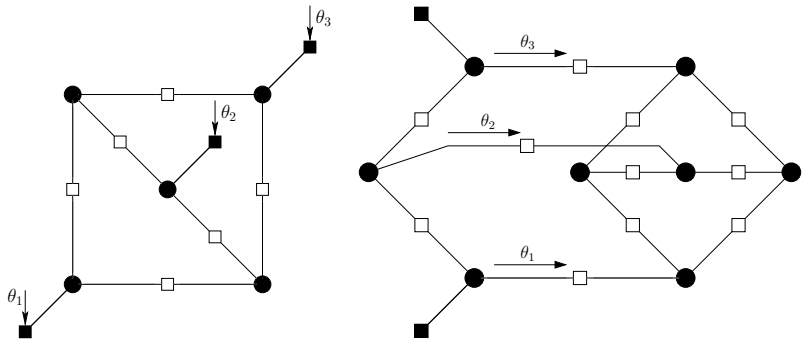

(a) (b)

Figure 2.9: (a) Initialization of a $\mathcal{T}(5,3)$. (b) $\mathcal{T}(5,3)$ + 3 variable nodes = $\mathcal{T}(8,2)$.

Table 2.10: Evolution of the messages entering a $\mathcal{T}(5,3)$

(a) Case 1

Iter.	$\theta_1^{(l)}$	$\theta_2^{(l)}$	$\theta_3^{(l)}$
1	$+L_1$	$+L_1$	$+L_1$
2	$+L_2$	$+L_2$	$+L_2$
3	$+L_2$	$+L_2$	$+L_2$
4	$+L_1$	$+L_1$	$+L_1$
5	0	0	0
6	$+L_1$	$+L_1$	$+L_1$
7	0	0	0
8	$+L_1$	$+L_1$	$+L_1$
9	$+L_1$	$+L_1$	$+L_1$
10	$+L_1$	$+L_1$	$+L_1$

(b) Case 2

Iter.	$\theta_{c_1}^{(l)}$	$\theta_{c_2}^{(l)}$	$\theta_{c_3}^{(l)}$
1	$+L_1$	$+L_1$	$+L_1$
2	$+L_2$	$+L_2$	$+L_1$
3	$+L_2$	$+L_1$	$+L_2$
4	$+L_2$	$-L_1$	$+L_1$
5	0	$+L_1$	0
6	$+L_2$	0	$+L_2$
7	$+L_2$	$+L_1$	$+L_1$
8	$+L_1$	0	$+L_1$
9	$+L_1$	$+L_1$	$+L_1$
10	$+L_1$	0	$-L_1$

Although we see that dynamic initialization vectors can accurately predict the decoder behavior, we restrict ourselves to using static initialization vectors in order to ensure computational feasibility in the analysis.

Our main intuition for defining the notion of noisy trapping sets is as follows. Let us consider a code whose graph G contains a subgraph H that is isomorphic to the topology $\mathcal{T}(a,b)$. Assume that a particular FAID is being used for decoding an error pattern where some (or all) of the variable nodes in H are initially in error and the nodes outside H are initially correct. During each iteration of decoding, different possible messages belonging to $\mathcal{M}$ will be passed into the nodes of H from outside of H depending on its neighborhood. The initialization vector can be considered as a possible snapshot of the messages entering H through its check nodes in some arbitrary iteration, and different initializations represent the different possible influences that the neighborhood of H can have. Therefore, analyzing the FAID under different initializations on a given $\mathcal{T}$ can provide a good indication of its error correction capability on a code whose graph contains H.

Although the initialization vector should ideally be iteration-dependent and include all messages passed to all check nodes of $\mathcal{T}(a,b)$ from outside of $\mathcal{T}(a,b)$, this would make analyzing a FAID on $\mathcal{T}(a,b)$ computationally intractable. Therefore we only include constant values that are passed to degree-one check nodes into the initialization vector. We now define the notion of *noisy critical number* which is an extension of the notion of critical number for FAIDs.

Definition 2.6. *The noisy critical number of a FAID* D *under an initialization vector* $\boldsymbol{\Theta}$ *on a TS* $\mathcal{T}(a,b)$ *is the smallest number of errors introduced in* $\mathcal{T}(a,b)$ *for which* D *fails on* $\mathcal{T}(a,b)$.

By determining the noisy critical number under every possible initialization vector $\mathbf{\Theta} \in \mathcal{M}^b$ on the TS $\mathcal{T}(a,b)$, a vector of noisy critical numbers, referred to as *noisy critical number vector* (NCNV), can be obtained for a particular FAID. Let N_Θ denote the number of all possible initialization vectors, i.e., $N_\Theta = |\mathcal{M}^b|$. The NCNV of a FAID denoted by D on a given TS $\mathcal{T}(a,b)$ is given by $\mathscr{N}_\mathrm{D}(\mathcal{T}(a,b), N_I) = (\zeta_1, \zeta_2, \ldots, \zeta_{N_\Theta})$, where ζ_i is the noisy critical number determined under a initialization vector $\mathbf{\Theta_i} \in \mathcal{M}^b$ on TS $\mathcal{T}(a,b)$ with N_I being the maximum number of decoding iterations. The NCNV can now be used as a parameter for decoder selection.

2.3.4 Choice of trapping sets for decoder selection

Since our approach for identifying good FAIDs relies on determining the NCNVs of FAIDs on different TS's, the first step in the decoder selection is to carefully select the harmful topologies that should be considered for the analysis. The selected TS's should be topologies that are known to exist in practical high-rate codes with dense graphs and are regarded as relatively harmful for existing iterative decoders. Also the TS's used should have notable differences in their topological structures, so that the candidate FAIDs identified from the analysis are more likely to be good on several codes rather than just on a single code.

We use the trapping set ontology (TSO) [60] to determine which harmful topologies to consider. The TSO is a systematic hierarchy of trapping sets that is based on their topological relations, and it is specified in the form of a *parent-child* relationship between the TS's. A trapping set $\mathcal{T}_1$ is said to be a parent of a TS $\mathcal{T}_2$ if $\mathcal{T}_2$ contains $\mathcal{T}_1$. For the decoder selection, the TS's are chosen such that they do not have many common parents, and that most of the parents (graphs of smaller size) in the TSO are considered. For simplicity, we ensure that all the TS's selected have the same value of b, so that the NCNVs determined from different TS's all have the same dimension.

2.3.5 Decoder domination

Having selected the harmful topologies, the next step in the decoder selection is to determine and be able to compare the NCNVs of different FAIDs on all the selected TS's. We introduce the notion of *decoder domination* in order to compare the NCNVs of different FAIDs.

Let the set of chosen TS's for the analysis of FAIDs be denoted by $\Lambda = \{\mathcal{T}_1, \mathcal{T}_2, \ldots, \mathcal{T}_{N_\Lambda}\}$ with cardinality N_Λ. Let $\mathcal{F} = \{\mathrm{D}_1, \ldots, \mathrm{D}_{N_\mathcal{F}}\}$ denote the set of N_s-level FAIDs considered for possible decoder selection with cardinality $N_\mathcal{F}$. Let $\mathscr{N}_{\mathrm{D}_k}(\mathcal{T}_j, N_I)$ denote the NCNV of a FAID $\mathrm{D}_k \in \mathcal{F}$ determined on a TS $\mathcal{T}_j \in \Lambda$, and let $\mathscr{N}^{(i)}_{\mathrm{D}_k}(\mathcal{T}_j, N_I)$ denote the i^{th} component of the NCNV, i.e., $\mathscr{N}^{(i)}_{\mathrm{D}_k}(\mathcal{T}_j, N_I) = \zeta_i$.

A FAID D_k is said to dominate a FAID D_l for a given initialization vector $\mathbf{\Theta_i}$, if

$$\mathscr{N}^{(i)}_{\mathrm{D}_k}(\mathcal{T}_j, N_I) \geq \mathscr{N}^{(i)}_{\mathrm{D}_l}(\mathcal{T}_j, N_I) \ \ \forall j \in \{1, 2, \ldots, N_\Lambda\} \tag{2.3}$$

In other words, D_k dominates D_l under a given initialization vector $\mathbf{\Theta_i}$ if the noisy critical number of D_k is not less than the noisy critical number of D_l on all the TS's in Λ.

The number of initialization vectors under which D_k dominates D_l is denoted by $\tilde{n}(\mathrm{D}_k, \mathrm{D}_l)$ and is given by

$$\tilde{n}(\mathrm{D}_k, \mathrm{D}_l) = \sum_{i=1}^{N_\Theta} \prod_{j=1}^{N_\Lambda} \mathbb{1}\left(\mathscr{N}^{(i)}_{\mathrm{D}_k}(\mathcal{T}_j, N_I) \geq \mathscr{N}^{(i)}_{\mathrm{D}_l}(\mathcal{T}_j, N_I)\right) \tag{2.4}$$

where $\mathbb{1}$ is the indicator function that outputs a one when the condition in its argument is true and zero otherwise.

If $\tilde{n}(\mathrm{D}_k, \mathrm{D}_l) \geq \tilde{n}(\mathrm{D}_l, \mathrm{D}_k)$, then D_k is said to dominate D_l with *domination strength* $\tilde{n}(\mathrm{D}_k, \mathrm{D}_l) - \tilde{n}(\mathrm{D}_l, \mathrm{D}_k)$. For simplicity we shall use the symbol $\rhd$ to denote domination, i.e., $(\mathrm{D}_k \rhd \mathrm{D}_i) = 1$ implies that D_k dominates D_i.

2.3.6 Methodology for selection: a general approach

For a given value of N_s, a methodology for identifying good N_s-level FAIDs can now be devised based on the notions of decoder domination and the NCNVs. We remind the reader that the main goal of our approach is to be able to identify a small subset of candidate N_s-level FAIDs, where each candidate FAID is potentially good on several codes. Let this small subset of selected FAIDs be denoted by $\mathcal{F}_c$. Ideally, if a candidate FAID could be selected solely based on how it dominates all the other FAIDs in $\mathcal{F}$, then one could possibly obtain an ordering of the FAIDs in $\mathcal{F}$ in terms of their dominance and conclude which ones are more likely to be good on a given code containing one or more of the TS's in Λ. Unfortunately, we have found that such an ordering does not exist since there can be many FAIDs that dominate a particularly good FAID (known a priori to be good) and yet perform poorly on certain codes.

Therefore, without going into the details, we shall describe a general approach for selection that utilizes pre-determined small sets of good FAIDs and bad FAIDs denoted by $\mathcal{F}_g$ and $\mathcal{F}_b$ respectively. The set $\mathcal{F}_g$ consists of N_s-level FAIDs that are known a priori to have good error floor performance on several codes of different rates and possibly containing different TS's. The set $\mathcal{F}_b$ consists of N_s-level FAIDs that were found to perform well on one particular code but perform poorly on other codes. We regard FAIDs in $\mathcal{F}_b$ to be bad since our goal is to identify FAIDs that are capable of surpassing BP on several codes.

We then evaluate whether a particular FAID $\mathrm{D}_k \in \mathcal{F}$ dominates or is dominated

by the FAIDs in the sets $\mathcal{F}_g$ and $\mathcal{F}_b$. By using the sets $\mathcal{F}_g$ and $\mathcal{F}_b$ to compare with, we are inherently trying to select FAIDs whose NCNVs have characteristics similar to the NCNVs of FAIDs in $\mathcal{F}_g$ but dissimilar to the NCNVs of the FAIDs in $\mathcal{F}_b$. Therefore, we define a cost function, $\mathscr{C}_{\tilde{n}}$, that is based on domination strengths, and whose value determines whether the FAID D_k should be accepted for inclusion into $\mathcal{F}_c$. We have observed that it is crucial for a candidate FAID to dominate most (or all) FAIDs in $\mathcal{F}_g$ and also not be dominated by most (or all) FAIDs in $\mathcal{F}_b$ for it to be considered potentially good. This is reflected in the cost function $\mathscr{C}_{\tilde{n}}$ defined below.

$$\begin{aligned}\mathscr{C}_{\tilde{n}}(\mathrm{D}_k) = &\sum_{\forall\ \mathrm{D}_i\in\mathcal{F}_g,\ (\mathrm{D}_k\rhd\mathrm{D}_i)=1} \big(\tilde{n}(\mathrm{D}_k,\mathrm{D}_i)-\tilde{n}(\mathrm{D}_i,\mathrm{D}_k)\big)\\ &+\sum_{\forall\ \mathrm{D}_j\in\mathcal{F}_b,\ (\mathrm{D}_k\rhd\mathrm{D}_j)=1} \big(\tilde{n}(\mathrm{D}_k,\mathrm{D}_j)-\tilde{n}(\mathrm{D}_j,\mathrm{D}_k)\big)\\ &-\sum_{\forall\ \mathrm{D}_i\in\mathcal{F}_g,\ (\mathrm{D}_i\rhd\mathrm{D}_k)=1} \big(\tilde{n}(\mathrm{D}_i,\mathrm{D}_k)-\tilde{n}(\mathrm{D}_k,\mathrm{D}_i)\big)\\ &-\sum_{\forall\ \mathrm{D}_j\in\mathcal{F}_b,\ (\mathrm{D}_j\rhd\mathrm{D}_k)=1} \big(\tilde{n}(\mathrm{D}_j,\mathrm{D}_k)-\tilde{n}(\mathrm{D}_k,\mathrm{D}_j)\big)\end{aligned} \tag{2.5}$$

The value of the cost function $\mathscr{C}_{\tilde{n}}$ is compared to a threshold τ. If $\mathscr{C}_{\tilde{n}}(\mathrm{D}_k) \geq \tau$, then the FAID D_k is selected as a candidate to be included in $\mathcal{F}_c$, else it is rejected. The cardinality of $\mathcal{F}_c$ depends on τ since a smaller τ accepts more FAIDs and a larger τ accepts less FAIDs. The choice of N_I also plays a role and should generally be chosen to be small (5 to 10 iterations).

Note that the approach we have presented in this chapter is slightly different from the one proposed in [73]. In [73], the selection algorithm assumes it has no a priori knowledge on the sets $\mathcal{F}_g$ and $\mathcal{F}_b$, and then tries to progressively build the sets before using them to identify good candidate FAIDs. By instead utilizing pre-determined sets of $\mathcal{F}_g$ and $\mathcal{F}_b$ in our approach, we have found that the selection procedure is greatly improved and we were able to obtain much better sets of candidate FAIDs $\mathcal{F}_c$ (in terms of their error floor performance). Note however that the approach of [73] is still applicable to the selection method presented here as it could still be used as an initial step for determining the sets $\mathcal{F}_g$ and $\mathcal{F}_b$.

Using our methodology, we were able to derive a set of good candidate 7-level FAIDs (which are 3-bit precision decoders) for column-weight-three codes. On a variety of codes of different rates and lengths, particularly good 7-level FAIDs chosen from $\mathcal{F}_c$ all outperformed the BP (floating-point) in the error floor. Moreover, the loss in the waterfall compared to BP was found to be very reasonable. The numerical results to support this statement are provided in the next section. Another interesting remark related to our selection procedure that we have found is that, although the DE threshold values were not at all used as parameters in the selection of FAIDs, the candidate

FAIDs that we obtained in set $\mathcal{F}_c$ were all found to have fairly good DE thresholds.

2.4 Numerical results

Earlier in Section 2.2, we demonstrated the capability of 5-level and 7-level FAIDs to outperform BP in the error floor on the $(155, 64)$ Tanner code. We now provide additional numerical results on the BSC to further illustrate the efficacy of FAIDs on column-weight-three codes of higher practical interest and validate our approach for decoder selection. The three codes used for the simulations were chosen to cover a broad variety of LDPC codes in terms of rate, length, and structure. They are: 1) an $R = 0.751$ $(2388, 1793)$ structured code based on latin squares, 2) an $R = 0.5$ $(504, 252)$ code, and 3) an $R = 0.833$ $(5184, 4322)$ quasi-cyclic code.

The $(2388, 1793)$ structured code with girth-8 was designed using the method of Nguyen *et. al* [62], which is based on latin squares and avoids certain harmful TS's in the code design. The $R = 0.5$ $(504, 252)$ code with girth-8 was designed using the progressive edge-growth (PEG) method of [74] while ensuring that it contains no $(5, 3)$ TS (see [60] for the topology). The $(5184, 4322)$ quasi-cyclic code is a high-rate girth-8 code with a minimum distance of 12.

Figures 2.10, 2.12, and 2.11 show the frame error-rate (FER) performance comparisons versus the cross-over probability α between the particularly good 7-level (3-bit precision) FAIDs we identified and the BP (floating-point). Table 2.1 defines the FAID used on the $(2388, 1793)$ and the $(5184, 4322)$ codes, while Table 2.3 defines the FAID used on the $(504, 252)$ PEG-based code. Note that both are 7-level NLT FAIDs and all decoders were run for a maximum of 100 iterations.

In all three codes, the 7-level FAIDs begin to surpass the BP at an FER$\simeq 10^{-5}$. Also notice the difference in the better slopes of the error floor for the 7-level FAIDs which can be attributed to their improved error correction capability. For instance, all FAIDs used on the $(155, 64)$ Tanner code in Fig. 2.2 guarantee a correction of 5 errors, whereas BP fails to correct several 5-error patterns. It must also be noted that the good 7-level FAIDs identified using our approach outperformed BP on several other tested codes as well. Therefore, the methodology is applicable to any column-weight-three code and provides to an extent "universally" good FAIDs, as they are all capable of surpassing BP on not just few but several codes.

2.5 First results on column-weight-four LDPC codes

To conclude this chapter, we provide a *practical* section in order to identify harmful structures, and design FAIDs for a given column-weight-four code. This section does not contain any theoretical work, but just relies on experiments, observations and intuition leading nevertheless to promising results.

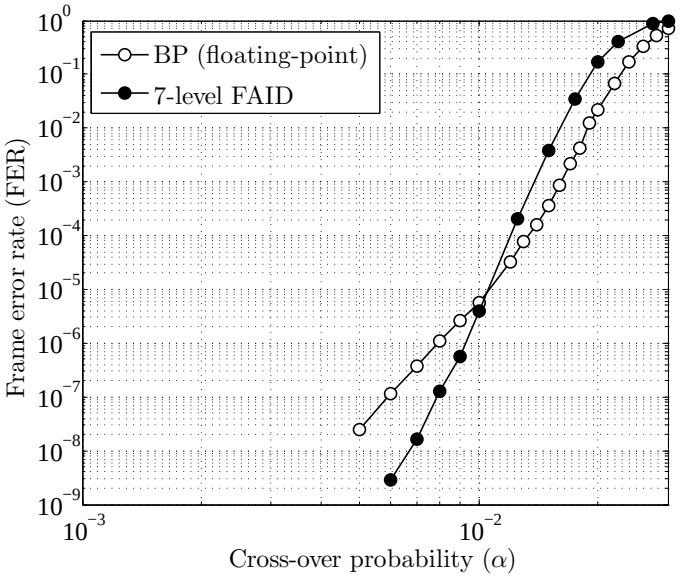

Figure 2.10: Performance comparisons between the BP (floating-point), the 7-level FAID defined by Table 2.1 on the $(2388, 1793)$ structured code.

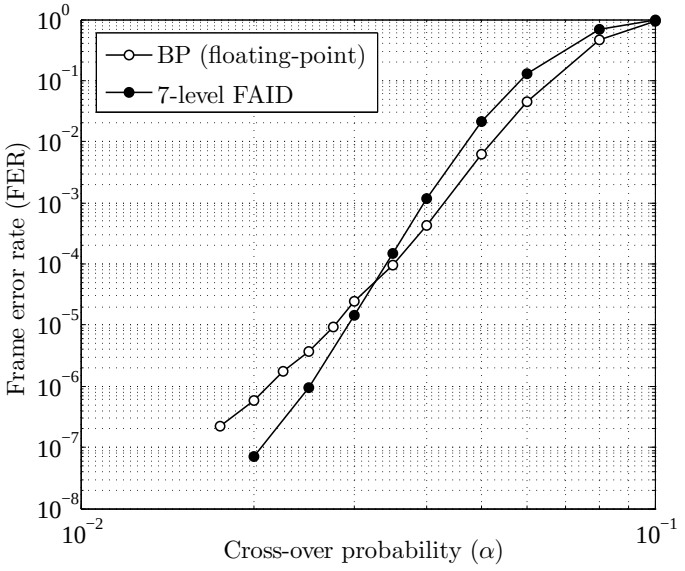

Figure 2.11: Performance comparisons between the BP (floating-point) and the 7-level FAID defined by Table 2.3 on the $(502, 252)$ quasi-cyclic code.

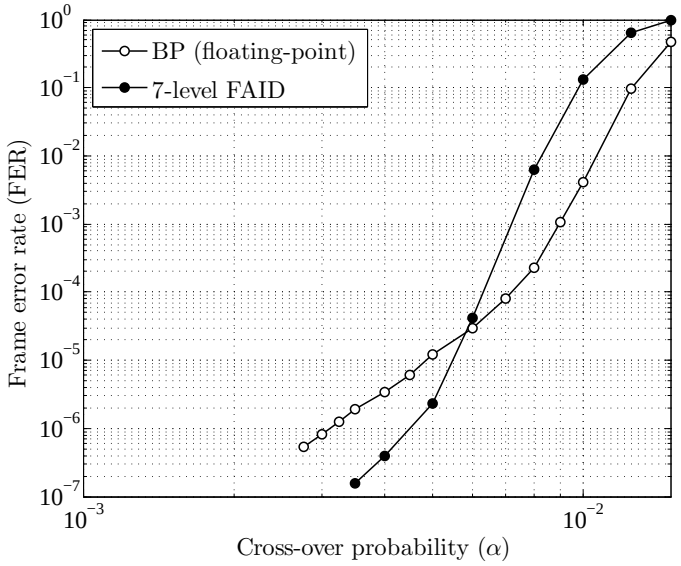

Figure 2.12: Performance comparisons between the BP (floating-point) and the 7-level FAID defined by Table 2.1 on the $(5184, 4322)$ quasi-cyclic code.

All the work performed previously considered column-weight-three girth-eight LDPC codes where the work on the harmful structures responsible for the error floor phenomenon of classical decoders was known. However for practical implementation (notably in storage systems), we need to address the case of a high-rate column-weight-four girth-six LDPC codes. In this section we propose a practical case of study of designing a FAID for such a given code on the BSC. The code we take as a practical test code is quasi-cyclic (QC) and has three different properties compared to the previous codes mentioned in this dissertation, which is column-weight four, girth-six and high-rate. The size of the code is $N = 4995$ and the rate is $R = 0.9$.

The FAIDs aim at improving the performance of an LDPC code in the error floor region. For column-weight-four and girth-six LDPC codes, the low-weight error patterns are not really known. Considering the length and the rate of the code, the exhaustive extraction of these structures cannot be done quickly and efficiently with the known algorithms. We choose another approach which consists in computing the performance of the BP/min-sum decoders on the BSC until the mid-SNR region, and then from the error patterns obtained, we derive some low-weight error patterns that are responsible for the error floor on the high SNR region. Due to the QC property of the code, the knowledge of a particular harmful attractor provides multiple ones. Finally the designed FAID should be able to correct some of the extracted structures, or at least improve the number of bits that can be corrected on them. Finding the minimum TS's of a given code is not an obvious issue, especially when this code is a high-rate code

with a high minimum distance. The existing algorithms suggest to focus on the Tanner graph and to derive some attractors with cycle enumerators in order to predict the error floor. Here we just want to identify some of the smallest TS's in order to design decoders with better performance on these TS's compared with the classical decoders (min-sum/BP).

On the QC-LDPC code of length 4995, it is not possible (in a reasonable simulation time) to obtain error patterns of weight less than 15. We simulate the performance of both min-sum and BP decoders on the BSC starting at a fixed α. We then collect the error patterns with a maximum weight of 40. The idea is next to claim that if a binary vector is an error event, it is because the bits initially in error in the Tanner graph are located in the neighborhood of an attractor from which he cannot escape. With this obvious statement we develop an iterative method to identify those attractors. From the error patterns collected, we run again the simulations on the BSC, recording for each bit the frequency of decision in error for each of them during the decoding (basically during 100 iterations maximum). From this records we can extract the indices of the variable nodes often decided in error (practically we use a threshold on the percentage of iterations spent by a variable decided in error). We then run again the decoding with this new vector as an input vector and we keep recording the indices of the variable nodes decided in error by eventually increasing the percentage. Once the method converges to a fix point, we obtain one attractor (with a low-weight) derived from the original error event.

Remark: This procedure does not necessarily converge to a TS, as it can also converge eventually to the original codeword sent: in this case no attractor is found. We want also to precise that we are not claiming that using this method, each error-pattern will output a low-weight harmful topology, but if this error pattern is "close enough" to an harmful structure, this procedure should capture the effect of it.

In the following we propose the formalization of the method, and then two examples are explained to show the extraction of two TS's containing 8 bits.

2.5.1 Scheme of the proposed algorithm

We consider a decoder $\mathcal{D}$ on the BSC with a transition probability α on a LDPC code of length N.

1. Simulate the frame error rate at $\alpha = \alpha_0$ in the mid-SNR region.

2. Take an error pattern $\underline{E_0}$ of weight w_0 (which is not already an attractor, ie. which evolves during the decoding).

3. Initialize $i = 0$, and the threshold percentage τ=50%

4. Simulate again E_i at $\alpha_{i+1} = \frac{w_i}{N}$

5. If E_i is still an error pattern :

   (a) Record the frequency $\underline{f^{(i)}} = \{f_1^{(i)}, f_2^{(i)}, ..., f_N^{(i)}\}$ of bits $\{b_1, ...b_N\}$ decided in error during the decoding

   (b) $\underline{E_{i+1}} = \{b_k | f_k^{(i)} \geq \tau\}_{(k=1...N)}$

   (c) $i = i + 1$ Redo step 4. until $\underline{E_{i+1}} = \underline{E_i}$

The idea of the algorithm is the following one : if a bit is decided in error more than half of the decoding time in error, it means that it is involved in some attractors that make the decoding fail. We point out that the selection of the original error event is very important. We need to select an error event that evolves during the decoding, which means that the decided output vector changes from one iteration to another.

A weakness of this algorithm concerns the time of convergence in the decoding. With a high length code, some vectors can be error events in 100 iterations, but they can be corrected in 150 iterations. We want here to select "real" error events, for which the decoder is trapped in an attractor no matter the number of iterations done. Practically the threshold percentage is iteration dependent. We obtained the best results with a low starting percentage (around τ=20%) and finishing at a very high percentage (around τ=90%).

To illustrate this algorithm we propose two examples. The first one with a constant percentage and the second one with an adaptive one.

2.5.2 Examples of the extraction of a minimal trapping set

2.5.2.1 Example 1 : Fix percentage - τ=50%

This first example shows that from an error event of weight 18, we derive a TS whose induced subgraph contains 8 variable nodes while keeping the threshold at 50%. The method starts with the original error event of weight 18 decoded with the BP decoder. At the end of the 100 decoding iterations we keep the bits decided in error more than 50% of the decoding time - there are 9 with an average number of iterations decided in error of 79. We feed these bits to the decoder as a new error event, and we record the bits decided in error more than 50% of the time. At the third iteration our algorithm has converged, the 8 bits decided more than 50% of the time in error are the same as the ones in error at the input of the decoder with an average number of iteration decided in error of 97. The induced subgraph of the corresponding bits is a TS. In three iterations of this procedure we obtained the TS shown in Fig 2.13. Moreover we checked that when the 8 bits of this TS are initially in error, the decoding fails.

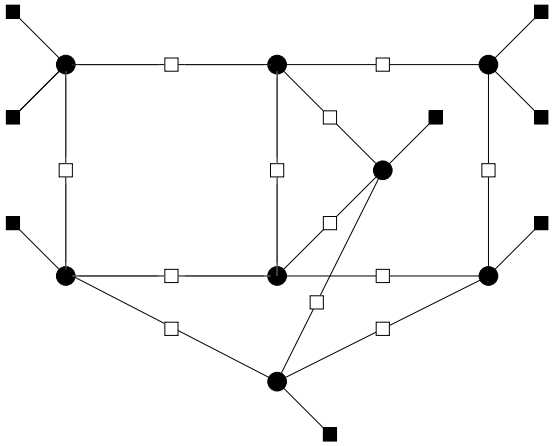

Figure 2.13: Extracted TS from Example 1 – denoted (8,4,2) TS.

2.5.2.2 Example 2 : Adaptative percentage - 30% $\leq \tau \leq$ 70%

This second example starts from an error event obtained of weight 16. The algorithm is slightly modified because the values of the percentage evolve with the iterations. Indeed we start with τ=30% to end up to τ=70%. We have to consider dynamic τ because we witnessed that the error event is quite far from the bad attractor we want to reach. By starting with a lower τ, we can "follow" better the evolution of the errors, and get closer to bad attractors.

During the first four iterations we then keep τ=30%. Once the output error event is the same as the input one, we increase τ to 55% and then to 70% until we obtain a low-weight error pattern, in this case with 8 bits. The evolution of the procedure for this example is summarized in the Table 2.11. The obtained TS is depicted in the Fig. 2.5.2.2. It is pretty easy to see that the absence of two odd-degree check nodes on one variable node, leads to a highly harmful structure, indeed the BP cannot correct all the 6-error event in it.

Table 2.11: Steps of the algorithm - Example 2

Iteration	Threshold τ	Error event weight	Number of bits with an error decision frequency $\geq \tau$	Average number of iterations for the bits with an error decision frequency $\geq \tau$
1	30%	16	9	56
2	30%	9	10	58
3	30%	10	11	77
4	30%	11	11	85
5	55%	11	9	92
6	70%	9	8	94

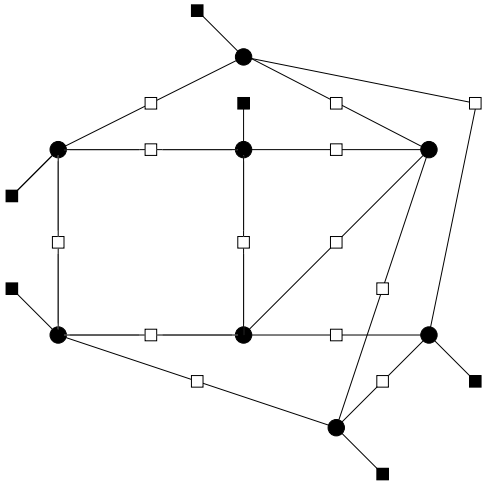

Figure 2.14: Extracted TS from Example 2 – denoted (8,6,0) TS

2.5.2.3 Structures extracted

Similarly to the two previous examples, we extracted the topological structures for the BP and/or the min-sum decoder. We used the two decoders, as we witnessed that some error events for the BP decoder were not harmful when the min-sum decoder was used. We extracted a small database of structures for which the classical decoders fail for 8, 7, 6 and even 5 errors. We present in the Table 2.12 the number of bits that a given decoder can correct on the whole code using the new notation we propose to denote TS for column-weight-four code:

Definition 2.1. *Let* $\mathbf{T}(\mathbf{y})$ *be a TS. This TS is denoted* (a, b, c) *TS, where* $a = |\mathbf{T}(\mathbf{y})|$*, whose induced subgraph has* b *variable nodes connected to one odd-degree parity-check node, and* c *variable nodes connected to two odd-degree parity-check nodes.*

Remark : For the column-weight-three LDPC code, the former notation still stands with a $(a, b, 0)$ TS.

The Fig. 2.15(a) presents one of the most harmful structures that we found in the QC-LDPC code, hence 5 errors cannot be corrected for the BP decoder. The Fig. 2.15(b) presents another structure on which the BP cannot correct more than 6 errors.

2.5.2.4 Proposed decoder on the BSC

We now present the decoders that have been designed for this particular QC high-rate code. The update function at the check nodes is still taken to be the update rule of the min-sum decoder presented in the beginning of the chapter in Eq. (2.1).

On the variable node we can still define a FAID map Φ_v as for the column-weight-three LDPC code with an array. With $d_v = 4$ this array for $y_i = -C$ for a 5-level FAID

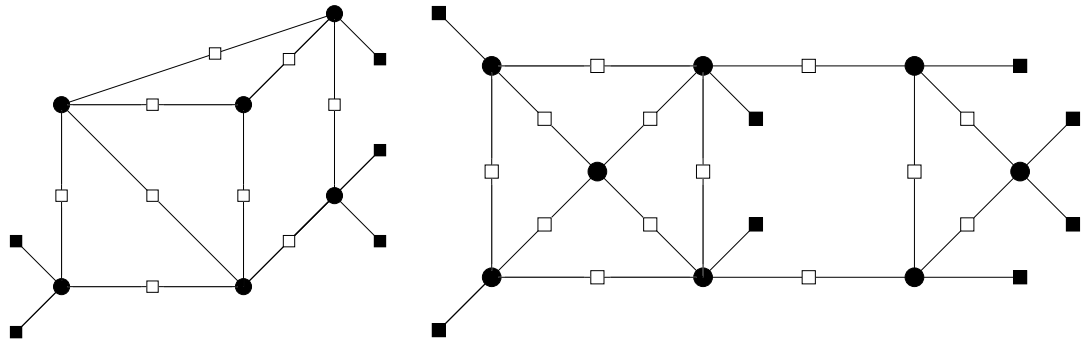

(a) (6,2,2) TS (b) $(8,6,1)_2$ TS

Figure 2.15: Two harmful TS's extracted from the given code.

is now a look-up table given by :

m_1	m_2	m_3	$\Phi_v(-C, m_1, m_2, m_3)$
$-L_2$	$-L_2$	$-L_2$	$-L_2$
$-L_2$	$-L_2$	$-L_2$	$-L_1$
$\vdots$	$\vdots$	$\vdots$	$\vdots$
$+L_2$	$+L_2$	$+L_2$	$+L_2$

where m_1, m_2, and m_3 are the incoming messages.

For $N_s = 7$ levels, this array contains 84 rows, which means we need 84 outputs to design our rule, for $N_s = 15$, this value increases to 680. The number of possible decoders is then very high as soon as we increase N_s. We can certainly not generate all the possible decoders, and then we choose the best one by looking at its characteristics. We then propose to design a FAID using a non-linear equation at the variable nodes, and afterwards we derive the corresponding look-up table.

We propose here the basis of the decoder used on the BSC. The update rule for the designed FAID with m_1, m_2, m_3 as incoming messages, is given by

$$\Phi_v(-C, m_1, m_2, m_3) = sign(S) \times \left\lfloor \max\left(\left(\sqrt{|S|} - \rho_{off} \right), \frac{N_s - 1}{2} \right) + 0.5 \right\rfloor \quad (2.6)$$

$$\text{where : } \begin{cases} S & = & s_1 m_1^2 + s_2 m_2^2 + s_3 m_3^2 + s_C C^2 \\ s_i & = & sign(m_i) \\ \lfloor . \rfloor & : & \text{Floor function} \\ |.| & : & \text{Abs function} \\ C & \in & \mathbb{R} \\ \rho_{off} & \in & [0, 1] \end{cases}$$

This decoder is a multi-level decoder, as the output of the variable node will belong to the alphabet due to the saturation value at $\frac{Ns-1}{2}$ and the floor function. Note that we assign integer value to the alphabet level, such that $\tilde{\mathcal{M}} = \{-\frac{Ns-1}{2}, ..., 0, ..., +\frac{Ns-1}{2}\}$. The idea of the decoder is to compute a quadratic sum taking into account the signs of the messages, and then flatten out the results with the square root. We add the offset parameter ρ_{off} to be able to design more decoders, and to improve its performance. The different value for C is providing different FAIDs, we select the FAIDs with the highest DE threshold as potential candidates, and then simulate them on the given code.

The 3-bit decoder presented in the next section (on 7 levels) has the parameters $|C| = 2.5$, $\rho_{off} = 0.2$. The 4-bit decoder presented in the next section (on 15 levels) has the parameters $|C| = 3.5$, $\rho_{off} = 0.5$. These two decoders are the best FAIDs we were able to design, although it is likely that better FAIDs for column-weight-four code can certainly be designed.

2.5.2.5 Performance of the decoder

The performance curves are shown in Fig. 2.16. We can observe the improvement in the performance with our decoder especially with 15-level FAID (performing on 4 bits of precision). Indeed this error rate curve of the designed FAID is stuck to the one of the min-sum decoder and slightly better in the beginning of the error floor. In order to illustrate the improvement of the performance of the designed FAIDs in the error floor, we compare their error correction capability on the structures extracted in the previous section with the min-sum and BP decoder. These results are summarized in the Table 2.12. We can see that the designed finite precision decoders correct at least the same number of errors, and even more in some cases. The TS of the Fig. 2.15(a) is actually a TS only for the min-sum and BP decoders, as the designed FAIDs can correct the 6 bits inside.

2.6 Conclusion

In this chapter we have introduced a new class of low-complexity iterative decoders, the FAIDs. After a complete description of their structures we have shown their outstanding performance in the error floor region, as we have shown that FAIDs on 7-level, hence using 3-bit of precision, were able to surpass the traditional BP decoding. Given the high number of possible FAIDs which can be designed, we tackle the issue of the selection of FAIDs. At first we studied deeply the famous Tanner code to show that based on the minimal codeword we could select the best 5-level and 7-level FAIDs on this particular code. For more complicated codes, where the codewords cannot be listed easily, we propose a methodology based on the concept of *noisy critical number*

Table 2.12: Maximum Number of correctable bits per FAID and per TS

	Maximum Number of bits correctable			
Trapping sets	Min-sum	BP	3-bit FAID	4-bit FAID
TS(6,2,2)	5	5	**6**	**6**
$TS(6,4,1)_1$	5	5	**6**	**6**
$TS(6,4,1)_2$	5	5	5	5
TS(7,2,2)	6	6	6	6
TS(7,4,2)	6	6	6	6
TS(8,4,2)	7	6	**7**	**7**
TS(8,6,0)	6	6	6	6
$TS(8,6,1)_1$	7	7	7	7
$TS(8,6,1)_2$	6	6	**7**	**7**
TS(9,2,3)	7	7	7	7
$TS(9,6,2)_1$	8	8	8	8
$TS(9,6,2)_2$	8	7	**8**	**8**
TS(10,4,2)	7	7	**8**	**8**

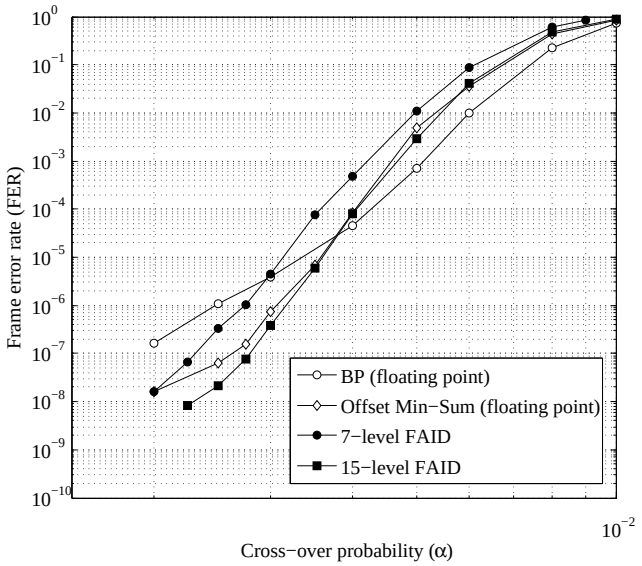

Figure 2.16: Performance comparisons between the floating point decoders: BP and offset min-sum, and the 7-level and 15-level FAIDs design for the given column-weight-four code.

and *decoder domination* to extract the best FAIDs on column-weight-three codes. We also provided an embryo of methodology for a girth-six column-weight-four LDPC code where harmful structures are not completely known. Based on the observations

of the min-sum and BP decoder during the decoding process, we were able to extract some harmful structures of the given code. We then designed finite precision FAIDs whose error correction capabilities were better than the min-sum and/or BP. The simulation results confirmed that a FAID using 3-bit can also surpass the BP for a column-weight-four LDPC codes.

The next work implies to find an efficient and systematic methodology to design FAIDs for column-weight-four codes possibly by deriving them from the identified good FAIDs for column-weight-three codes, although it is now obvious that good FAIDs for column-weight-three codes will engender good FAIDs for column-weight-four codes. The next step is obviously to tackle the more common channel, the AWGNC, in which the issue of the quantization of the channel will be the core of the analysis.

Chapter 3

Compressed Sensing: Introduction and Reconstruction Methods

In this chapter we present a descriptive review of the work done in the last few years in the emerging field of compressed sensing, also called compressive sensing. We remind the original problem setting, and the main relevant reconstruction methods proposed in the last few years.

For the sake of clarity of the manuscript, we only refer to algorithms that we found worth mentioning among the large amount of methods in the literature regarding compressed sensing.[1]

3.1 Introduction

The Compressed Sensing (CS) problem as it has been suggested by Candès, Romberg and Tao [77, 78] and Donoho [79] aims at detecting a compressed or compressible signal with many less measurements than the Nyquist-Shannon sampling theorem would suggest. In the case of an analogous signal, the sampling theorem demonstrates that the number of samples that needed to be taken to recover completely the original signal needs to be at least twice its bandwidth. However in the case of a sparse signal (potentially in a certain basis), the Compressed Sensing provides a different approach which reduces drastically the number of samples that need to be acquired and then stored for a signal. This property of reducing the number of samples taken in a sparse signal explains the massive interest around this recent field of the signal processing.
The applications of the Compressed Sensing are numerous, as the assumption of spar-

[1] An important database of papers on the compressed sensing topic can be found in the Digital Signal Processing group website at Rice University [75] and some up-to-date articles and papers as well as some interesting discussions in [76].

sity can make sense in many topics of the signal processing. To name a few, let us remind that the wavelet decomposition [80] generally provides a sparse approximation of a given image. We remind a well known decomposition on the Fig. 3.1. It is pretty clear that the majority of the coefficients of this image have a small absolute value and can be considered as sparse, or pseudo-sparse if we consider that the sparsity is defined by the number of non-zero coefficients. Other domains of the signal processing are concerned by compressed sensing, like the radar [81], imaging [82], the digital communications [83] or even the biomedical [84] as long as a sparse representation of a signal exists in some basis. Applications of compressed sensing can also be found in genetics, as it is stated in [85], in the case we want to study n genes doing some analysis on m patients. Commonly only a few genes will be active for each patient, hence the sparsity. Many other examples can be found in the literature. We continue this chapter by introducing rigorously the compressed sensing setting.

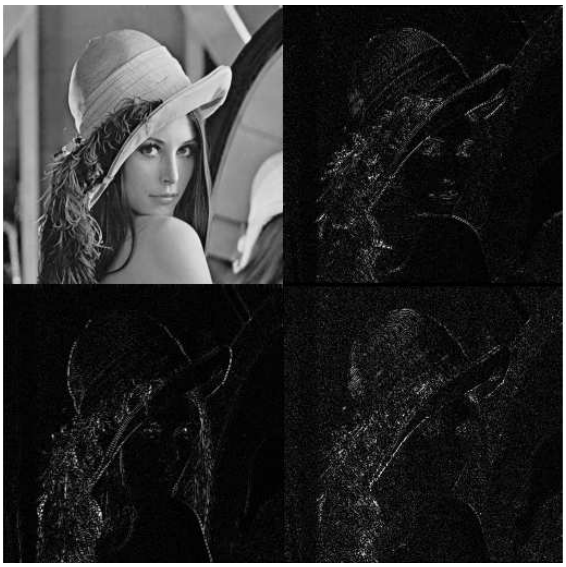

Figure 3.1: Wavelet decomposition of Lena image

3.2 Problem setting and original solver methods

The original Compressed Sensing problem is to recover a high-dimensional vector from a lower dimension set of linear equations. We then consider a signal $\mathbf{s} \in \mathbb{R}^N$, and we suppose that a certain basis $\mathbf{\Psi}$ provides a K-sparse representation of $\mathbf{s}$ such that $\mathbf{s} = \mathbf{\Psi x}$ with $\|\mathbf{x}\|_0 = K$. This vector $\mathbf{s}$ is not measured directly, but instead M projections of $\mathbf{s}$ are taken where $M < N$. The projection vector is denoted $\mathbf{y}$ such that

$$\mathbf{y} = \mathbf{\Phi s} \tag{3.1}$$

with $\mathbf{y}$ a $M \times 1$ column vector and $\mathbf{\Phi} \in \mathbb{R}^{M \times N}$ being the measurement matrix, also called the sampling matrix. Since $M < N$ the recovery of the signal $\mathbf{x}$ from $\mathbf{y}$ is in general not possible; however the assumption of a sparse signal makes the reconstruction possible and practical.

As the sparse representation of $\mathbf{s}$ in the basis $\mathbf{\Psi}$ is $\mathbf{x}$, the recovery of $\mathbf{s}$ from $\mathbf{y}$ can be formulated as the ℓ_0-norm minimization problem on $\mathbf{x}$:

$$\tilde{\mathbf{x}} = argmin \|\mathbf{x}\|_0 \text{ s.t. } \mathbf{y} = \Phi\mathbf{s} = \mathbf{\Phi\Psi x}. \tag{3.2}$$

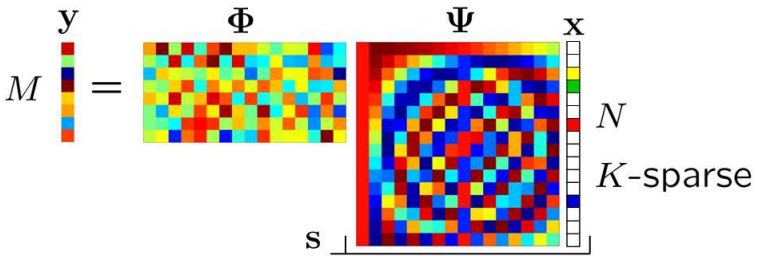

Figure 3.2: Traditional vision of the compressed sensing

This problem is often depicted as the Fig. 3.2 where $\mathbf{\Psi}$ is the basis matrix providing a sparse approximation of $\mathbf{s}$, and $\mathbf{\Phi}$ being the measurement matrix. In other words we look for the sparsest vector $\mathbf{x}$ such that $\mathbf{y} = \mathbf{\Phi\Psi s}$. This problem can be also viewed as finding a K-term approximation to $\mathbf{y}$ from the columns of the basis $\mathbf{\Phi\Psi}$, which is called the *holographic basis* because of the complex pattern in which it encodes the sparse signal coefficients [79]. This problem is sometimes called *recovery via combinatorial optimization* and is known to be NP-hard as the decoder needs to perform a combinatorial enumeration of all the $\binom{N}{K}$ possible sparse subspaces. Hence it cannot be used for practical applications.

Practically, a much easier problem yields an equivalent solution by solving for the ℓ_1-sparsest coefficients $\mathbf{x}$ that agree with the measurements $\mathbf{y}$. This reconstruction is known as the ℓ_1-norm minimization, or the *recovery via convex optimization*

$$\tilde{\mathbf{x}} = argmin \|\mathbf{x}\|_1 \text{ s.t. } \mathbf{y} = \mathbf{\Phi s} = \mathbf{\Phi\Psi x}. \tag{3.3}$$

This optimization is more tractable and can be solved by a linear programming technique called *Basis Pursuit (BasP)* [86]. The complexity of this technique is polynomial in N, more precisely $\mathcal{O}(N^3)$.

In the sequel we will only consider the reconstruction of the sparse vector $\mathbf{x}$ from the observation vector $\mathbf{y}$ with the measurement matrix $\mathbf{A}$ such that we are trying to

solve

$$\mathbf{y} = \mathbf{A}\mathbf{x}. \tag{3.4}$$

In other words we either assume the basis $\mathbf{\Psi}$ being taken as the identity matrix and $\mathbf{A} = \mathbf{\Phi}$, and hence our signal is sparse in the basis of the study, or that $\mathbf{\Phi\Psi} = \mathbf{A}$. This little modification in the problem will simplify the notations for the rest of the manuscript.

In [78] it has been shown that the ℓ_1-norm minimization technique performs the exact reconstruction of the vector $\mathbf{x}$ for a sufficient sparsity and a properly chosen measurement matrix $\mathbf{A}$. The conditions on the measurement matrix were expressed in terms of the *Restricted Isometry Property* (RIP).
We say that $\mathbf{\Phi}$ has RIP of order K if for every K-sparse vector $\mathbf{v}$, and for constant $0 \leq \epsilon \leq 1$

$$(1-\epsilon)\left\|\mathbf{v_K}\right\|_2^2 \leq \left\|\mathbf{A_K v_K}\right\|_2^2 \leq (1+\epsilon)\left\|\mathbf{v_K}\right\|_2^2 \tag{3.5}$$

where $\mathbf{v_K}$ is the mutilated vector $\mathbf{v}$ constituted of the K non-zero elements of $\mathbf{v}$, and $\mathbf{A_K}$ corresponding to the matrix formed by the extracted columns of $\mathbf{A}$ which corresponds to the K indices of the non-zero elements of $\mathbf{v}$. In other words the RIP indicates that the matrix $\mathbf{A}$ does not distort too much the ℓ_2-norm of any K-sparse vector.

The RIP gives the following interesting property: for a K-sparse vector $\mathbf{x}$ we can take the number of measurements M on the order of $K\log(N/K)$. It is also important to notice that the RIP provides an insurance of the output of the BasP to be the same output as the ℓ_0 minimization, however it can be different from the original vector $\mathbf{x}$.

3.3 Iterative reconstruction methods

3.3.1 Introduction

Soon after the seminal works of Candès, Tao, Romberg and Donoho, many studies have been led in order to tackle the complexity of the ℓ_1-minimization reconstruction technique. The main goal was to propose a variation of the LP solver providing good reconstruction performance with a lower complexity. Among all the proposed methods, we cite here some famous greedy algorithms like the Matching Pursuit [87], the Orthogonal Matching Pursuit (OMP)[88, 89], or Stagewise OMP [90]. The main idea of these greedy algorithms consists in the iterative approximation of the coefficients of the sparse signal to recover. They are known to be very fast and easy to implement, and guarantee the performance to be close to the original ℓ_1-minimization. Many other algorithms exist in the literature, the chapter 8 of [91] presents an overview of the greedy algorithms used in compressed sensing.

Other methods for recovering sparse signal from an undetermined system of equations have been suggested equivalently to the message-passing decoder in channel coding. The first work mentioning this type of reconstruction methods is in [92]. In this chapter we give an overview of the iterative reconstruction methods starting by exploring the link between message-passing algorithms in compressed sensing and in channel coding. Then we present the current knowledge in the use of LDPC matrices as measurement matrix. Finally we explore some of the iterative reconstruction methods.

3.3.2 Motivation for message-passing reconstruction methods

The success of sparse codes in channel coding such as the Low-Density Parity-Check (LDPC) codes [1, 15] has strongly suggested that the use of sparse compressed matrices needed to be explored in the compressed sensing case.

As we already mentioned, in a communication system, a codeword x containing N bits is transmitted through a noisy channel. The noise added by the channel to the original information can be modeled as an error vector $\mathbf{e}$ added to the codeword $\mathbf{x}$. In the case of the binary symmetric channel (BSC) this error vector is binary, in the case of an AWGNC, the samples of $\mathbf{e}$ are drawn for a Gaussian distribution. The output vector is defined as $\mathbf{y} = \mathbf{x}+\mathbf{e}$, and the addition is proceeded accordingly to the channel (binary addition for the BSC, real addition for the AWGNC). Although this has been already presented, let us briefly remind that an LDPC code is defined by its parity-check matrix $\mathbf{H}$ of size $M \times N$ with $N > M$. The particularity of $\mathbf{H}$ is its sparsity, as the number of non-zero elements in $\mathbf{H}$ decreases in $1/N$. The sparsity of $\mathbf{H}$ and then its equivalent bipartite Tanner graph [16] plays a key role in the decoding process. Indeed the decoding will be simplified by running a low-complexity message-passing algorithm (such as the belief propagation, or the FAID presented in the chapter 1) to decode $\mathbf{y}$ and then recover $\mathbf{x}$.

One possible link between compressed sensing and LDPC codes stands in the property of $\mathbf{H}$. Indeed we remind that, from the construction of $\mathbf{x}$ we have $\mathbf{Hx} = \mathbf{0}$. If we consider a sparse noisy vector $\mathbf{e}$, the output of the channel can be transformed in $\tilde{\mathbf{y}} = \mathbf{Hy} = \mathbf{H}(\mathbf{x} + \mathbf{e}) = \mathbf{He}$. Then $\mathbf{H}$ can be viewed as a measurement matrix, and by applying the reconstruction method of the compressed sensing, we can recover $\mathbf{e}$ and then $\mathbf{x}$.
In the following we consider $\mathbf{H}$ as equivalently a parity-check matrix, or a measurement matrix.

3.3.3 LDPC measurement matrices

The relation between the theory of LDPC codes and compressed sensing was explored in the work of Dimakis and Vontobel [93], who studied the relation between two linear

programs: the BasP of compressed sensing which can be restated as a Linear Program (LP) and the so-called LP-decoder [94] of a related LDPC code. (The LP decoder is a sub-optimal decoder whose performance is governed by the parity-check matrix used to define the LP constraints.) It was shown in [93] that a binary matrix $\mathbf{H}$ which is a good parity-check matrix for LP decoding of the corresponding LDPC code is also a good measurement matrix for BasP in the respective compressed sensing problem over a binary alphabet. The contraposition gives that "bad" measurement matrices in compressed sensing will have "bad" performance results in the channel coding side. Besides it is shown that the basis pursuit using the matrices constructed by Gallager [1] form the best known sparse measurement matrices that maximize the recovery of sparse signals using these sparse measurement matrices. We already mentioned that a *sufficient* condition to certify that a given measurement matrix is "good" is that this matrix follows the RIP. However the RIP is an incomplete characterization of the LP relaxation of "good" measurement matrices [95]. A *necessary and sufficient condition* for a measurement matrix to be "good" requires that the matrix $\mathbf{H}$ respects the *nullspace* condition. The attribute "good" means here that the ℓ_0-minimization and the ℓ_1-minimization (BasP) outputs the same estimate $\hat{\mathbf{x}}$. Dimakis *et al.* [96] presented a necessary and sufficient condition for a good measurement matrix for k-sparse signals. While Restricted Isometry Property (RIP) provides a sufficient condition for a good measurement matrix for compressed sensing, Null Space Property (NSP) which is defined below, provides the necessary and sufficient condition for a good compressed sensing measurement matrix. Let V be the set of columns of a measurement matrix $\mathbf{H}$ and the null-space $\mathrm{NSpace}(\mathbf{H}) = \{\omega \in \mathbb{R}^n : \mathbf{H}\omega = \mathbf{0}\}$. The measurement matrix H has the Null Space Property (NSP) if for $k \in \mathbb{Z}_{\geq 0}$, $c \in \mathbb{R}_{\geq 0}$ and $I' = V \backslash I$.

$$c\| \omega_I \|_1 \leq \| \omega_{I'} \|_1 \ \forall\, \omega \in \mathrm{NSpace}(\mathbf{H}),\ \forall I \subseteq V,\ |I| \leq k$$

Before giving the main result representing the connection between channel coding and compressed sensing, a summary of LP decoding and some related definitions are explained.

Let $\mathcal{C}$ be a binary linear code and let $\mathbf{H}$ be a parity-check matrix of $\mathcal{C}$ with the set of columns V and the set of rows C. For every $j \in C$, let h_j be the j^{th} row of H and let

$$\mathrm{Null}_{\mathcal{C}}(j) = \{x \in \{0,1\}^n | \sum_{i \in V} h_{ji}.x_i = 0 \mod 2\}.$$

Then, the *fundamental polytope P* of $\mathbf{H}$ is defined as $P(\mathbf{H}) = \bigcap_{j \in C} \mathrm{conv}(\mathrm{Null}_{\mathcal{C}}(j))$, where $\mathrm{conv}(\mathrm{Null}_{\mathcal{C}}(j))$ is the convex hull of $\mathrm{Null}_{\mathcal{C}}(j)$. The conic hull of $\mathbf{H}$ is called *fundamental cone* and is denoted by $\mathcal{K}(\mathbf{H})$. Hence,

$$\mathcal{K}(\mathbf{H}) = \mathrm{conic}(P(\mathbf{H})) = \bigcap_{j \in C} \mathrm{conic}(\mathrm{Null}_{\mathcal{C}}(j)).$$

The LP decoding [94] tries to solve the following optimization problem.

$$\text{minimize} \ \sum_{i=1}^{n} \lambda_i . f_i \quad \text{s.t.} \quad f \in P(\mathbf{H})$$

where $\lambda_i = \log \frac{\Pr(y_i|0)}{\Pr(y_i|1)}$ and $\mathbf{y} = (y_1, y_2, ..., y_n)$ is the received word. In analyzing the performance of LP decoder, it is assumed that the all-zero codeword is transmitted. So, the LP decoder will succeed on decoding when the all-zero codeword has the lowest value on the cost function $\sum_{i=1}^{n} \lambda_i . f_i$ compared to the all non-zero vectors in $\mathcal{K}(\mathbf{H})$. With these preliminaries, the fundamental connection between channel coding and compressed sensing is provided as follows.

Let $\mathbf{H}$ be a zero-one measurement matrix, then

$$\omega \in \text{NSpace}(H) \Rightarrow |\omega| \in \mathcal{K}(\mathbf{H}).$$

This result was also extended to a measurement matrix $\mathbf{H}$ with entries in $\mathbb{C}$ such that $|H_{ij}| \in \{0, 1\}$ for all $(i, j) \in V \times C$ (*Lemma 12* [96]). Also, based on definitions of *pseudo-weight* on BSC, BEC and AWGNC, they provided some results for performance guarantee of compressed sensing LP-decoder. The minimum binary symmetric channel (BSC) pseudo-weight $w_p^{BSC,min}(\mathbf{H})$ is defined in the Definition 9 of [93], and brings the following theorems:

Theorem 3.1. *If* $\mathbf{H}$ *is a parity-check matrix of a LDPC code* $\mathcal{C}$ *and* $w_p^{BSC,min}(\mathbf{H}) > 2K$ *then linear programming decoding will successfully decode any output from the BSC with at most* K *errors.*

Theorem 3.2. *If* $\mathbf{H}$ *is a 0-1 measurement matrix that satisfies* $w_p^{BSC,min}(\mathbf{H}) > 2K$ *and* $\mathbf{x}$ *is* K*-sparse then BasP and the* ℓ_0*-minimization will output the same estimate* $\hat{\mathbf{x}}$ *given* $\mathbf{y} = \mathbf{H}\mathbf{x}$*.*

Moreover, using expander graphs, they obtained threshold results (strong and weak bounds [96]) for compressed sensing LP-decoder and provided a discussion on construction of good measurement matrices with large girth.

3.3.4 Message-passing reconstruction methods

To tackle the issue of the complexity of LP solver, and similarly to channel coding, low-complexity algorithms have been introduced. These algorithms primarily used the graphical representation of the measurement matrix to exchange information iteratively to recover the original vector $\mathbf{x}$. As for the Tanner graph of LDPC codes, the columns of the measurement matrix are associated with the variable nodes corresponding to the vector $\mathbf{x}$, and the rows of the measurement matrix correspond to the summation

nodes, also called measurement nodes, or even check nodes to make the bridge with the graphical representation of an LDPC matrix.

3.3.4.1 Message-passing and approximate message-passing

A first message-passing algorithm was introduced by Donoho *et al.* in [92] for noise free measurements. The variables in message-passing algorithms are associated with edges in the bipartite graph representation of the matrix $\mathbf{A}$. Messages are updated according to the rules

$$\begin{aligned} x_{i\to a}^{(l+1)} &= \eta_l\Big(\sum_{b\in N(i)\setminus a} A_{b,i} z_{b\to i}^{(l)}\Big) \\ z_{a\to i}^{(l)} &= y_a - \sum_{j\in N(a)\setminus i} A_{a,j} x_{j\to a}^{(l)} \end{aligned} \tag{3.6}$$

where a and b are measurement nodes, i and j are variable nodes, η_l is a sequence of threshold functions (applied componentwise), $\mathbf{x}^{(l)} \in \mathbb{R}^n$ is the current estimate of the solution $\mathbf{x}$, $\mathbf{z}^{(l)} \in \mathbb{R}^n$ is the current residual and $N(v)$ is the set of neighbor nodes of the node v in the Tanner graph.

Donoho's *et al.* [92] iterative thresholding algorithm, called the *approximate message-passing* (AMP) follows from the message-passing algorithm given in (3.6). The authors of [92] argue that the right side of the equation for update of messages $x_{i\to a}^{(l)}$ in (3.6) does not depend strongly on the index a (specially if the matrix A is dense in which case only one out of n terms is excluded). They also argue that the right-hand side of the equation for updating $z_{a\to i}^{(l)}$ does not depend strongly on i. If these two dependencies are neglected, the messages are associated to graph vertices (x to variable nodes and z to summation nodes), and the algorithm has a flavor of a bit flipping algorithm [97]. In contrast to message-passing which in general has to update nm messages, the bit flipping algorithms update only n variable nodes and m summation nodes.

The first algorithm [92] starts from an initial guess $\mathbf{x}^{(0)} = \mathbf{0}$ and $\mathbf{z}^{(0)} = \mathbf{y}$, and iteratively proceeds by calculating

$$\begin{aligned} \mathbf{x}^{(l+1)} &= \eta_l(\mathbf{A}^T\mathbf{z}^{(l)} + \mathbf{x}^{(l)}) \\ \mathbf{z}^{(l)} &= \mathbf{y} - \mathbf{A}\mathbf{x}^{(l)} + \frac{1}{\delta}\mathbf{z}^{(l-1)}\langle \eta'_{l-1}(\mathbf{A}^T\mathbf{z}^{(l-1)} + \mathbf{x}^{(l-1)})\rangle, \end{aligned}$$

where η_l is a sequence of threshold functions (applied componentwise), $\mathbf{x}^{(l)} \in \mathbb{R}^n$ is the current estimate of the solution $\mathbf{x}$, $\mathbf{A}^T$ denotes the transpose of $\mathbf{A}$ and $\eta'(\mathbf{u}) = \partial\eta(\mathbf{u})/\partial\mathbf{u}$. The bracket $\langle\rangle$ operator applied on a vector $\mathbf{v} = (v_i)_{1\le i\le n}$ gives $\langle\mathbf{v}\rangle = (1/n)\sum_{1\le i\le n} v_i$. The role of the additional term in the update of $\mathbf{z}^{(l)}$ is to cancel

the correlation between the present vector estimates and their past values. A typical thresholding function η is the *soft thresholding* given by

$$\eta(\mathbf{x};\lambda) = \text{sgn}(\mathbf{x})(|x| - \lambda)_+$$

where the subscript $(u)_+ = u\mathbb{I}(u \geq (0))$, and $\mathbb{I}$ is the indicator function equal to one when the Boolean expression in his argument is true, and zero otherwise. An algorithm by Tropp and Wright [98] uses slightly modified update equations

$$\begin{aligned} \mathbf{x}^{(l+1)} &= \eta_l((1/c)\mathbf{A}^T\mathbf{z}^{(l)} + \mathbf{x}^{(l)}) \\ \mathbf{z}^{(l)} &= \mathbf{y} - \mathbf{A}\mathbf{x}^{(l)}, \end{aligned}$$

where the constant c is chosen to help the convergence.

Pham *et al.* [99] introduced two low-complexity algorithms, list decoding and multiple-basis belief propagation. The basic idea behind using BP in these algorithms is to identify the columns of the measurement matrix $\mathbf{A}$ that maximizes the correlation with $\mathbf{y}$. The measurement matrix $\mathbf{A}$ is constructed in the following manner. First, an LDPC code $\mathcal{C}$ of length n is considered. Then, all codewords of $\mathcal{C}$ are converted to their Binary Phase Shift Keying (BPSK) images and are normalized by $\frac{1}{\sqrt{n}}$. The normalized BPSK images of codewords are used as the columns of $\mathbf{A}$. In list-based BP algorithm, a list of T vectors based on $\mathbf{y}$, a biasing value b and sparsity parameter k is constructed. A binary parity-check matrix $\mathbf{H}$ of $\mathcal{C}$ with the row-weight d_c is chosen uniformly from the ensemble of binary matrices of the same size and with the row-weight d_c. Running the BP algorithms gives a list of binary words $\mathbf{w_1}, \mathbf{w_2}, ..., \mathbf{w_T}$. The repeated words or those which do not satisfy $\mathbf{Hw_i} = 0$ are deleted. The outputs are at most k words whose (BPSK) images have the largest correlation with $\mathbf{y}$.

In case of a non-binary vector $\mathbf{x}$, they proposed another algorithm, multiple basis belief propagation (MBBP) which uses more than one parity-check matrix to find the columns of $\mathbf{A}$ with the largest correlation with $\mathbf{y}$. The MBBP algorithm begins with initializing the sparsity parameter k, the measurement vector $\mathbf{y}$ and γ parity-check matrices $\mathbf{H_1}, \mathbf{H_2}, ..., \mathbf{H}_\gamma$. The interference is modeled as a zero-mean Gaussian variable with the variance $\sigma^2 = \max(|\mathbf{y}|)\frac{k-1}{k}$. Running BP algorithm for the received vector $\mathbf{y}$ and using the parity-check matrix $\mathbf{H_i}$ $(i = 1, 2, ..., \gamma)$ outputs a word $\mathbf{w_i}$. The words $\mathbf{w_i}$ which do not satisfy $\mathbf{H_i w_i} = 0$ are deleted and the codeword whose BPSK image has the largest correlation with $\mathbf{y}$ is set to be output.

Combination of the list decoding with Orthogonal Matching Pursuit (OMP), (*Algorithm 2: BP-OMP Algorithm* in [99]), has an asymptotic optimal performance with computational complexity $O(kT \log n)$. Also, the simulation results show that both algorithms, list decoding and MBBP, have good performance for recovery of sparse signals.

In the rest of this chapter we present 2 low-complexity algorithms, starting with the

Sparse Matching Pursuit.

3.3.4.2 Sparse matching pursuit

In [100] the authors suggest an algorithm called *Sparse Matching Pursuit* for compressed sensing with sparse measurement matrices. This algorithm can be described as a message-passing algorithm in the context of a K sparse signal. We keep here the scheme $y = Ax$.
Let us remind that the rows of $\mathbf{H}$, labeled $m = 1, \ldots, M$, are the check nodes of the graph representing the values of $\mathbf{y_m}$, and the columns of $\mathbf{H}$, labeled $n = 1, \ldots, N$, are the variable nodes representing the values of $\mathbf{x_n}$. At the l^{th} iteration the message from a variable node n to a check node m is denoted $\mu^{(l)}_{n\to m}$, and the message from a check node m to a variable node n is denoted $\mu^{(l)}_{m\to n}$. These two messages exist only on the edges of the Tanner graph, in other words if $A_{m,n} = 1$. $\mathcal{N}(n)$ (resp. $\mathcal{N}(m)$ denotes the neighbors of the variable node n (resp. check node m). The algorithm of the Sparse Matching Pursuit is given by the Algorithm 1. This algorithm requires a

Algorithm 1: Sparse Matching Pursuit Reconstruction Algorithm

Initialization : $\mu^{(0)}_{m\to n} = y_m$
for *iteration* $l = 1, \ldots, L$ **do**
  for $n = 1, \ldots, N$ **do**
    for $\forall m \in \mathcal{N}(n)$ **do**
      $\mu^{(l)}_{n\to m} = \underset{m' \in \mathcal{N}(n)\setminus m}{median} \left(\mu^{(l-1)}_{m'\to n}\right)$;
  for $m = 1, \ldots, M$ **do**
    for $\forall n \in \mathcal{N}(m)$ **do**
      $\mu^{(l)}_{m\to n} = y_m - \sum_{n' \in \mathcal{N}(m)\setminus n} \left(\mu^{(l)}_{n'\to m}\right)$;

number of measurement M to be on the order of $Klog(N/K)$. The performances are the same asymptotically as the BasP.

Finally, we conclude this introductive chapter on compressed sensing by presenting in detail the most simple algorithm that can be imagined to recover a sparse high-dimensional vector from a set of linear measurements.

3.3.4.3 Verification decoding

In order to reconstruct strictly sparse signals, Zhang and Pfister [101] used two decoding algorithms, LM1 and LM2, based on verification algorithm. The reconstruction method is an iterative algorithm in which the messages correspond to the vertices (variable and check nodes in the factor graph) not to the edges. Hence, the algorithm can be considered as a bit flipping algorithm as introduced in [97]. The decoder is analyzed using density evolution to find the average fraction of verified messages. Then, for each decoder and for regular LDPC code ensembles and strictly sparse signals with $k_n = \lfloor \delta n \rfloor$, they provided a threshold δ^* such that for all $\delta < \delta^*$, iterative decoding can recover the original signal with high probability as $n \to \infty$. Using stopping set analysis, they analyzed the performance of regular LDPC codes in the high-rate regime and found thresholds below than given by density evolution [102]. Then, they generalized their results to the reconstruction of strictly sparse signals in compressed sensing using both uniform reconstruction and non-uniform (randomized) reconstruction. For uniform reconstruction, stopping set analysis and for non-uniform reconstruction, density evolution were used to evaluate the performance of these reconstruction compressed sensing systems. They also showed that randomized reconstruction compressed sensing has linear-time reconstruction for strictly sparse signals.

In this algorithm each variable node can have two states; one *unverified state* (no value has yet been estimated), and one *verified state* (the variable node has been estimated). Note that when a variable has been verified, it cannot be changed anymore. This algorithm is summarized in the following steps and is described in the Algorithm 2:

- **Step** 1. Variable nodes which are the neighbors of zero-value check nodes are verified as 0.
- **Step** 2. Variable nodes connected to check nodes with degree one (only one edge connected) are verified as the value of the check node.
- **Step** 3. A single variable node connected to two check nodes with the same measurement value is verified to the common value of the check nodes.
- **Step** 4. Subtract the values of the verified variable nodes from the neighboring check nodes and then remove all verified variable nodes and edges connected to them.

Steps 1 to 4 are repeated until reconstruction succeeds or no more progress can be done. The Fig. 3.3(a) 3.3(a) and 3.3(c) sketch the Steps 1, 2 and 3. Note that the verification decoding was originally introduced for the q-ary Symmetric Channel [101] . The justification of Step 3 is based on the observation that, over large alphabets, the probability that two independent random numbers are equal (or equivalently two

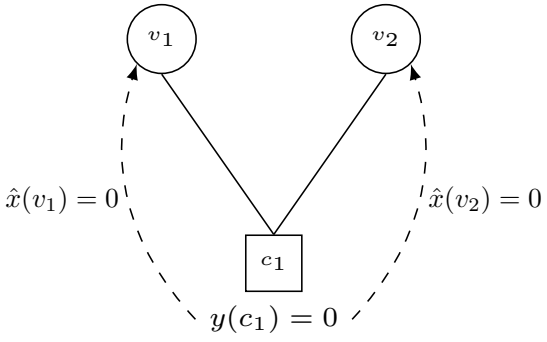

(a) Step 1

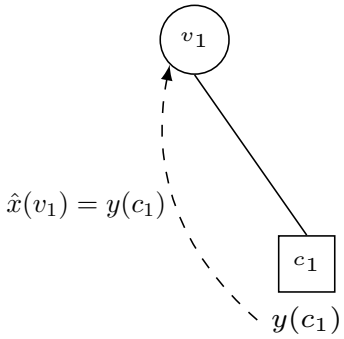

(b) Step 2

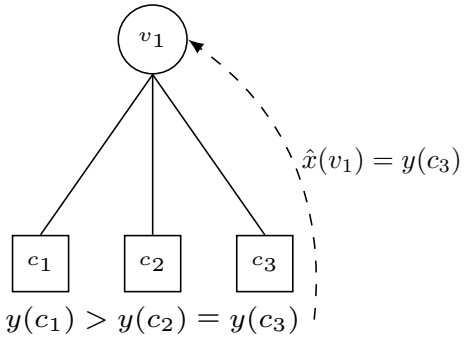

(c) Step 3

Figure 3.3: Steps of the verification decoding algorithm

independent measurements) is quite small. This leads to consider that any two common measured values (during decoding) are generated by the same set of non-zero data. This observation holds for large alphabets and then for the real numbers too. Note that in the Algorithm 2, we added one condition to the Step 3 (Fig. 3.3(b)) to avoid that at one iteration, the value on one check node becomes negative. In the Algorithm 2, L is the maximum number of iterations for the decoding, [*] denotes the unverified state and δ is a precision threshold to check the correct recovery of our signal (practically $\delta \sim 10^{-3}$).

It is pretty easy to see that for a sparse signal $\mathbf{x}$, and a sparse measurement matrix $\mathbf{A}$, the first step will decrease the number of edges that need to be considered and then the complexity will be drastically reduced from one iteration to another. This very low-complexity reconstruction algorithm will provide a benchmark in terms of recovery performance, and we will then be able to estimate the performance of the low-complexity algorithm presented in the next chapter.

Algorithm 2: Verification Decoding

Input : $\mathbf{y}$ and $\mathbf{A}$ such that $\mathbf{y} = \mathbf{Ax}$, L, δ.
Output: $\hat{\mathbf{x}}$ the estimate of $\mathbf{x}$.
$l = 0$;
$\hat{x} = [*, \ldots, *]$;
while $\mathbb{E}\left[|\hat{\mathbf{x}} - \mathbf{x}|^2\right] > \delta$ *or* $l < L$ **do**
1 **foreach** c_j *such that* $y(c_j) = 0$ **do**
$\hat{x}\left(\mathcal{N}(c_j)\right) = 0$;
2 **foreach** c_j *such that* $CheckDegree(c_j) = 1$ **do**
$\hat{x}\left(\mathcal{N}(c_j)\right) = y(c_j)$;
$y\left(\mathcal{N}(v_i)\right) = y\left(\mathcal{N}(v_i)\right) - y(c_j)$ with $v_i = \mathcal{N}(c_j)$;
3 **foreach** (c_j, c_k) *such that* $|\mathcal{N}(c_j) \cap \mathcal{N}(c_k)| = 1$ *and* $y(c_j) = y(c_k)$ **do**
$v_i = \mathcal{N}(c_j) \cap \mathcal{N}(c_k)$;
if $y\left(\mathcal{N}(v_i)\right) - y(c_j) \geq 0$ **then**
$\hat{x}(v_i) = y(c_j)$;
$y\left(\mathcal{N}(v_i)\right) = y(\mathcal{N}(v_i)) - y(c_j)$;
4 **foreach** v_i *such that* $\hat{x}(v_i)$ *is verified* **do**
$A\left(\mathcal{N}(v_i), v_i\right) = 0$;
$l = l + 1$;

Chapter 4

Interval-Passing Algorithm: Description and Analysis

AFTER the review done in the previous chapter on the compressed sensing and the presentation of some reconstruction algorithms we present in this chapter the low-complexity message-passing algorithm developed for the reconstruction of sparse signal, called Interval-Passing Algorithm. This algorithm uses sparse non-negative measurement matrices and has the advantage to perform at a very low complexity, and its performance is very decent compared to some other complex reconstruction methods.

We first provide a complete description of this algorithm with some simulation results and then we provide an complete analysis of it. We also present the link between the reconstruction failures of this algorithm and some particular structures of the graphical representation of the measurement matrix.

4.1 Interval-passing algorithm

Chandar *et al.* [103] introduced a simple message passing algorithm for reconstructing non-negative signals using sparse binary measurement matrices. We modified this algorithm in order to deal with non-negative real-valued measurement matrices and refer to it as interval-passing algorithm (IPA) [104, 105, 106]. From [103], the complexity of the algorithm is $\mathcal{O}(n(\log(\frac{n}{k}))^2 \log(k))$ which is a good trade-off between the polynomial complexity of the LP reconstruction, and the linear complexity of the simple verification decoding [102] presented in the last chapter.

4.1.1 Description of the algorithm

The IPA is an iterative algorithm, and thus messages are associated with the graphical representation of the measurement matrix to perform the reconstruction. Let $V = \{v_1, v_2, ..., v_n\}$ and $C = \{c_1, c_2, ..., c_m\}$ be respectively the sets of variable nodes and measurement nodes[1] in the graphical representation of the measurement matrix $\mathbf{A} = \{a_{j,i}\}$ for $1 \leq j \leq m$ and $1 \leq i \leq n$. The graphical representation of $\mathbf{A}$ is actually the Tanner graph [16] of the binary image[2] of $\mathbf{A}$, whose edges are labeled by the real values corresponding to the non-zero position in $\mathbf{A}$. The graphical representation of $\mathbf{A}$ has the flavor of a non-binary LDPC code Tanner graph [107, 108].

In the IPA, the messages passing through edges are intervals $[\mu, M]$ corresponding to the lower and upper bounds of the estimation of the connected variable node. At each iteration l, the message update from the variable v_i to the measurement node c_j is given by:

$$\mu_{v_i \to c_j}^{(l)} = \max_{c'_j \in \mathcal{N}(v_i)} \left(\mu_{c'_j \to v_i}^{(l-1)} \right) \times a_{j,i} \tag{4.1}$$

$$M_{v_i \to c_j}^{(l)} = \min_{c'_j \in \mathcal{N}(v_i)} \left(M_{c'_j \to v_i}^{(l-1)} \right) \times a_{j,i} \tag{4.2}$$

and the messages from the measurement node c_j to the variable node v_i are updated as:

$$\mu_{c_j \to v_i}^{(l)} = \max \left\{ 0, \frac{y_j - \sum_{v'_i \in \mathcal{N}(c_j) \setminus \{v_i\}} M_{v'_i \to c_j}^{(l)}}{a_{j,i}} \right\} \tag{4.3}$$

$$M_{c_j \to v_i}^{(l)} = \frac{y_j - \sum_{v'_i \in \mathcal{N}(c_j) \setminus \{v_i\}} \mu_{v'_i \to c_j}^{(l)}}{a_{j,i}} \tag{4.4}$$

where $\mathcal{N}(v_i)$ (resp. $\mathcal{N}(c_j)$) is the set of measurement (resp. variable) nodes which are the neighbors of v_i (resp. c_j) in the Tanner graph of $\mathbf{A}$. Updating messages from a variable (resp. measurement) node to a measurement (resp. variable) node is shown in Fig. 4.1 and 4.2, respectively.

The IPA is formally given in the Algorithm 3, where L represents the maximum number of reconstruction iterations. So far we consider the reconstruction in a noise

[1] Analogous to check nodes in LDPC codes.

[2] A matrix $\mathbf{H} = \{h_{j,i}\}$ is said to be the binary image of a matrix $\mathbf{A} = \{a_{j,i}\}$ if $h_{j,i} = 1$ if $a_{j,i} \neq 0$ and $h_{j,i} = 0$ if $a_{j,i} = 0$

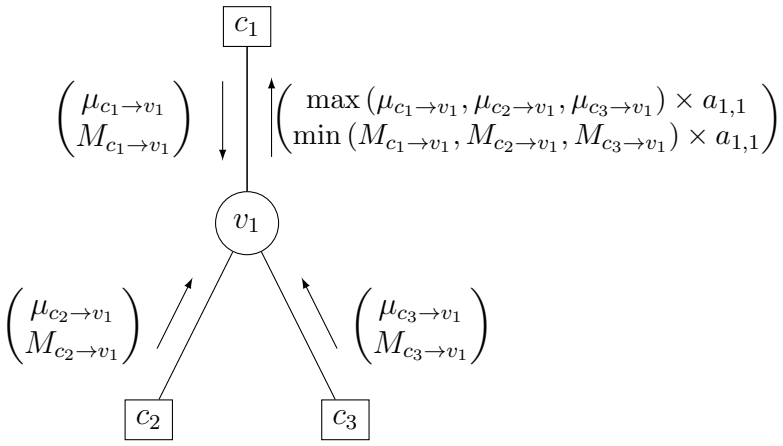

Figure 4.1: IPA: Updating messages from the variable node v_1 to the measurement node c_1.

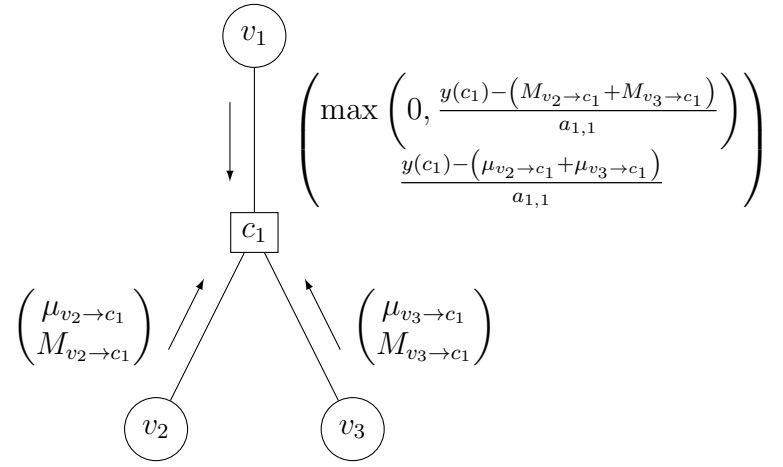

Figure 4.2: IPA: Updating messages from the measurement node c_1 to the variable node v_1.

Algorithm 3: Interval-Passing Algorithm

Input : $\mathbf{y}$ and $\mathbf{A}$ such that $\mathbf{y} = \mathbf{A}\mathbf{x}$, L.

Output : $\hat{\mathbf{x}}$ the estimate of $\mathbf{x}$.

Initialization: $\forall c_j \in C, \forall v_i \in \mathcal{N}(c_j)$, $\mu^{(0)}_{c_j \to v_i} = 0$ and $M^{(0)}_{c_j \to v_i} = y(c_j)/a_{j,i}$;

for $l = 1$ *to* L **do**

1 **foreach** $v_i \in V$ **do**

foreach $c_j \in \mathcal{N}(v_i)$ **do**

$$\mu^{(l)}_{v_i \to c_j} = \max_{c'_j \in \mathcal{N}(v_i)} (\mu^{(l-1)}_{c'_j \to v_i}) \times a_{j,i};$$

$$M^{(l)}_{v_i \to c_j} = \min_{c'_j \in \mathcal{N}(v_i)} (M^{(l-1)}_{c'_j \to v_i}) \times a_{j,i};$$

2 **foreach** $c_j \in C$ **do**

foreach $v_i \in \mathcal{N}(c_j)$ **do**

$$\mu^{(l)}_{c_j \to v_i} = \frac{1}{a_{j,i}} \left(y(c_j) - \sum_{\substack{v'_i \in \mathcal{N}(c_j) \\ v'_i \neq v_i}} M^{(l)}_{v'_i \to c_j} \right);$$

if $\mu^{(l)}_{c_j \to v_i} < 0$ **then**

$\mu^{(l)}_{c_j \to v_i} = 0$;

$$M^{(l)}_{c_j \to v_i} = \frac{1}{a_{j,i}} \left(y(c_j) - \sum_{\substack{v'_i \in \mathcal{N}(c_j) \\ v'_i \neq v_i}} \mu^{(l)}_{v'_i \to c_j} \right);$$

3 **for** $v_i \in V$ **do**

if $(l > 1 \;\&\; \mu^{(l)}_{v_i \to \mathcal{N}(v_i)} = M^{(l)}_{\mathcal{N}(v_i) \to v_i}) \parallel l = L$ **then**

$\hat{x}(v_i) = \mu^{(l)}_{v_i \to \mathcal{N}(v_i)}$;

free environment. The reconstruction process stops when the maximum number of iterations is reached, or the lower bound and the upper bound of the interval from variable nodes to measurement nodes has converged to a common value for every variable node. This common value is set as the estimate of each connected variable node value. When the lower bound and he upper bound did not converge, we arbitrarily set the estimate value to the lower bound.

4.1.2 Simulation results

4.1.2.1 Performance comparisons

We now compare the IPA performance using the non-negative real valued measurement matrix with the complex LP reconstruction algorithm, and with simple verification decoding. We used the LDPC matrix design from an array of permutation matrices from [62] to design our measurement matrices as quasi-cyclic (QC) LDPC matrices. We designed a $(2, 3)$-regular LDPC matrix with $m = 159$ and $n = 265$ and then substituted the non-zero elements in the LDPC matrix by a random number drawn from the uniform distribution in $(0, 1)$ to obtain the matrix $\mathbf{A}$.

For each sparsity k, at least 75 random k-sparse signals $\mathbf{x}$ are generated and 50 reconstruction iterations are performed. The proportion of correct reconstruction results is summarized in the plot of the Fig. 4.3 for the IPA, the verification decoding algorithm, and the LP reconstruction. A random k-sparse vector is said to be correctly recovered if each of its n samples is correctly estimated as close as 10^{-6}. We can see then that the IPA is a good trade-off between performance and complexity.

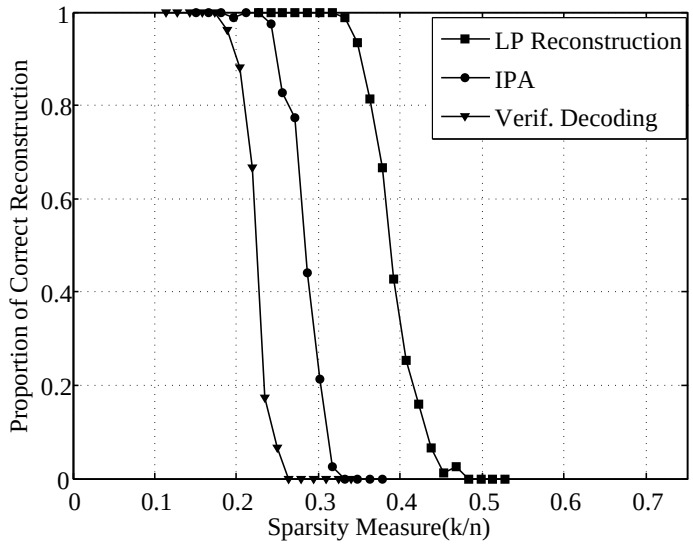

Figure 4.3: Simulation results using the designed measurement matrix $\mathbf{A}$.

4.1.2.2 Influence of the rate

In this section we present the reconstruction performance of the IPA by using different measurement matrices that are still QC-LDPC matrices of lengths 120, 1800 with column weight $d_v = 4$. We still used the method from [62] to design different measurement matrices. For each length we design 4 measurement matrices which have different rates, $R = 0.2$, $R = 0.33$, $R = 0.5$, $R = 0.67$. The results in terms of proportion of correct reconstruction using noise-free measurements for each measurement matrix are shown in Fig. 4.4. We observe, as expected, that the reconstruction performance decreases when the rate of the code increases. Indeed from the channel coding side, we know that increasing the rate decreases the redundancy present in the code. From the compressed sensing point of view, increasing the rate of the measurement matrix leads to obtain less measurements, which means less linear combinations of the input which intuitively leads to a harder problem to solve. Moreover, the results show that the measurement matrix of length $n = 120$ and rate $R = 0.67$ cannot be a good candidate to reconstruct data, as in a noise-free environment it cannot even recover a 1-sparse vector.

4.2 Reconstruction analysis

In this section, we study the recovery of the IPA on non-negative real-valued signals. We present the analysis on binary measurement matrices for the sake of clarity, but the extension of these results to non-negative real-valued measurement matrices is straightforward. First, we give a theorem given in [104] which proves the failure of the IPA on stopping sets. A stopping set is defined as follows.

Definition 4.1 ([109])**.** *A stopping set T is a subset of the set of variable nodes V such that all neighbors of T are connected to T at least twice.*

The cardinality of a stopping set is called the size of the stopping set.

Theorem 4.1 ([104])**.** *Let $\mathbf{A_{m\times n}}$ be a binary measurement matrix. The IPA fails on the recovery of a signal $\mathbf{x}$ if the non-zero entries contain a stopping set in $\mathbf{A}$.*

Proof. We prove that if all variable nodes in T have non-zero values, the IPA cannot recover them. In other words, we prove that the bounds of the intervals passing through the edges of the graphical representation of $\mathbf{A}$ never converge, i.e. we show that $\forall v \in T$ such that $x(v) > 0$, then $\mu^{(l)}_{v\to c} < x(v) < M^{(l)}_{v\to c}$, $\forall l \geq 0, \forall c \in \mathcal{N}(v)$.
Suppose $\forall v \in T$, $x(v) > 0$, from the definition of a stopping set $\forall c \in \mathcal{N}(v)$, $y(c) > x(v)$. Then, at the initialization ($l = 0$) we have:

$$\mu^{(0)}_{c\to v} = 0 < x(v) < y(c) = M^{(0)}_{c\to v} \tag{4.5}$$

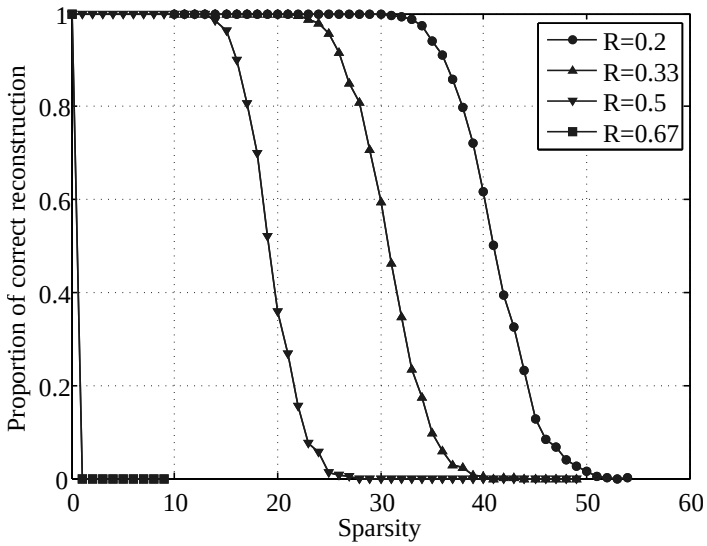

(a) $n = 120$

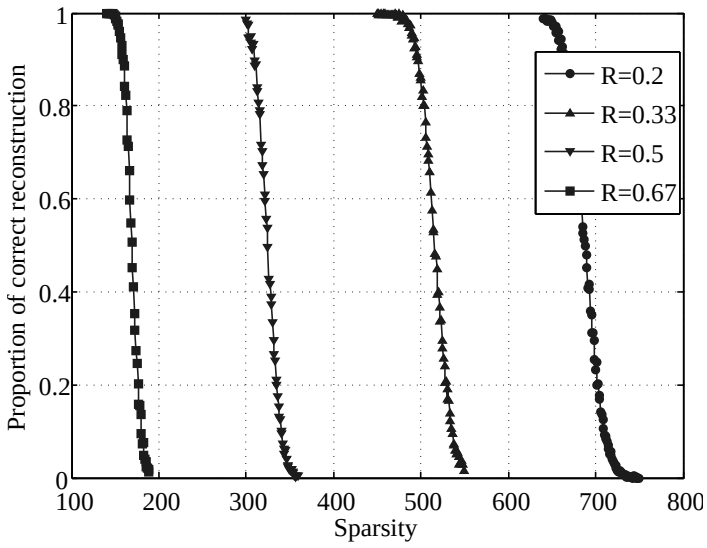

(b) $n = 1800$

Figure 4.4: Reconstruction of noise free measurements with QC-LDPC measurement matrices of lengths $n = 120$ and $n = 1800$ and column weight $d_v = 4$ for different rates.

At the first iteration we have:

$$\mu_{v\to c}^{(1)} = \max_{c\in\mathcal{N}(v)} \left(\mu_{c\to v}^{(0)}\right) = 0 < x(v) \tag{4.6}$$

$$M_{v\to c}^{(1)} = \min_{c\in\mathcal{N}(v)} \left(M_{c\to v}^{(0)}\right) > x(v) \tag{4.7}$$

Now consider the update at the measurement node. For the lower bound of the interval we have:

$$\begin{aligned}
\mu_{c\to v}^{(1)} &= \max\left(0, y(c) - \sum_{v'\in\mathcal{N}(s)\setminus\{v\}} M_{v'\to c}^{(1)}\right) && (4.8)\\
&< \left(y(c) - \sum_{v'\in\mathcal{N}(s)\setminus\{v\}} x(v')\right) && (4.9)\\
&= x(v) && (4.10)
\end{aligned}$$

The last equation stands from the initialization $x(v) < y(c) = M_{v\to c}^{(1)}$. Similarly, for the upper bound at the measurement node we have:

$$\begin{aligned}
M_{c\to v}^{(1)} &= y(c) - \sum_{v'\in\mathcal{N}(s)\setminus\{v\}} \mu_{v'\to c}^{(1)} && (4.11)\\
&> y(c) - \sum_{v'\in\mathcal{N}(s)\setminus\{v\}} x(v') && (4.12)\\
&= x(v) && (4.13)
\end{aligned}$$

The last equation results from the initialization $x(v) > y(c) = \mu_{v\to c}^{(1)}$.

Thus we obtain $\mu_{c\to v}^{(1)} < x(v) < M_{c\to v}^{(1)}$. For $l > 1$ the messages from variable nodes to check nodes are simply the intersection of intervals from the check nodes at the previous iteration, and then we still have $\mu_{v\to c}^{(l)} < x(v) < M_{v\to c}^{(l)}$. The proof is completed by induction for every $l > 0$. □

Theorem 4.1 also indicates that the IPA fails on reconstruction of a signal $\mathbf{x}$ whose non-zero values form the smallest stopping set in the measurement matrix $\mathbf{A}$. However, as we explain in the following example, the smallest stopping set is not the smallest configuration on which the IPA fails.

Example 4.1. *Consider a stopping set of size four as given in Fig. 4.5. According to Theorem 4.1, the IPA cannot recover a signal* $\mathbf{x}$ *with non-zero values on* $\{v_1, v_2, v_3, v_4\}$. *The algorithm also fails on a 2-sparse signal* $\mathbf{x}$ *whose non-zero values are* $\{v_1, v_3\}$ *or* $\{v_2, v_4\}$, *which implies that the variable nodes forming one of the smallest stopping*

set are not necessarily the smallest configuration on which the IPA fails. However, the IPA can recover a 2-sparse signal with non-zero values on $\{v_1, v_2\}$ *or* $\{v_1, v_4\}$.

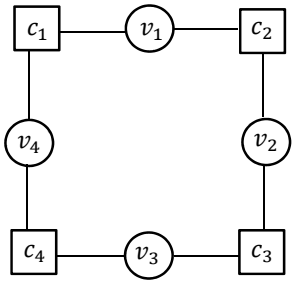

Figure 4.5: A stopping set of size 4.

Example 4.1 shows the main difference between the iterative decoding on the BEC and the signal recovery of the iterative IPA in compressed sensing. The iterative decoder over the BEC fails if and only if the erasures contain a stopping set, while the IPA fails even if the non-zero values do not involve a stopping set. The following results identify recoverable signals whose non-zero values are subsets of stopping sets. First, we show that every zero-value variable node is recoverable by the IPA. In this paper, we say that a node is zero if its value is equal to zero.

Lemma 4.1. *The IPA can recover all zero variable nodes.*

Proof. Suppose v is a variable node with value 0 and $\{c_1, c_2, ..., c_{d_v}\}$ is the set of the d_v measurement neighboring nodes of v with measurement values $\{\alpha_1, \alpha_2, ..., \alpha_{d_v}\}$. At each iteration of the IPA, the message which is sent from c_j ($j = 1, ..., d_v$) to v is either $[0, 0]$ or $[0, \beta_j]$ where $0 < \beta_j \leq \alpha_j$. If v receives at least one $[0, 0]$ from one of its neighbors, the value of v is recovered as 0. If all messages from every c_j to v are $[0, \beta_j]$, the decision rule of the algorithm leads to recover the value of v to the maximum value of lower bounds of the intervals $[0, \beta_j]$, which is 0. □

Since all zero variable nodes are recovered by the IPA, it is enough to study the recovery of non-zero variable nodes. We note that reconstruction of all zero variable nodes does not necessarily result that the IPA can be used to estimate the support of the signal, since it is possible that the IPA fails to recovery of a non-zero variable node and recovers the value of the non-zero variable node to zero.

Definition 4.2. *A set of variable nodes* S *is called a minimal stopping set, if* S *forms a stopping set and it does not contain a smaller stopping set.*

It is clear that the smallest stopping set in a measurement matrix $\mathbf{A}$ is a minimal stopping set while a minimal stopping set is not necessarily the smallest stopping set. The size of the smallest stopping set is called the *stopping distance* [110] and plays a significant role in iterative decoding of LDPC codes over the BEC.

Theorem 4.2. *Let $\mathbf{A_{m\times n}}$ be a binary measurement matrix and $V_S = \{v_1, v_2, ..., v_k\}$ be a subset of variable nodes forming a minimal stopping set. Let $\mathbb{R}^n_{\geq 0}$ be a set of non-negative real vectors in $\mathbb{R}^n$ and $\mathbf{x} = [x_1, x_2, ..., x_n]^t \in \mathbb{R}^n_{\geq 0}$ be a signal with at most $k-2$ non-zero values, i.e. $\| \mathbf{x} \|_0 \leq k-2$, such that the set of non-zero variables is a subset of V_S. Then, the IPA can recover $\mathbf{x}$ if there exists at least one zero measurement node among the neighbors of V_S.*

Proof. Let $M = \{c_1, c_2, ..., c_q\}$, $1 \leq q \leq m$ be the set of measurement nodes connected to V_S. Suppose that c_1 is the only zero measurement node. Since V_S forms a stopping set, there exist at least two zero variable nodes, say v_1, v_2, connecting to c_1 and there exist non-zero value measurement nodes connected to v_1, v_2. Moreover, V_S is a minimal stopping set, so there exists at least one measurement node, $c_2 \in M\backslash\{c_1\}$ with only one neighbor in $V_S\backslash\{v_1, v_2\}$, namely v_3. Otherwise, $V_S \backslash\{v_1, v_2\}$ will be a smaller stopping set, which is a contradiction. Suppose c_2 has the value α. At the first iteration, c_1 sends $[0, 0]$ to v_1 and v_2 and v_1 and v_2 send $[0, 0]$ to their neighbors. Based on the above explanation, c_2 is a neighbor of v_1 or v_2 or both of them with only one neighbor in $V_S \backslash\{v_1, v_2\}$. At the second iteration, c_2 will send $[\alpha, \alpha]$ to the only variable node v_3. So, the value of the variable node v_3 is recovered to α. Since the value of this variable node is recovered, we can consider this variable node to have value zero by subtracting α from the value of all measurement nodes which are the neighbors of v_3. Now, we have three variable nodes v_1, v_2, v_3 whose values have been determined. Again, with the same discussion, there exists a measurement node $c_3 \in M\backslash\{c_1, c_2\}$ with only one neighbor in $V_S\backslash\{v_1, v_2, v_3\}$ which can be recovered in the next iteration. Continuing the same process will recover all variable nodes. □

Example 4.2. *Fig. 4.6 illustrates the previous theorem considering the recovery of a signal with 4 non-zero variable nodes in a minimal stopping set of size 6 in which there exists one zero measurement node c_1 and two zero variable nodes v_1 and v_2. Let $\alpha, \beta, \gamma, \delta, \eta$ be the non-zero values of c_2, c_3, c_4, c_5 and c_6, respectively. Note that c_2 is one the measurement nodes with exactly one neighbor among $\{v_3, v_4, v_5, v_6\}$. At initialization, the zero measurement node c_1 sends $[0, 0]$ to v_1 and v_2. And c_2 sends $[0, \alpha]$ to v_2 and v_3. At the first iteration, v_2 sends $[0, 0]$ to c_2, which causes c_2 to send $[\alpha, \alpha]$ to v_3. Thus, the value of v_3 is recovered as α. Another measurement node with only one neighbor in $\{v_4, v_5, v_6\}$ is c_3. Again this measurement node sends $[\beta, \beta]$ to v_4 and so the value of v_4 is recovered as β. The same process results in the recovery of all variable nodes.*

In Theorem 4.2 we proved that the existence of at least one zero measurement node is enough to reconstruct a signal $\mathbf{x}$ whose non-zero values are a subset of a minimal stopping set. As we will show in the following Lemma and Corollary, in regular measurement matrices we can give an upper bound on the number of variable nodes

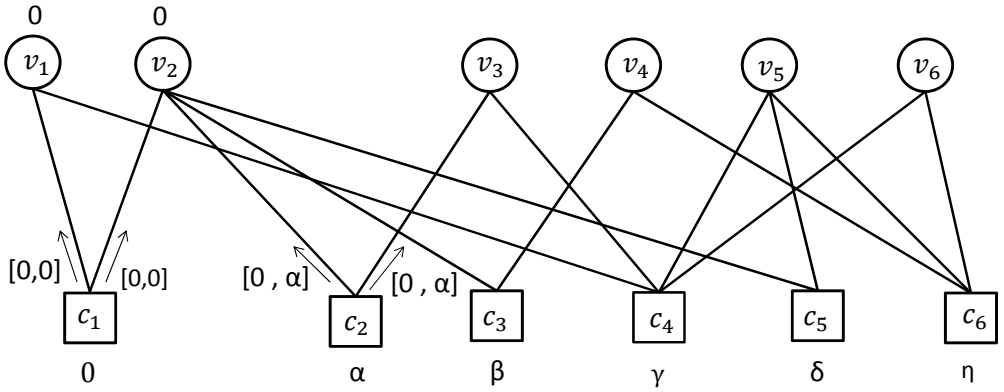
0
0
v_1
v_2
v_3
v_4
v_5
v_6
[0,0]
[0,0]
[0 , α]
[0 , α]
c_1
c_2
c_3
c_4
c_5
c_6
0
α
β
γ
δ
η

(a)

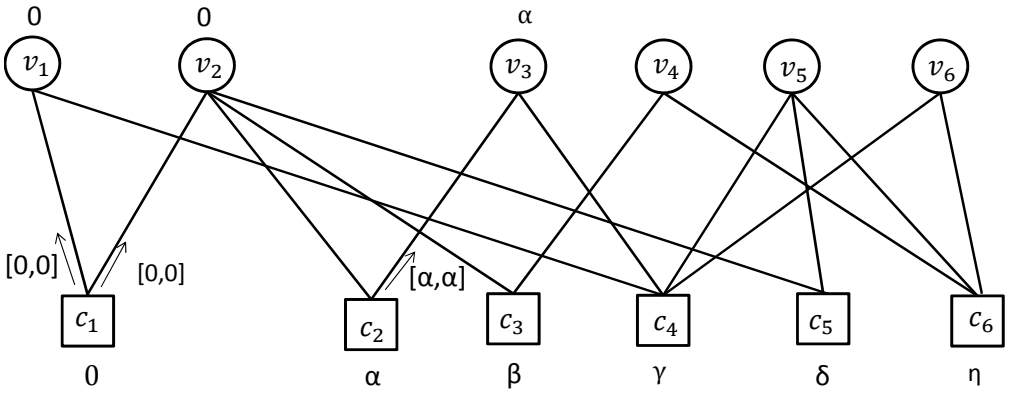
0
0
α
v_1
v_2
v_3
v_4
v_5
v_6
[0,0]
[0,0]
[α,α]
c_1
c_2
c_3
c_4
c_5
c_6
0
α
β
γ
δ
η

(b)

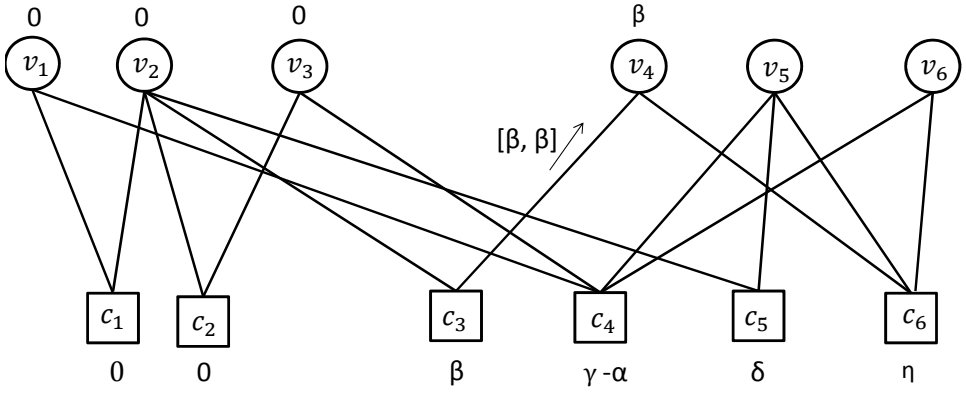
0
0
0
β
v_1
v_2
v_3
v_4
v_5
v_6
[β, β]
c_1
c_2
c_3
c_4
c_5
c_6
0
0
β
γ -α
δ
η

(c)

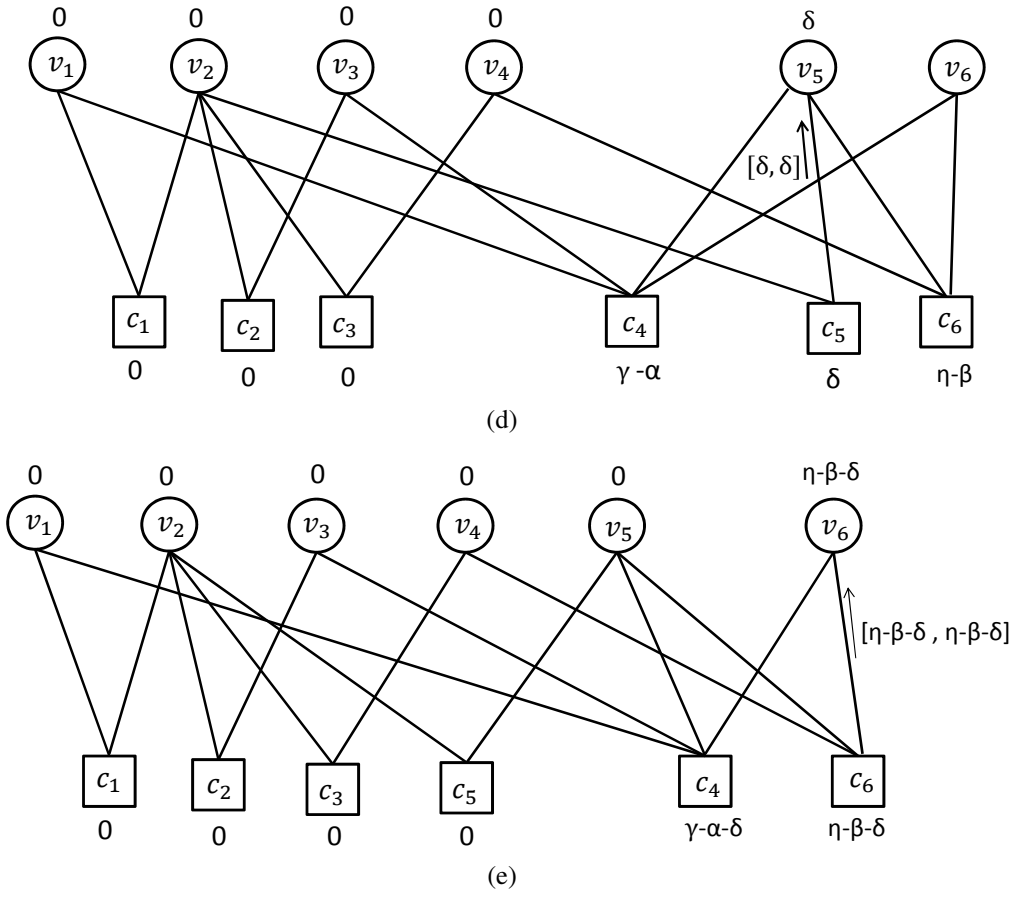

Figure 4.6: Reconstruction of a signal with non-zero elements in a minimal stopping set of size 6 with the IPA when there exists one zero measurement node. (a) the first messages sending from measurement nodes to variable nodes, (b) messages from the measurement nodes to variable nodes in the first iteration (recovery of v_3), (c) the message to v_4 in the second iteration (recovery of v_4), (d) the message to v_5 in the third iteration (recovery of v_5), (e) the message to v_6 in the fourth iteration (recovery of v_6).

forming a subset of a minimal stopping set S such that there exists at least one measurement node among the neighbors of S with no connection to this subset of variable nodes. This result shows that in a minimal stopping set, if the number of non-zero values is bounded by a fixed number, the IPA can recover the signal $\mathbf{x}$.

Lemma 4.2. *Let $\mathbf{A_{m\times n}}$ be a binary (d_v, d_c)-regular measurement matrix and let $g = 2r$ be the girth of the Tanner graph corresponding to $\mathbf{A}$. Then, every subset N of variable nodes such that*

$$|N| < \frac{\sum_{i=0}^{r-1}(d_v-1)^{\lceil \frac{i}{2} \rceil}(d_c-1)^{\lfloor \frac{i}{2} \rfloor}}{d_v} \tag{4.14}$$

contains a measurement node which does not have any neighbor in N.

Proof. The proof is obtained by using lower bounds on the number of measurement nodes given in [111]. According to this bound,

$$m \geq \sum_{i=0}^{r-1}(d_v-1)^{\lceil \frac{i}{2} \rceil}(d_c-1)^{\lfloor \frac{i}{2} \rfloor}. \tag{4.15}$$

Now, suppose N is a subset of variable nodes. Since the matrix is regular, the maximum number of measurement nodes that can be connected to the variable nodes in N is at most $|N|d_v$. If $|N|d_v < \sum_{i=0}^{r-1}(d_v-1)^{\lceil \frac{i}{2} \rceil}(d_c-1)^{\lfloor \frac{i}{2} \rfloor}$ which results $|N| < \frac{\sum_{i=0}^{r-1}(d_v-1)^{\lceil \frac{i}{2} \rceil}(d_c-1)^{\lfloor \frac{i}{2} \rfloor}}{d_v}$, there exists at least one measurement node which does not have any connection to N. □

Corollary 4.1. *Suppose $\mathbf{A_{m\times n}}$ is a binary (d_v, d_c)-regular measurement matrix with girth $g = 2r$. Let N be a subset of k variable nodes that forms a minimal stopping set. If $|N| < \frac{\sum_{i=0}^{r-1}(d_v-1)^{\lceil \frac{i}{2} \rceil}(d_c-1)^{\lfloor \frac{i}{2} \rfloor}}{d_v}$, then the IPA can recover a signal $\mathbf{x}$ with non-zero values in N. In the case that the girth is 6, $|N|$ is bounded by $|N| \leq \frac{(d_v-1)d_c}{d_v} = \frac{(d_v-1)k}{m}$. If the girth is 8, $|N|$ is bounded by $|N| \leq \frac{(d_v-1)d_c+(d_v-1)(d_c-1)}{d_v}$.*

The following theorem gives a sufficient condition on exact recovery of a signal whose support is a subset of a minimal stopping set and all neighboring measurement nodes are non-zero.

Theorem 4.3. *Let $\mathbf{A_{m\times n}}$ be a binary measurement matrix and $V_S = \{v_1, v_2, ..., v_k\}$ be a subset of variable nodes forming a minimal stopping set. Let $\mathbf{x} = [x_1, x_2, ..., x_n]^t \in \mathbb{R}^n_{\geq 0}$ be a signal with at most $k-1$ non-zero values, i.e. $\| \mathbf{x} \|_0 \leq k-1$ such that the set of non-zero variables is a subset of V_S. Suppose all measurement nodes have non-zero values. Then, the IPA can recover $\mathbf{x}$ if*
1. There exists at least one measurement node c_j such that the variable nodes $\{v_1, v_2, ..., v_p\}$

which are connected to c_j have non-zero values and do not share a measurement node other than c_j and
2. The measurement nodes $\{c_1, c_2, ..., c_l\}$ connected to $\{v_1, v_2, ..., v_p\}$ do not have non-zero neighboring variable nodes excluding $\{v_1, v_2, ..., v_p\}$.

Proof. Suppose $\{v_1, v_2, ..., v_p\}$ have non-zero values $\{\alpha_1, \alpha_2, ..., \alpha_p\}$. Since $\{c_1, c_2, ..., c_l\}$ are connected to zero variable nodes except for $\{v_1, v_2, ..., v_p\}$ and $\{c_1, c_2, ..., c_l\}$ are not shared by more than one variable node in $\{v_1, v_2, ..., v_p\}$, the value of every measurement node in $\{c_1, c_2, ..., c_l\}$ lies in $\{\alpha_1, \alpha_2, ..., \alpha_p\}$. There exists a measurement node in $\{c_1, c_2, ..., c_l\}$ that has only one neighbor in $V_S \backslash \{v_1, v_2, ..., v_p\}$. Otherwise, $V_S \backslash \{v_1, v_2, ..., v_p\}$ will be a smaller stopping set. Without loss of generality, suppose c_1 is a measurement node with this property which is connected to v_1 with the value α_1. In the first iteration, c_j sends $\sum_{i=1}^{p} \alpha_i$ to its neighbors in $\{v_1, v_2, ..., v_p\}$ and c_1 sends $[0, \alpha_1]$ to its neighbors. In the second iteration, c_j sends $[\alpha_1, \sum_{i=1}^{p} \alpha_i]$ to v_1 and c_1 and other neighbors of v_1 send intervals with the upper bound α_1 to v_1 which results that the message $[\alpha_1, \alpha_1]$ is sent from v_1 to its neighbors. Thus, the value of v_1 is recovered as α_1 and all measurement nodes which are the neighbors of v_1 are satisfied. So, c_1 is satisfied and its value can be considered as zero. The recovery of the other variable nodes is followed by Theorem 4.2 which implies that the existence of at least one zero measurement node is enough to recover all the variable nodes in a configuration forming a stopping set. □

The following example shows how the IPA can recover a vector $\mathbf{x}$ under the conditions of the Theorem 4.3.

Example 4.3. *Fig. 4.7 depicts the recovery of the three non-zero variable nodes in $\{v_1, v_2, v_3\}$ a minimal stopping set of size 5 in which all measurement nodes are non-zero. First, note that the measurement node c_1 and the variable nodes v_1, v_2, v_3 satisfy the two conditions of Theorem 4.3. Thus, if the non-zero variable nodes v_1, v_2, v_3 have values α, β, γ, then c_1 has value $\lambda = \alpha + \beta + \gamma$ and other measurement nodes c_2, c_3, c_4, c_5 have the values α, β, γ and γ respectively. For simplicity, we just show how the value of the variable node v_3 is recovered. At initialization, c_1 sends $[0, \alpha+\beta+\gamma]$ to v_3 and c_5 sends $[0, \gamma]$ to v_3. In the first iteration, c_1 receives $[0, \alpha]$ and $[0, \beta]$ from v_1 and v_2, respectively and c_5 receives $[0, \min(\alpha, \gamma)]$ from v_5. Then, c_1 sends $[\gamma, \alpha + \beta + \gamma]$ to v_3 and c_5 sends $[0, \gamma]$ or $[\gamma - \min(\alpha, \gamma), \gamma] = [\gamma - \alpha, \gamma]$ to v_3. In the second iteration, v_3 sends $[\gamma, \gamma]$ to its neighbors which makes c_5 is satisfied and can be considered as a zero measurement node. Now, there exists a zero measurement node in this minimal stopping set. Theorem 4.2 results in the recovery of other variable nodes.*

Theorems 4.2 and 4.3 give sufficient conditions on the recovery of signals whose non-zero values form a subset of a minimal stopping set. To show how small stopping sets affect the performance of the IPA, we provide simulation results of the performance of the IPA in the next section.

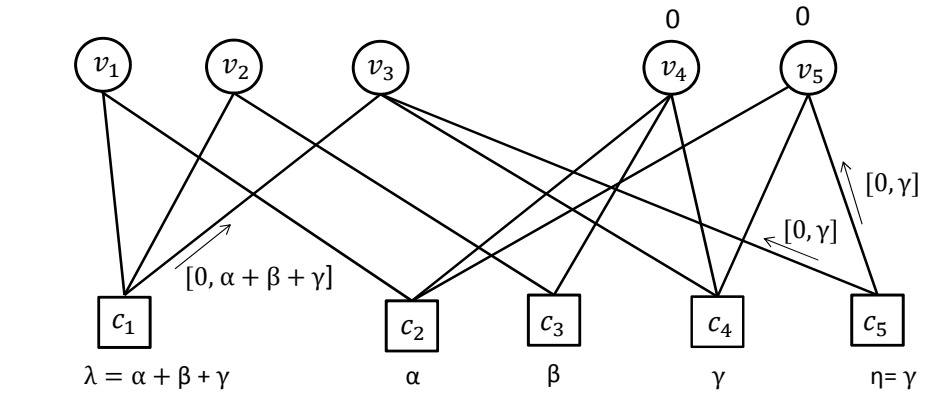

(a)

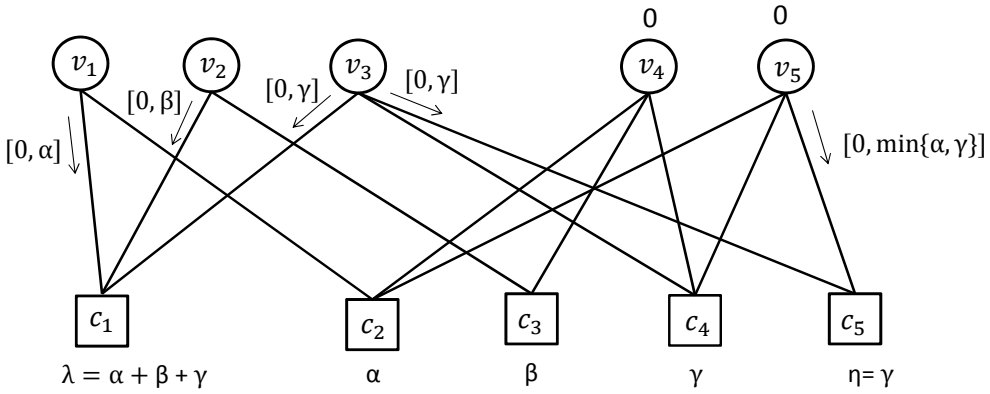

(b)

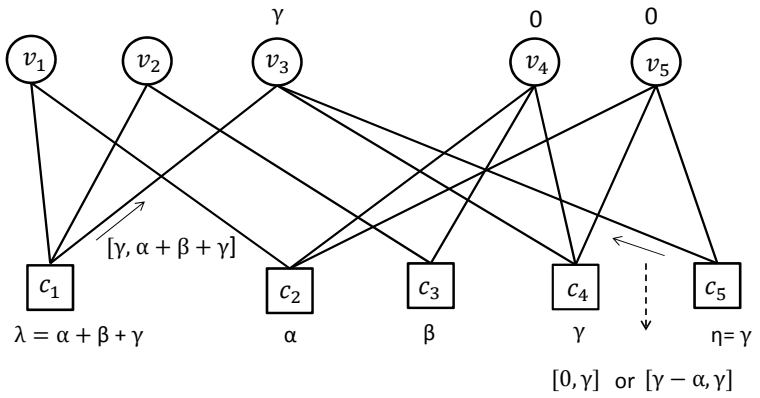

(c)

Figure 4.7: Reconstruction of a signal with non-zero elements in a support of a stopping set of size 5 with IPA and with no zero measurement node. (a) the first messages which are sent from check nodes to variable nodes, (b) messages from variable nodes in the first iteration, (c) messages from check nodes in the second iteration.

4.3 Numerical results

4.3.1 Preliminaries

In this section we provide simulation results of the reconstruction performance of the IPA by establishing the link with the analysis done previously related to stopping sets. From Theorem 4.1, we know that if the support of the signal $\mathbf{x}$ is, or contains, a stopping set, the IPA cannot recover it. The stopping sets in the measurement matrix $\mathbf{A}$ are then responsible for most of the failures of the reconstruction via the IPA.

Orlitsky *et al.* derived a formula to obtain the average distribution $E(s)$ for any size s of stopping sets for a (d_v, d_c)-regular LDPC code of size n [43]:

$$E(s) = \binom{n}{s} \frac{\text{coef}\left(\left((1+x)^{d_c} - xd_c\right)^{\frac{d_v}{d_c}n}, x^{sd_v}\right)}{\binom{nd_c}{sd_v}} \tag{4.16}$$

where coef $(p(x), x^i)$ denotes the coefficient of x^i in the polynomial $p(x)$. The average distribution of stopping sets can theoretically be computed using the previous formula, however it has to be done by numerical methods due to its large complexity. To be able to practically find stopping sets, algorithms have been proposed as in [57] and [112] in the channel coding context. In their recent work, Rosnes *et al.* [57, 113] provide the stopping set repartition on various LDPC codes based on their algorithm to find small stopping sets. In [113] they focused more specifically on the LDPC codes from the IEEE 802.16e standard [114], referred as the Wimax codes. These codes are circulant-based LDPC codes, and the IEEE standard provides the design of codes for 19 different lengths. Also, one model matrix to design codes with rates 1/2, and 5/6 is provided, and two model matrices are provided for codes with rates 2/3 and 3/4 (denoted by A and B). In the sequel we will use the matrix of the IEEE 802.16e standard as measurement matrix for two different length, $n = 768$, and $n = 2304$. We remind in the Tables 4.1 and 4.2 the stopping set spectrum for each of the six that can be designed for each length in which we adopted the notation of Rosnes *et al.* [113].

4.3.2 Simulation results on the Wimax codes

In order to see the influence of stooping set on the performance of the IPA, we have generated all the codes of length $n = 768$ and $n = 2304$ according to the IEEE standard. We used these six codes for each length as measurement matrices and we simulate the recovery performance via the IPA. The simulation results are shown in Fig. 4.8 4.9 where the proportion of correct reconstruction of sparse signals is plotted versus the sparsity measure k/n. For each sparsity k and for each matrix, 500 k-sparse signals are generated, and a maximum of 50 iterations of the IPA for the reconstruction

Table 4.1: Stopping distance s_{min} for the length $n = 768$ LDPC codes from the IEEE802.16 standard with different rates R. The number of stopping sets of weight s_{min} is denoted $N_{s_{min}}$ (from [57] and [113]).

R	s_{min}	$N_{s_{min}}$	$N_{s_{min}+1}$	$N_{s_{min}+2}$	$N_{s_{min}+3}$	$N_{s_{min}+4}$
1/2	14	32	32	0	32	32
2/3 A	8	64	0	0	160	160
2/3 B	12	64	128	384	1120	3352
3/4 A	9	32	128	576	2192	9696
3/4 B	4	16	0	0	32	216
5/6	6	96	672	5376	36512	280128

Table 4.2: Stopping distance s_{min} for the length $n = 2304$ LDPC codes from the IEEE802.16 standard with different rates R. The number of stopping sets of weight s_{min} is denoted $N_{s_{min}}$ (from [57] and [113]).

R	s_{min}	$N_{s_{min}}$	$N_{s_{min}+1}$	$N_{s_{min}+2}$	$N_{s_{min}+3}$	$N_{s_{min}+4}$
1/2	28	96	96	288	288	624
2/3 A	15	96	0	96	480	768
2/3 B	15	96	0	0	0	0
3/4 A	12	48	0	0	0	0
3/4 B	12	16	96	0	672	1824
5/6	9	192	288	1920	8616	43584

are done.

These results emphasize the connection between the stopping set distribution and the performance of the IPA from the theorems of the previous section. For instance, it is clear when comparing the numbers of Table 4.1 and the plot of Fig. 4.8, or between Table 4.2 and the Fig. 4.9 that the stopping set distribution is responsible for most of the failures of the IPA. For example in the case of $n = 768$, at a constant rate (e.g. 2/3), the measurement matrix with higher stopping distance has a slightly better performance. However, we can see that even if the matrix A with rate 3/4 has a better stopping distance than the rate 5/6 matrix, it performs better. This observation comes from the stopping set distribution as matrix A with rate 3/4 has only 16 stopping sets of weight 4, and the next ones have weight 7 (and there are a few of them) whereas for the rate 5/6, the number of stopping sets of weight 6 or 7 are very numerous. Then, although the stopping set distribution gives an insight of the performance of the IPA on a given measurement matrix, it is not obvious to foresee this performance because it depends on the stopping distance and on the number of stopping sets of each weight. These observations hold for the case of $n = 2304$.

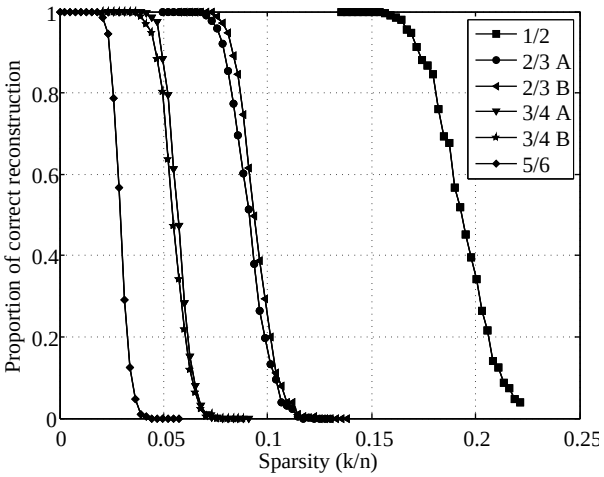

Figure 4.8: IPA performance on the IEEE 802.16e LDPC codes of length $n = 768$ for the different available rates.

4.4 Conclusion and discussion

In this chapter we have introduced the IPA, a low-complexity iterative reconstruction algorithm for compressed sensing in which sparse non-negative matrices are considered as measurement matrices. We showed that the IPA has good reconstruction results in a noise free case. We also demonstrated that there exists a close link between the

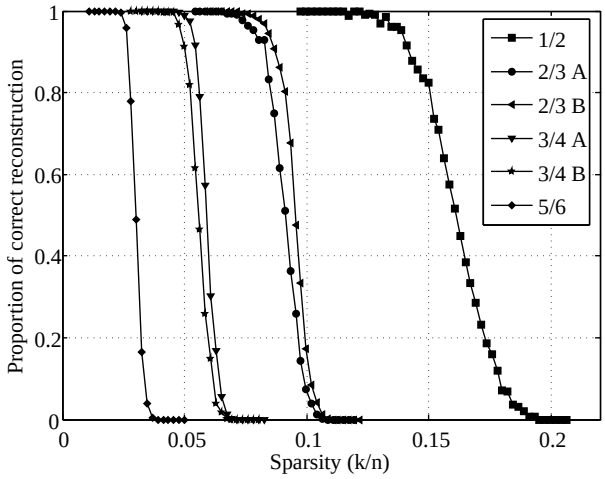

Figure 4.9: IPA performance on the IEEE 802.16e LDPC codes of length $n = 2304$ for the different available rates.

failures of the IPA and some topological structures of its equivalent graphical representation, known as stopping sets in the case of LDPC decoding.

The major perspective for this work is to adapt the IPA in a noisy case. However this adaptation raises some questions. Indeed the IPA dealing primarily with non-negative measurements, the noise added could flip the sign of some measurements. The decision will also be an issue, as the intervals are likely not to converge to a single value. However the first experiments tend to show that IPA can recover at least the support of the sparse signal.

For instance we took a 10-sparse vector $\mathbf{x}$ of length $n = 265$ with non-zero values between 0 and 255 (as in a grayscale image). We then use a sparse binary matrix $\mathbf{A}$ of size $m \times n$ with $m = 159$ (this measurement matrix is designed, as in the previous sections, as arrays of permutation matrices). We then measure $\mathbf{x}$ via $\mathbf{A}$, but with addition of a Gaussian noise, such that $\mathbf{y} = \mathbf{Ax} + \mathbf{z}$, where $\mathbf{z}$ is drawn for the Gaussian distribution with variance σ^2. The SNR being defined here as $E_b/N_0 = 1/2\sigma^2$. Fig. 4.10 depicts the first results concerning the reconstruction of IPA in a noisy setting where we applied a noise of 2dB on the measurements. This figure shows in x-axis the indices of the sparse signal, and in y-axis its original value (denoted with a $\times$), as well as the interval which is computed for each location of the signal. Moreover, we introduced some prior information in the setting, as we assume to know, while performing the reconstruction, the minimum value for the non-zero values in x, this removes the false alarms. We then notice that although the approximation of the intervals is not quite accurate, it is pretty promising as it allows to detect, at least, the support of the original vector $\mathbf{x}$. It is our belief, that under certain conditions on the signals (more

prior knowledge, particular structure of the original vector...) the adaptation of the IPA to noisy measurements is possible. This will lead to make it more practical for certain applications, as in the image processing using wavelets decomposition.

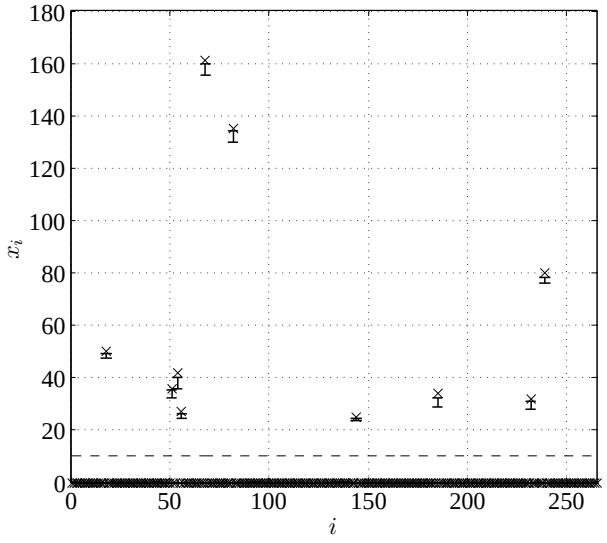

Figure 4.10: First results on the IPA reconstruction in a noisy case.

Conclusion and perspectives

The presence of iterative algorithms in many digital systems demonstrates their extraordinary efficiency in systems used to communicate, entertain and even work. With the increasing number of users of digital technologies, the need in fast and large-scale iterative methods will definitely keep growing.

In digital communications, traditional decoders, such as belief propagation (BP) used for the decoding of low-density parity-check (LDPC) codes present an abrupt degradation of the error-rate performance at a high signal-to-noise ratio. Recently a class of finite precision iterative decoders, called finite alphabet iterative decoders (FAIDs) was proposed to improve the performance in this particular region using a very low complexity. In addition, it has been shown that FAIDs can surpass BP using only 3 bits of precision on column-weight-three codes, and we even present in this dissertation a 3-bit and 4-bit FAID surpassing the BP in the error floor region for a column-weight-four code. As the number of possible FAIDs is very large for a given number of precision bits, we have proposed two methodologies to select potential good FAIDs for column-weight-three codes. The first one relying on the particular knowledge of a code, specifically the knowledge of its minimal codewords, and the second one is more general and aims at selecting good FAID for any column-weight-three code based on the analysis of potential harmful structures in a code.

The work done in this thesis on this topic leads to different perspectives. The complete extension on FAIDs for column-weight-four codes is crucial for the practical applications, and can be addressed by two different ways. The first one is to extend the work done for column-weight-three codes, which is, to know better the harmful topologies for this type of codes and possibly design a trapping set ontology, and from there design FAIDs able to surpass BP in the error floor. However this technique will be limited by the number of potential FAIDs that can be designed, necessarily more numerous than in column-weight-three. The second approach can rely on the derivation of FAIDs for column-weight-four codes from a combination of FAIDs for column-

weight-three codes. This would definitely lead to a design at a lower complexity, but the combination of FAIDs for column-weight-three codes is not trivial to realize, while ensuring a good error correction capability. Nevertheless we know thanks to this work that FAIDs for column-weight-four codes are able to surpass BP in the error floor.

The second perspective of this work concerns the modification of the channel. We have considered the Binary Symmetric channel, but designing good FAIDs on Additive White Gaussian Noise channel (AWGNC) is a challenge, as the values of the channels are not binary anymore. The major issue for this will certainly be the quantization of the real values received from the channel to a discrete alphabet. Adapting FAIDs on AWGNC using column-weight-four codes will definitely promote the FAIDs as serious candidate decoders in the storage industry for hard-drive, or flash memories systems.

In the second part of the dissertation we have shown the potential of iterative algorithms in compressed sensing, an emerging field in signal processing, in which the sampling of a signal can be done below the Nyquist sampling rate if the signal is sparse in a certain basis. We presented in this dissertation a modified version of a low-complexity iterative reconstruction algorithm called Interval-Passing algorithm (IPA) whose reconstruction performance is a good trade-off between other low-complexity methods and complex reconstruction algorithms. This algorithm uses non-negative measurement matrices, and the analysis of the failures of the IPA establishes a link between the failures of iterative decoder on the Binary Erasure channel and the graphical representation of the measurement matrix.

Further work in this topic includes the analysis of the reconstruction possibilities of the IPA under noisy measurements which will help to design measurement matrices to improve the performance. Another related perspective for this work relies on the computation of the mutual information between the original signal and its measurements, and find a connexion between the maximization of this mutual information and the failures of the IPA with the goal of designing measurement matrices maximizing the reconstruction performance.

Bibliography

[1] R. G. Gallager, *Low Density Parity Check Codes*. Cambridge, MA: M.I.T. Press, 1963.

[2] R. W. Hamming, "Error detecting and error correcting codes," *Bell Sys. Tech. Journal*, vol. 29, pp. 147–160, Apr., 1950.

[3] M. J. E. Golay, "Notes on digital coding," *Proc. IEEE*, 37, pp. 657, 1949.

[4] D. E. Muller, "Application of boolean algebra to switching circuit design and to error detection," *IRE Trans. on Electronic Computers*, vol. 3, pp. 6–12, Sep. 1954.

[5] Irving S. Reed, "A class of multiple-error-correcting codes and the decoding scheme," *Trans. of the IRE Professional Group on Inform. Theory*, vol 4, pp. 38–49, Sep. 1954.

[6] C.E. Shannon, "A Mathematical Theory of Communication," *Bell Sys. Tech. Journal*, vol. 27, pp. 379–423, 623–656, July, October, 1948.

[7] A. Hocquenghem, "Codes correcteurs d'erreurs," *Chiffres*, vol. 2, pp. 147–156, Sep. 1959.

[8] R. C. Bose, D. K. Ray-Chaudhuri, "On A Class of Error Correcting Binary Group Codes," *Information and Control*, vol. 3, pp. 68–79, Mar. 1960.

[9] I. S. Reed, G. Solomon, "Polynomial Codes over Certain Finite Fields," *J. Soc. Indust. Appl. Math.*, vol. 8, pp. 300–304, Jun. 1960.

[10] E. R. Berlekamp, "Factoring Polynomials Over Finite Fields," *Bell System Technical Journal*, vol. 46, pp. 1853–1859, May 1967.

[11] P. Elias, "Coding for noisy channels," *IRE Conv. Rep.*, Pt. 4, pp. 37–47, 1955.

[12] A. J. Viterbi, "Error bounds for convolutional codes and an asymptotically optimum decoding algorithm," *IEEE Trans. Inf. Theory*, vol. 13, no. 4, pp. 260–269, Apr. 1967.

[13] L. Bahl, J. Cocke, F. Jelinek, and J. Raviv, "Optimal decoding of linear codes for minimizing symbol error rate," *IEEE Trans. Inf. Theory*, vol. 20, no. 3, pp. 284–287, Mar. 1974.

[14] C. Berrou, A. Glavieux, and P. Thitimajshima, "Near Shannon limit error-correcting coding and decoding: Turbo codes," *Proc. Int. Conf. on Commun.*, Geneva, Switzerland, pp. 1064–1070, May 1993.

[15] D. J. C. MacKay and R. M. Neal, "Good codes based on very sparse matrices," *Proc. 5th IMA Conf. Cryptography and Coding*, Cirencester, UK, no. 1025, pp. 100–111, Dec. 1995.

[16] R. Tanner, "A recursive approach to low complexity codes," *IEEE Trans. Inf. Theory*, vol. 27, no. 5, pp. 533–547, Sep. 1981.

[17] N. Wiberg, " Codes and Decoding on General Graphs," *PhD Dissertation*, 1996.

[18] F. R. Kschischang, B. J. Frey and H.-A. Loeliger, "Factor Graphs and the Sum-Product Algorithm," *IEEE Trans. Inf. Theory*, vol. 47, pp. 498–519, Feb. 2001.

[19] T. Richardson and R. Urbanke, "The capacity of LDPC codes under message-passing decoding," *IEEE Trans. Inf. Theory*, vol. 47, pp. 599–618, Feb. 2001.

[20] J. Chen, A. Dholakia, E. Eleftheriou, M. Fossorier, and X.-Y. Hu, "Reduced-complexity decoding of LDPC codes," *IEEE Trans. Commun.*, vol. 53, no. 8, pp. 1288–1299, Aug. 2005.

[21] M. Fossorier, M. Mihaljevic, H. Imai, "Reduced complexity iterative decoding of low-density parity check codes based on belief propagation," *IEEE Trans. Commun.*, vol. 47, no. 5, pp. 673–680, May 1999.

[22] J. Lee, J. Thorpe, "Memory-efficient decoding of LDPC codes," *Proc. Int. Symp. Inform. Theory*, Adelaide, Australia, pp. 459–463, Sep. 2005.

[23] M. Sipser and D. A. Spielman, "Expander codes," *IEEE Trans. Inf. Theory*, vol. 42, pp. 1710–1722, Nov. 1996.

[24] D. Burshtein and G. Miller, "Expander graph arguments for message passing algorithms," *IEEE Trans. Inf. Theory*, vol. 47, pp. 782–790, Feb. 2001.

[25] J. Feldman, M. J. Wainwright, and D. R. Karger, "Using linear programming to decode binary linear codes ," *IEEE Trans. Inf. Theory*, vol. 51, no. 3, pp. 954–972, Mar. 2005.

[26] M. P. C. Fossorier, "Quasi-cyclic low-density parity-check codes from circulant permutation matrices," *IEEE Trans. Inf. Theory*, vol. 50, pp. 1788–1793, Aug. 2004.

[27] J. Thorpe, "Low density parity-check codes constructed from protographs," *JPL INP Progress Report*, 42-154, Aug. 15, 2003.

[28] D. Divsalar, S. Dolinar, C. R. Jones, K. Andrews, "Capacity-approaching protograph codes," *IEEE J. Select. Areas Commun.*, vol. 27, no. 6, pp. 876–888, Aug. 2009.

[29] L. Lan, L. Zeng, Y. Y. Tai, L. Chen, S. Lin, and K. Abdel-Ghaffar, "Construction of quasi-cyclic LDPC codes for AWGN and binary erasure channels: A finite field approach," *IEEE Trans. Inf. Theory*, vol.53, pp. 2429–2458, Jul. 2007.

[30] Kou Y. Kou, S. Lin and M. C. Fossorier, "Low-Density Parity-Check Codes Based on Finite Geometries: A Rediscovery and New Results," *IEEE Trans. on Inf. Theory*, vol. 47, no. 7, pp. 2711–2736, Nov. 2001.

[31] B. Vasic, O. Milenkovic, "Combinatorial construction of low-density parity-check codes for iterative decoding," *IEEE Trans. Inf. Theory*, vol. 50, no.6, pp. 1156–1176, Jun. 2004.

[32] R. M. Tanner, "Convolutional codes from quasi-cyclic codes: A link between the theories of block and convolutional codes," *Univ. Calif. Santa Cruz, Tech. Rep.*, 1987.

[33] A. Feltström and K. S. Zigangirov, "Periodic time-varying convolutional codes with low-density parity-check matrix," *IEEE Trans. Inf. Theory*, vol. 45, no. 5 pp. 2181–2190, Sept. 1999.

[34] M. Lentmaier, A. Sridharan, D. J. Costello, and K. S. Zigangirov, "Iterative Decoding Threshold Analysis for LDPC Convolutional Codes," *IEEE Trans. Inf. Theory*, vol. 56, no. 10, 5274–5289, Oct. 2010.

[35] S. Lin and D. J. Costello, "*Error Control Coding: Fundamentals and Applications*," second edition, Prentice Hall: Englewood Cliffs, NJ, 2005.

[36] E. Sharon, S. Litsyn and J. Goldberger, "Efficient serial message-passing schedule for LDPC decoding," *IEEE Trans. on Inf. Theory*, vol. 53, no. 11, pp. 4076–4091, Nov. 2007.

[37] J. Pearl, *Probablisitic Reasoning in Intelligent Systems*, San Francisco, CA, USA: Kaufmann, 1988.

[38] B. J. Frey, *Graphical models for machine learning and digital communication*, Cambridge, MA, USA: MIT Press, 1998.

[39] D. MacKay and M. Postol, "Weaknesses of Margulis and Ramanujan-Margulis low-density parity-check codes,", *Electron. Notes in Theoretical Comput. Sci.*, vol. 74, 2003.

[40] B. J. Frey, R. Koetter, and A. Vardy, "Signal-space characterization of iterative decoding," *IEEE Trans. Inf. Theory*, vol. 47, no.2, pp. 766–781, Feb. 2001.

[41] G. D. Forney, Jr., R. Koetter, F. R. Kschischang, and A. Reznick, "On the effective weights of pseudocodewords for codes defined on graphs with cycles," *Codes, systems and graphical models*, pp. 101–112, Springer, 2001.

[42] C. Di, D. Proietti. I. E. Teletar, T. J. Richardson, and R. L. Urbanke, "Finite length analysis of low-density parity-check codes on the binary erasure channels," *IEEE Trans. Inf. Theory*, vol. 48, no. 6, pp. 1576–1579, Jun. 2002.

[43] A. Orlitsky, K. Viswanathan, and J. Zhang, "Stopping set distribution of LDPC code ensemble," *IEEE Trans. Inf. Theory*, vol. 51, no. 3, pp. 929–953, Mar. 2005.

[44] T. Richardson, "Error floors of LDPC codes," in *Proc. Allerton Conf. on Commun., Control and Computing*, Monticello, Illinois, USA, Oct. 2003.

[45] M.G. Stepanov, V. Chernyak, M. Chertkov, B. Vasić, "Diagnosis of weakness in error correction codes: a physics approach," *Phys. Rev. Lett.*, vol. 95, Nov. 2005.

[46] S. K. Chilappagari, S. Sankaranarayanan, and B. Vasić, "Error floors of LDPC codes on the binary symmetric channels," in *Proc. IEEE Int. Conf. on Commun.*, Istanbul, Turkey, pp. 1089–1094, Jun. 2006.

[47] L. Dolecek, Z. Zhang, M. J. Wainwright, V. Anantharam, and B. Nikolic, "Analysis of Absorbing Sets for Array-Based LDPC Codes," in *Proc. IEEE Int. Conf. on Commun.*, Glasgow UK, pp. 6261–6268, Jun., 2007.

[48] S. K. Chilappagari and B. Vasić, "Error-correction capability of column-weight-three LDPC codes," *IEEE Trans. Inf. Theory*, vol. 55, no. 5, pp. 2055–2061, May 2009.

[49] P. O. Vontobel and R. Koetter, "Graph-cover decoding and finite-length analysis of message-passing iterative decoding of LDPC code," *Corr arXiv:cs/0512078v1*, Dec. 2005.

[50] C. A. Kelley and D. Sridhara, "Pseudocodewords of Tanner graphs," *IEEE Trans. Inf. Theory*, vol. 53, no. 11, pp. 4013–4038, Nov. 2007.

[51] R. Smarandache, A. Pusane, P. Vontobel, and D.J. Costello, "Pseudocodeword performance analysis for LDPC convolutional codes," *IEEE Trans. Inform. Theory*, vol. 55, no. 6, pp. 2577–2598, Jun. 2009.

[52] S. Laendner and O. Milenkovic, "Algorithmic and combinatorial analysis of trapping sets in structured LDPC codes," in *Proc. IEEE Int. Conf. on Wireless Networks, Commun. and Mobile Computing*, Hawaii, USA, pp. 630–635, Jun. 13-16, 2005.

[53] A. McGregor and O. Milenkovic, "On the hardness of approximating stopping and trapping sets in LDPC codes," *IEEE Trans. Inform.Theory*, vol. 56, no. 4, pp. 1640–1650, Apr. 2010.

[54] O. Milenkovic, E. Soljanin, and P. Whiting, "Asymptotic spectra of trapping sets in regular and irregular LDPC code ensembles," *IEEE Trans. Inf. Theory*, vol. 53, no. 1, pp. 39–55, Jan. 2007.

[55] C. Cole, S. Wilson, E. Hall, and T. Giallorenzi, "A general method for finding low error rates of LDPC codes," May 2006.

[56] S. Abu-Surra, D. Declercq, D. Divsalar, and W. Ryan, "Trapping set enumerators for specific LDPC codes," in *Proc. Inform. Theory and Applicat. Workshop*, San Diego, CA, USA, pp. 1–5, Jan. 31- Feb. 5, 2010.

[57] E. Rosnes and O. Ytrehus, "An efficient algorithm to find all small-size stopping sets of low-density parity-check matrices," *IEEE Trans. Inf. Theory*, vol. 55, no. 9, pp. 4167–4178, Sept. 2009.

[58] M. K. Dehkordi and A. H. Banihashemi, "An efficient algorithm for finding dominant trapping sets of LDPC codes," in *Proc. 6th Int. Symp. Turbo Codes Iterat. Inf. Process.*, pp. 444–448, Brest, France, Sep. 6-10, 2010.

[59] X. Zhang and P. H. Siegel, "Efficient algorithms to find all small error-prone substructures in LDPC Codes," in *Proc. IEEE Globecom.*, Houston, TX, USA, Dec. 5–9, 2011.

[60] B. Vasić, S. K. Chilappagari, D. V. Nguyen, and S. K. Planjery, "Trapping set ontology," in *Proc. Allerton Conf. on Commun., Control and Computing*, Monticello, IL, USA, pp. 1–7, Sept. 2009.

[61] S. K. Chilappagari, M. Chertkov, M. G. Stepanov, and B. Vasić, "Instanton-based techniques for analysis and reduction of error floors of LDPC codes," *IEEE JSAC on Capacity Approaching Codes*, vol. 27, no. 6, pp. 855–865, Aug. 2009.

[62] D. V. Nguyen, S. K. Chilappagari, M. W. Marcellin, and B. Vasic, "On the construction of structured LDPC Codes free of small trapping sets," *IEEE Trans. Inf. Theory*, vol. 58, no. 4, pp. 2280–2302, Apr. 2012.

[63] S. K. Planjery, D. Declercq, L. Danjean, and B. Vasic, "Finite alphabet iterative decoders for LDPC codes surpassing floating-point iterative decoders," *IET Electron. Lett.*, vol. 47, no. 16, , pp. 919–921, Aug. 2011.

[64] S. K. Planjery, S. K. Chilappagari, B. Vasic, D. Declercq, and L. Danjean, "Iterative decoding beyond belief propagation," in *Proc. Inform. Theory and App. Workshop*, San Diego, CA, USA, pp. 41–43, Jan. 2010.

[65] G. Kuperberg, "Symmetries of plane partitions and the permanent-determinant method," *J. Comb. Theory A*, vol. 68, pp. 115–151, 1994.

[66] S. K. Chilappagari and B. Vasić, "Error-correction capability of column-weight-three LDPC codes," *IEEE Trans. Inf. Theory*, vol. 55, no. 5, pp. 2055–2061, May 2009.

[67] S. K. Planjery, D. Declercq, S. K. Chilappagari, and B. Vasić, "Multilevel decoders surpassing belief propagation on the binary symmetric channel," in *Proc. IEEE Int. Symp. on Inf. Theory*, Austin, TX, USA, pp. 769–773, Jun. 2010.

[68] R. M. Tanner, "A [155,64,20] sparse graph (LDPC) code," in *Recent results session, IEEE Int. Symp on Inf. Theory*, Sorrento, Italy, Jun. 2000.

[69] R. Tanner, D. Srkdhara, and T. Fuja, "A class of group-structured LDPC codes," in *Proc. of Int. Symp. of Commun. Theory and Applic.*, Ambleside, UK, pp. 365–370, Jul. 2001.

[70] D. J. Costello, Jr., A. Sridharan, D. Sridhara, and R. Tanner, "A construction of Low density parity check convolutional codes based on quasi-cyclic block codes," in *Proc.of IEEE Int. Symp. on Inf. Theory*, Lausanne, Switzerland, p. 481, Jun. 30–Jul. 5 2002.

[71] M. Karimi and A. Banihashemi, "An efficient algorithm for finding dominant trapping sets of ldpc codes," *IEEE Trans. Inf. Theory*, Aug. 2012.

[72] D. Declercq and M. Fossorier, "Improved impulse method to evaluate the low weight profile of sparse binary linear codes," in *Proc. of IEEE Int. Symp. on Inf. Theory*, Toronto, Canada, pp. 1963-1967, Jul. 2008.

[73] L. Danjean, D. Declercq, S. K. Planjery, and B. Vasic, "On the selection of finite alphabet iterative decoders for LDPC codes on the BSC," in *Proc. IEEE Inform. Theory Workshop*, Paraty, Brazil, pp. 345–349, Oct. 2011.

[74] E. E. X. Y. Hu and D. M. Arnold, "Regular and irregular progressive edge-growth tanner graphs," *IEEE Trans. Inf. Theory*, vol. 51, no. 1, pp. 386–398, Jan. 2005.

[75] "Compressed sensing resources," Rice University. [Online]. Available: http://dsp.rice.edu/cs

[76] "Nuit blanche blog." [Online]. Available: http://nuit-blanche.blogspot.com

[77] E. R. J. Candes and T. Tao, "Robust uncertainty principles: exact signal reconstruction from highly incomplete frequency information," *IEEE Trans. Inf. Theory*, vol. 52, no. 2, pp. 489–509, Feb. 2006.

[78] E. J. Candes and T. Tao, "Decoding by linear programming," *IEEE Trans. Inf. Theory*, vol. 51, no. 12, pp. 4203–4215, Dec. 2005.

[79] D. Donoho, "Compressed sensing," *IEEE Trans.Inf. Theory*, vol. 52, no. 4, pp. 1289–1306, 2006.

[80] S. Mallat, *A Wavelet Tour of Signal Processing, Third Edition: The Sparse Way*, 3rd ed, Academic Press, 2008.

[81] Z. Lei and Q. Chunting, "Application of compressed sensing theory to radar signal processing," in *Proc 3rd IEEE Int. Conf. on Comput. Sci. and Inform. Technology*, vol. 6, Chengdu, China, pp. 315–318, Jul. 2010.

[82] J. Romberg, "Imaging via compressive sampling," *IEEE Signal Process. Mag.*, vol. 25, no. 2, pp. 14–20, Mar. 2008.

[83] W. Bajwa, J. Haupt, A. Sayeed, and R. Nowak, "Compressed channel sensing: A new approach to estimating sparse multipath channels," *Proceedings of the IEEE*, vol. 98, no. 6, pp. 1058–1076, Jun. 2010.

[84] J. Provost and F. Lesage, "The application of compressed sensing for photo-acoustic tomography," *IEEE Trans. Med. Imag.*, vol. 28, no. 4, pp. 585–594, Apr. 2009.

[85] G. Kutyniok, "Compressed sensing: Theory and applications," *CoRR*, vol. abs/1203.3815, 2012.

[86] S. S. Chen, D. Donoho, and M. A. Saunders, "Atomic decomposition by basis pursuit," *SIAM Journal on Scientific Computing*, vol. 20, no. 1, pp. 33–61, 1998.

[87] S. Mallat and Z. Zhang, "Matching pursuit with time-frequency dictionaries," *IEEE Trans. Signal Process.*, vol. 41, pp. 3397–3415, 1993.

[88] J. Tropp and A. Gilbert, "Signal Recovery from partial information via orthogonal matching pursuit," *IEEE Trans. Inform. Theory*, vol. 53, no. 12, pp. 4655–4666, Dec. 2007.

[89] ——, "Signal recovery from random measurements information via orthogonal matching pursuit," *IEEE Trans. Inf. Theory*, vol. 53, no. 12, pp. 4655–4666, Dec. 2007.

[90] D. L. Donoho, Y. Tsaig., I. Drori., and J.-L. Starck, "Sparse solution of underdetermined linear equations by stagewise orthogonal matching pursuit," Tech. Rep., 2006.

[91] Y. C. Eldar and G. Kutyniok, *Compressed Sensing: Theory and Applications*. Cambridge University Press, 2012.

[92] D. L. Donoho, A. Maleki, and A. Montanari, "Message passing algorithms for compressed sensing," *Proc. Nat. Acad. Sci.*, vol. 106, no. 45, pp. 18 914–18 919, Sep. 2009.

[93] A. G. Dimakis and P. Vontobel, "LP decoding meets LP decoding: a connection between channel coding and compressed sensing," in *Proc. 47th Allerton Conf. on Commun., Control, and Computing*, Monticello, Illinois, USA, pp. 8–15, Sep. 30–Oct. 2 2009.

[94] J. Feldman, M. Wainwright, and D. Karger, "Using linear programming to decode binary linear codes," *IEEE Trans. Inf. Theory*, vol. 51, no. 3, pp. 954–972, Mar. 2005.

[95] J. D. Blanchard, C. Cartis, and J. Tanner, "Compressed sensing: How sharp is the restricted isometry property," *SIAM Review*, 2010.

[96] A. Dimakis, R. Smarandache, and P. O. Vontobel, "LDPC codes for compressed sensing," *IEEE Trans. Inf. Theory.*, vol. 58, no. 5, pp.3093–3114, May. 2012.

[97] M. Sipser and D. Spielman, "Expander codes," *IEEE Trans. Inf. Theory*, vol. 42, no. 6, pp. 1710–1722, Nov. 1996.

[98] J. Tropp and S. Wright, "Computational methods for sparse solution of linear inverse problems," in *Proc. of the IEEE*, vol. 98, no. 6, pp. 948–958, Jun. 2010.

[99] H. V. Pham, W. Dai, and O. Milenkovic, "Sublinear compressive sensing reconstruction via belief propagation decoding," in *Proc. IEEE Int. Symp. Inform. Theory*, Seoul, Korea, pp. 674–678, Jun. 28–Jul. 3 2009.

[100] R. Berinde, P. Indyk, and M. Ruzic, "Practical near-optimal sparse recovery in the L1 norm," in *Proc. 46th Allerton Conf. on Commun., Control, and Computing*, Urbana-Champaign, IL, USA, pp. 198–205, Sep. 23–26 2008.

[101] F. Zhang and H. Pfister, "Compressed sensing and linear codes over real numbers," in *Inf. Theory and Applicat. Workshop*, San Diego, CA, USA, pp. 558–561, Feb. 2008.

[102] F. Zhang and H. D. Pfister, "Verification decoding of high-rate LDPC codes with applications in compressed sensing," *IEEE Trans. Inf. Theory*, vol. 58, no. 8, pp. 5042,5058, Aug. 2012.

[103] V. Chandar, D. Shah, and G. Wornell, "A simple message-passing algorithm for compressed sensing," in *Proc. IEEE Int. Symp. Inform. Theory*, Austin, TX, USA, Jun. 13–18 2010, pp. 1968–1972.

[104] A. R. Krishnan, S. Sankararaman, and B. Vasic, "Graph-based iterative reconstruction of sparse signals for compressed sensing," in *Proc. Int. Conf. on Telecommun. in Modern Satellite, Cable and Broadcasting Services*, Nis, Serbia, pp. 133–137, Oct. 5–8 2011.

[105] L. Danjean, V. Ravanmehr, D. Declercq, and B. Vasic, "Iterative reconstruction algorithms in compressed sensing," in *Proc. 19th Telecommun. Forum*, Belgrade, Serbia, pp. 537–541, Nov. 22–24 2011.

[106] V. Ravanmehr, L. Danjean, D. Declercq, and B. Vasic, "On iterative compressed sensing reconstruction of sparse non-negative vectors," in *Proc. Int. Symp. on Appl. Sci. in Biomedical and Commun. Technologies*, Barcelona, Spain, Oct. 26–29 2011.

[107] M. C. Davey and D. J. C. MacKay, "Low-density parity check codes over GF(q)," *IEEE Commun. Lett.*, vol. 2, no. 6, pp. 165–167, Jun. 1998.

[108] D. Declercq and M. Fossorier, "Decoding Algorithms for Nonbinary LDPC Codes Over GF(q)," *IEEE Trans. Commun.*, vol. 55, no. 4, pp. 633–643, Apr. 2007.

[109] C. Di, D. Proietti, I. Telatar, T. Richardson, and R. Urbanke, "Finite-length analysis of low-density parity-check codes on the binary erasure channel," *IEEE Trans. Inf. Theory,*, vol. 48, no. 6, pp. 1570–1579, Jun. 2002.

[110] M. Schwartz and A. Vardy, "On the stopping distance and the stopping redundancy of codes," *IEEE Trans. Inf. Theory*, vol. 52, no. 3, pp. 922–932, Mar. 2006.

[111] S. Hoory, "The size of bipartite graphs with a given girth," *J. Combinatorial Theory Series B*, vol. 86, no. 2, pp. 215–220, Nov. 2002.

[112] G. Richter, "Finding small stopping sets in the tanner graphs of LDPC codes," in *Proc. Int. Symp. on Turbo Codes Related Topics and Int. ITG-Conf. on Source and Channel Coding*, Munich, Germany, pp. 1–5, Apr. 3–7 2006.

[113] E. Rosnes, O. Ytrehus, M. Ambroze, and M. Tomlinson, "Addendum to: An efficient algorithm to find all small-size stopping sets of low-density parity-check matrices," *IEEE Trans. Inf. Theory,*, vol. 58, no. 1, pp. 164–171, Jan. 2012.

[114] "IEEE standard for local and metropolitan area networks part 16: Air interface for fixed and mobile broadband wireless access systems amendment 2: Physical and medium access control layers for combined fixed and mobile operation in licensed bands and corrigendum 1," *IEEE Std 802.16e-2005 and IEEE Std 802.16-2004/Cor 1-2005 (Amendment and Corrigendum to IEEE Std 802.16-2004)*, Feb. 2006.